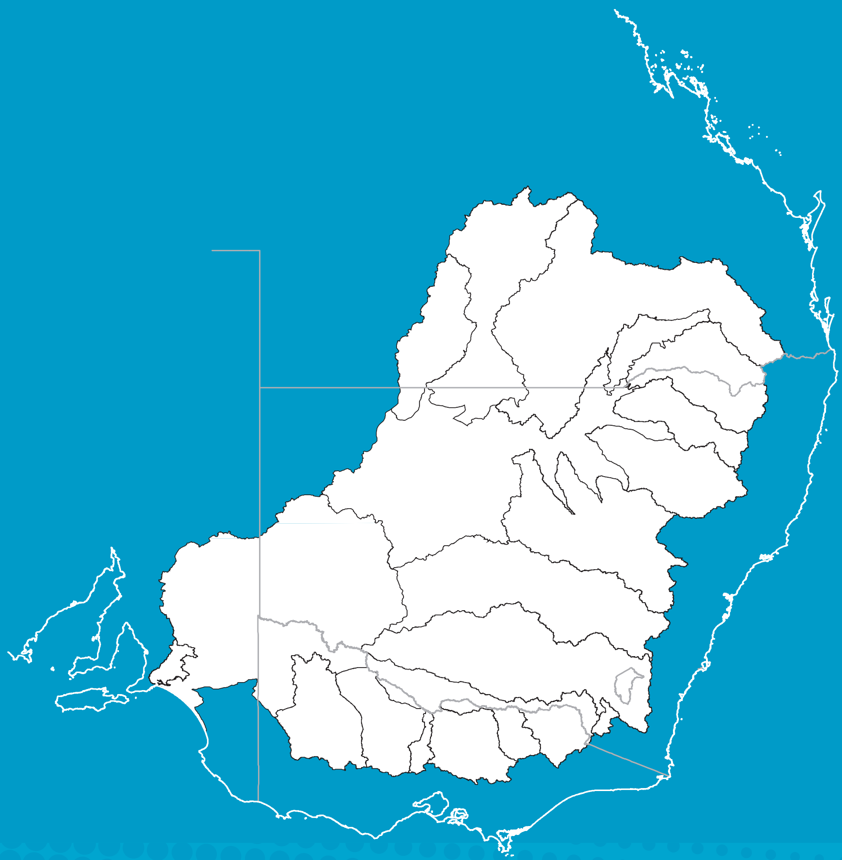

Diffuse groundwater recharge modelling across the Murray-Darling Basin

A report to the Australian Government from the CSIRO Murray-Darling Basin Sustainable Yields Project

Russell Crosbie, James McCallum, Glen Walker and Francis Chiew

September 2008

www.csiro.au

Murray-Darling Basin Sustainable Yields Project acknowledgments

The Murray-Darling Basin Sustainable Yields project is being undertaken by CSIRO under the Australian Government's Raising National Water Standards Program, administered by the National Water Commission. Important aspects of the work were undertaken by Sinclair Knight Merz; Resource & Environmental Management Pty Ltd; Department of Water and Energy (New South Wales); Department of Natural Resources and Water (Queensland); Murray-Darling Basin Commission; Department of Water, Land and Biodiversity Conservation (South Australia); Bureau of Rural Sciences; Salient Solutions Australia Pty Ltd; eWater Cooperative Research Centre; University of Melbourne; Webb, McKeown and Associates Pty Ltd; and several individual sub-contractors.

Citation

Crosbie RS, McCallum JL, Walker GR and Chiew FHS (2008) Diffuse groundwater recharge modelling across the Murray-Darling Basin. A report to the Australian government from the CSIRO Murray-Darling Basin Sustainable Yields Project. CSIRO, Australia. 108pp.

Enquiries should be addressed to:
Russell Crosbie
russell.crosbie@csiro.au

Publication Details

ISSN 1835-095X

Preface

This is a report to the Australian Government from CSIRO. It is an output of the Murray-Darling Basin Sustainable Yields Project which assessed current and potential future water availability in 18 regions across the Murray-Darling Basin (MDB) considering climate change and other risks to water resources. The project was commissioned following the Murray-Darling Basin Water Summit convened by the then Prime Minister of Australia in November 2006 to report progressively during the latter half of 2007. The reports for each of the 18 regions and for the entire MDB are supported by a series of technical reports detailing the modelling and assessment methods used in the project. This report is one of the supporting technical reports of the project. Project reports can be accessed at http://www.csiro.au/mdbsy.

Project findings are expected to inform the establishment of a new sustainable diversion limit for surface and groundwater in the MDB – one of the responsibilities of a new Murray-Darling Basin Authority in formulating a new Murray-Darling Basin Plan, as required under the Commonwealth Water Act 2007. These reforms are a component of the Australian Government's new national water plan 'Water for our Future'. Amongst other objectives, the national water plan seeks to (i) address over-allocation in the MDB, helping to put it back on a sustainable track, significantly improving the health of rivers and wetlands of the MDB and bringing substantial benefits to irrigators and the community; and (ii) facilitate the modernisation of Australian irrigation, helping to put it on a more sustainable footing against the background of declining water resources.

Executive Summary

The Murray-Darling Basin Sustainable Yield Project aims to investigate the water resources of the Murray-Darling Basin (MDB) now and into the future. Groundwater recharge is only a small component of the water balance but has an influence on the amount of water available for consumptive use and sustaining ecosystems. Prudent management of our water resources requires that all threats to water availability are investigated and assessed for uncertainty. Climate change is one threat to our water resources and its impact upon groundwater recharge has been investigated here.

This report aims to investigate the impact of a future climate upon the diffuse groundwater recharge of the MDB. Never before has a project sought to model the impact of climate change on a region as large as the MDB and for so many different climate scenarios. The scale of what was attempted for this project required that a methodology be established that is different to what has been done in previous climate change studies of groundwater recharge.

Groundwater recharge was modelled at selected points using the WAVES model for a variety of soil and vegetation types. Recharge scaling factors were calculated for each climate scenario at those selected points. The point scale estimates of the recharge scaling factors were then upscaled to the entire MDB using soil type, vegetation type and change in rainfall as covariates to create rasters of recharge scaling factors for each scenario.

The climate scenarios investigated here are a climate sequence based upon the previous ten years and three future climate scenarios (high, medium and low global warming) as predicted by 15 different global climate models. The outputs of this report are a series of rasters for the change in recharge throughout the MDB at a resolution of 0.05°× 0.05°for each of these 46 climate scenarios. The results are presented as a composite of the different global climate models to create a wet, mid and dry scenario. These rasters were aggregated to provide recharge scaling factors for each region and groundwater management unit throughout the MDB. The recharge scaling factors are used to assess the groundwater resources of the MDB, as reported elsewhere.

Under the scenario based on the last ten years of climate observations, recharge decreases by up to 50% in the southern parts of the MDB and in the Condamine, while in the remainder of the northern parts of the MDB recharge increases by up to 20%. Under the dry climate change scenario, recharge reduces in all parts of the MDB though not as extremely as under the climate scenario based on the last ten years. Under the mid climate change scenario, little change in recharge is observed throughout the MDB with small decreases in the south and small increases in the north. Under the wet climate change scenario, recharge increases in all regions with up to a 50 percent increase in the north and down to a 5 percent increase in the south.

Table of Contents

Figures

Tables

1 Introduction

1.1 Project scope

At the November 2006 Summit on the Southern Murray-Darling Basin, the Prime Minister asked CSIRO to investigate the sustainable yield of the Murray-Darling Basin (MDB) both now and into the future. This has required the modelling of the surface water and groundwater in each region of the MDB under historical climate conditions, under predicted global warming climate conditions and under both current and future levels of development. This report is one of many technical reports underpinning the 18 regional reports for the Murray-Darling Basin Sustainable Yields Project. It considers the dryland diffuse recharge of rainfall to groundwater.

1.2 Modelling recharge

Recharge is the addition of water to the groundwater store. There are many different mechanisms of groundwater recharge. In urban areas leaking pipes contribute to recharge. In irrigation areas the leaching fraction of water applied may become recharge. In some areas losing streams are the dominant form of groundwater recharge. This technical report only considers dryland diffuse recharge. For this report, recharge is defined as water that infiltrates the soil from rainfall, passes through the root zone and crosses the plane of the watertable.

Recharge is difficult to measure in the field and is often modelled. Recharge modelling can vary from simple relationships with rainfall to full deterministic models. At its simplest recharge can be modelled as a fixed proportion of rainfall or as a threshold and then a fixed proportion of ranfall. The next step up in complexity are models that account for land use differences and a relationship with rainfall. Soil-vegetation-atmosphere transfer (SVAT) models have the advantage of simulating the growth of vegetation and the routing of water through the soil zone. SVAT models are water balance models. They take rainfall (some models include irrigation) as inputs to the land surface and partition this input into evapotranspiration runoff and recharge, and they are often the preferred method of simulating recharge. SVAT models vary widely in their complexity with regard to how they treat vegetation growth and soil physics.

Most SVAT models are point or one-dimensional models. To be useful in a spatial context they need to be extended to all points of the landscape. Some approaches rely on one-dimensional models embedded in a GIS system to allow the one-dimensional model to be run on a grid (Beverly et al., 2005; Littleboy et al., 2003), while fully three-dimensional models are rare (Tuteja et al., 2005). SVAT models run spatially are computationally expensive and require a large amount of data.

The other alternative is to upscale the one-dimensional model results from the point scale to the working scale using covariates. This approach is more often used with field measurements (Brunner et al., 2004; Cook et al., 1989; Sophocleous, 1992).

1.3 Climate change

Climate change has been defined as ‘a change of climate which is attributed directly or indirectly to human activity that alters the composition of the global atmosphere and which is in addition to natural climate variability observed over comparable time periods’ (UNFCCC, 1992). This definition is wider than the often used ‘global warming’ as it encompasses all aspects of climate, e.g. temperature, precipitation, solar radiation, humidity etc.

Global climate models (GCMs) are used to predict change in climate from increased CO_2 (and other greenhouse gases) in the atmosphere. There is considerable uncertainty about the predictions made by GCMs and it is common practice to use the outputs of multiple models to assess scenarios.

Climate drives the hydrological cycle and any change in climate will have consequential changes in the hydrological cycle. Precipitation is the largest term in the water balance of a catchment and as such the hydrological cycle is most sensitive to changes in rainfall. In temperate, semi-arid and arid regions evapotranspiration is the second largest component of the water balance and so is affected not only by the availability of water but also by any changes in other aspects of climate (e.g. temperature). Recharge is often the smallest component of the water balance and is calculated as the residual after subtracting evapotranspiration and runoff from precipitation.

A common approach to assessing water budgets is to use a model to distribute precipitation into evapotranspiration, surface runoff and recharge. There are a wide variety of models available and they vary widely in their complexity. Two of the most popular models used for investigating the change in recharge due to climate change are SWAT (Neitsch et al., 2000) and HELP (Schroeder et al., 1994). They are both bucket models for soil moisture but SWAT uses a more complex vegetation routine. HELP seems to be the favoured model of North American researchers (Allen et al., 2004; Jyrkama and Sykes, 2007; Scibek and Allen, 2006) and SWAT has been used on both sides of the Atlantic (Eckhardt and Ulbrich, 2003; Rosenberg et al., 1999). Other approaches to the estimation of climate change impacts on groundwater include a scaling relationship with runoff (Loáiciga et al., 2000) or simple relationships with rainfall (Hsu et al., 2007; Kirshen, 2002). In all reported cases an increase in rainfall leads to an increase in recharge and a decrease in rainfall leads to a decrease in recharge.

Most recharge studies have been small in scale and so do not represent more than a pixel in a GCM. There are only three studies greater than 5000 km^2 reported in the scientific literature. Jyrkama and Sykes (2007) describe a study in the 7000 km^2 Grand River watershed in Ontario. In this study the general predictions from the IPCC (2001) were used to find that an increase in rainfall leads to an increase in recharge although it is not spatially uniform due to differences in soils and land use. In the 15,000 km^2 Edwards BFZ aquifer in Texas, Loáiciga et al. (2000) used a single pixel from a single GCM to derive a scaling factor for runoff that was then applied to recharge. (In this aquifer recharge is derived from losing streams.) This study found that the predicted decrease in streamflow and increase in demand would place excessive stress on the aquifer leading to decreased security of water supply, decreased water quality and a detrimental impact on GDEs. The largest area reported for climate change impacts on recharge is the 450,000 km^2 Ogallala aquifer in central US (Rosenberg et al., 1999). Due to the large scale of the study the same GCM could predict an increase in precipitation in one river basin and a decrease in another river basin. Overall, every scenario investigated resulted in less recharge leading to an accelerated decline in aquifer pressure in an aquifer already being mined.

1.4 Aims of project

This technical report describes a small portion of an overall larger project. The Murray-Darling Basin Sustainable Yield Project aims to estimate the amount of water available throughout the MDB for every catchment and aquifer under a series of historical and future climate scenarios.

This report describes the groundwater recharge component of this work. This project aims to:

- provide a methodology for estimating the change in diffuse groundwater recharge with a change in climate
- provide estimates of the change in recharge caused by a change in climate for all catchments and groundwater management units (GMUs) in the MDB. The change in recharge will be expressed as a series of scaling factors.

2 Description of the Murray-Darling Basin

The MDB is Australia's largest and most important river system. It is home to about 2,000,000 people and provides the potable water supply to another 1,000,000 outside the MDB. The MDB provides the water for 75% of Australia's irrigation industry and this underpins the MDB providing 34% of Australia's agricultural output (ABS, 2003). The MDB is also home to several wetlands of international importance that are protected under international treaties (DFA, 1974; DFAT, 1986; Ramsar Convention Bureau, 1971).

The MDB covers 1,060,000 km^2 or roughly one-seventh of the Australian continent. Its climate varies from sub-tropical in the north, Mediterranean in the south, alpine in the south-east and semi-arid in the west. The MDB has been sub-divided into 19 catchments that are used as regions for this project (Figure 2-1).

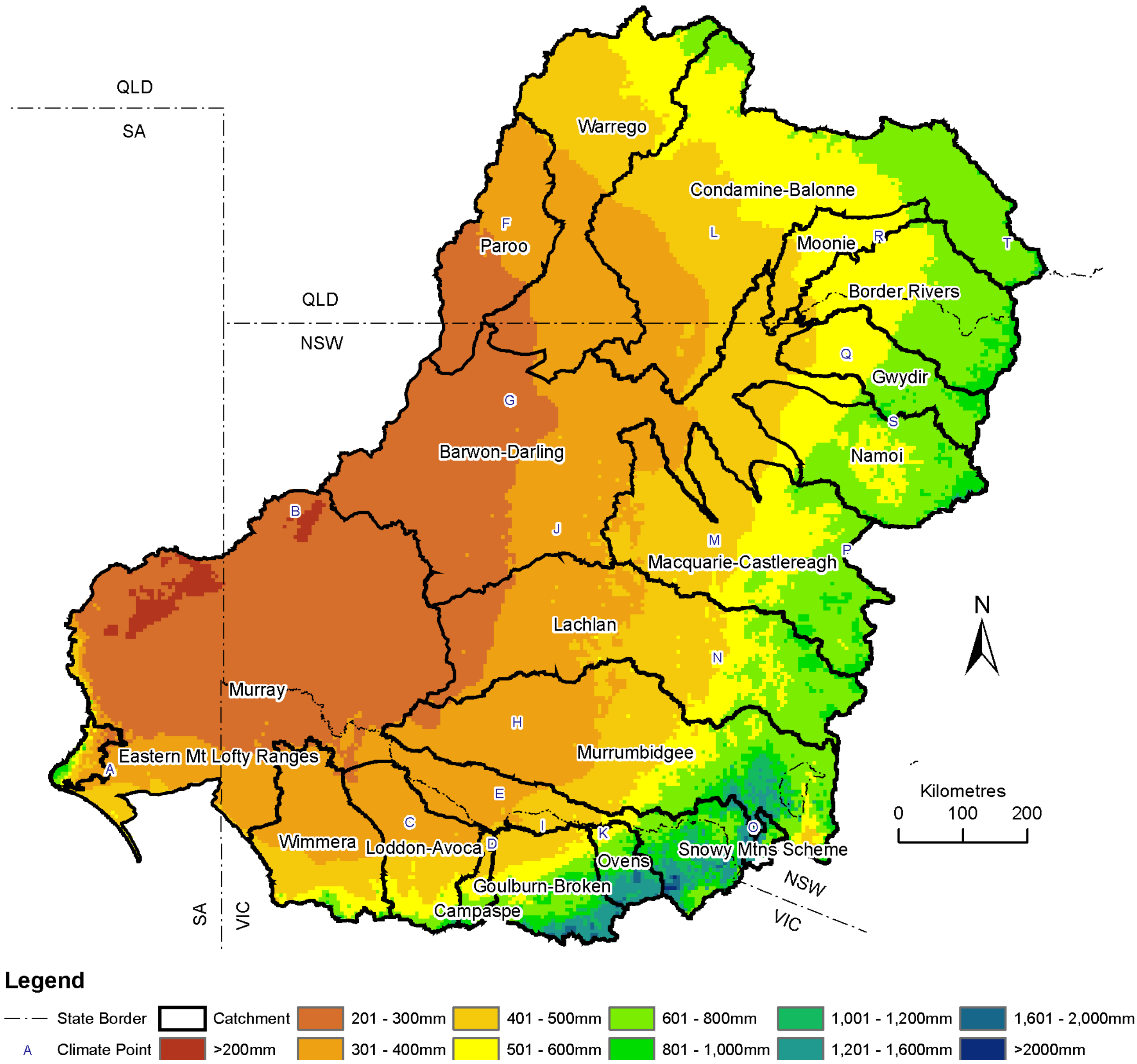

Figure 2-1. Annual average rainfall (1895 to 2006) across the Murray-Darling Basin. Also shown are the boundaries of regions used for reporting and the climate points used for WAVES modelling

According to the most recent IPCC report, the impact of climate change upon the MDB will be higher average temperatures, greater potential evapotranspiration, lower mean annual rainfall in the south, and greater daily extreme rainfall events (Christensen et al., 2007). These conclusions have been reinforced in a recent Australian study (CSIRO and BOM, 2007).

Knowing how much water is available for extraction both now and under future climate scenarios is essential for the wise management of the resource; groundwater recharge is one small part of this equation.

3 Methods

Recharge is a difficult part of the water balance to estimate, even with detailed field measurements. The scope of this project means that recharge had to be modelled. It was also important that the methods used can respond appropriately to climate and thus changes in climate variables. Modelling recharge can be just as uncertain as measuring recharge. For this reason it was the change in recharge between the baseline and the scenario that was investigated here.

Recharge was modelled at a select number of locations to derive recharge scaling factors (RSFs); these RSFs were upscaled to the entire MDB before being aggregated to the scale of a region or GMU. This section describes the methods developed in detail.

3.1 Point scale recharge

The model chosen for the unsaturated zone modelling in this project was WAVES (Zhang and Dawes, 1998). It is a SVAT model that can be used to estimate the components of an unsaturated zone water balance. It achieves a balance in its modelling complexity between soil physics, plant physiology, energy and solute balances. WAVES has been used extensively for recharge modelling studies in Australia (Salama et al., 1999; Zhang et al., 1999). Some changes were made to the model code to tailor its use for this project, as detailed in section 3.1.1.

The WAVES model requires three different data sets: climate, soil and vegetation inputs. The input files for the model were generated automatically using a simple Fortran program developed for this project. Similarly the output files from WAVES were summarised using another simple program.

A 4 m soil profile was modelled with a free draining lower boundary condition. It was assumed that the deep drainage from the bottom of the model was groundwater recharge and did not become lateral flow. The assumption was made that diffuse recharge in dryland areas was not affected by groundwater; this assumption will result in errors where the watertable is close to the surface.

The output of the point scale modelling was 22,560 model runs of WAVES. This was comprised of 20 locations, 3 vegetation types, 8 soils and 47 climate scenarios. These are described below.

3.1.1 Changes to the model code

One of the authors of the model made two changes to the WAVES model to suit its application to this project (Warrick Dawes, pers. comm. 2007). For a full description of the WAVES model the reader is referred to the technical manual (Zhang and Dawes, 1998).

In its standard form, WAVES v3.5 has a hard coded parameter for CO_2 concentration that is used in the calculation of stomatal conductance (equation 2.75 in Zhang and Dawes (1998)). This was altered for this project to become a variable:

$$r_s = (g_s)^{-1} = \left\{ \frac{g_0 + g_1 A}{(C_s - \Gamma)\left(1 + \frac{D_c}{D_{co}}\right)} \right\}^{-1} \qquad (1)$$

where r_s is the canopy resistance, g_s is the leaf stomatal conductance, g_0 is the residual stomatal conductance, g_1 is an empirical coefficient, A is the maximum carbon assimilation rate, C_s is the CO_2 mole fraction of the air at the canopy surface, Γ is the CO_2 compensation point, D_c is the vapour pressure deficit at the canopy surface, and D_{co} is an empirical coefficient.

The other change to the standard WAVES code that was required is in the Integrated-Rate-Methodology (IRM) weighting for relative assimilation. In WAVES this is a three-parameter model with relative assimilation based upon the availability of light, nutrients and water (equation 2.67 in (Zhang and Dawes, 1998)):

$$r = \frac{1 + w_H + w_N}{\dfrac{1}{\eta_T \chi_L} + \dfrac{w_H}{\chi_H} + \dfrac{w_N}{\chi_N}} \qquad (2)$$

where r is relative assimilation, w_H is the weighting of water relative to light, w_N is the weighting of nutrients relative to light, χ_H, χ_N, χ_L are the relative resource availabilities of water, nutrients and light respectively, and η_T is a modifier of light availability relative to temperature.

For this project relative assimilation has been expanded to a four-parameter model as used by Hatton et al. (1992):

$$r = \frac{1 + w_H + w_N + w_C}{\dfrac{1}{\eta_T \chi_L} + \dfrac{w_H}{\chi_H} + \dfrac{w_N}{\chi_N} + \dfrac{w_C}{\eta_V \chi_C}} \qquad (3)$$

where w_C is the weighting factor for CO_2 relative to light, χ_C is the relative resource availability of CO_2, and η_V is a modifier of CO_2 availability relative to vapour pressure.

3.1.2 Selection of points to model

With each run of the WAVES model taking up to two minutes to complete, it was impractical to model the entire MDB at the same scale as the climate data (~5 km grid). A series of points were selected across the MDB to reflect the rainfall gradient, the seasonal changes in rainfall and a bias toward the tier 1 GMUs. Three transects were selected to cover the rainfall gradient from the highest rainfall along the Great Dividing Range to the semi-arid western boundary of the MDB. One transect was in the north to account for the summer-dominated rainfall climatic region, the second transect was in the equi-seasonal rainfall climatic region, and the third transect was in the south where there is winter-dominated rainfall. Additional points were added in some tier 1 GMUs to arrive at a total of 20 points that were selected for detailed modelling (Table 3-1, Figure 2-1).

Table 3-1. Location of points selected for detailed unsaturated zone modelling

Location code	Longitude	Latitude	Region
A	139.5	35.2	Eastern Mt Lofty Ranges
B	142	31.6	Murray
C	143.6	35.95	Loddon Avoca
D	144.65	36.25	Campaspe
E	144.85	35.55	Murray
F	144.95	27.6	Paroo
G	145	30.05	Barwon-Darling
H	145.1	34.55	Murrumbidgee
I	145.45	36	Murray
J	145.65	31.85	Barwon-Darling
K	146.3	36.1	Ovens
L	147.85	27.7	Condamine-Balonne
M	147.85	32.05	Macquarie-Castlereagh
N	147.9	33.65	Lachlan
O	148.4	36.15	Murrumbidgee
P	149.65	32.15	Macquarie-Castlereagh
Q	149.7	29.4	Gwydir
R	150.15	27.75	Moonie
S	150.35	30.35	Namoi

Location code	Longitude	Latitude	Region
T	151.95	27.85	Condamine-Balonne

3.1.3 Climate

There were four climate and development scenarios modelled as part of this project, as detailed in (Chiew et al., 2008a):

- Scenario A – current climate, current development
- Scenario B – recent climate, current development
- Scenario C – future climate (~2030), current development
- Scenario D – future climate (~2030), future development.

The time frame modelled for each scenario is 112 years, beginning 1 January 1895 and ending 31 December 2006.

For Scenario A the interpolated historical climate sequence was extracted from the Queensland Department of Natural Resources and Water SILO website (Jeffrey et al., 2001) (http://www.nrw.qld.gov.au/silo/ppd/index.html) for each of the 20 points selected for modelling. The CO_2 concentration was estimated as 380 ppm based upon the 379 ppm recorded for 2005 (IPCC, 2007).

Scenario B was modelled using the climate averages of the previous ten years to modify the historical climate sequence. A full description of this procedure can be found in (Chiew et al., 2008a). As the development level for Scenario B was to be the same as Scenario A, the CO_2 concentration was also kept the same as Scenario A at 380 ppm.

For Scenario C there were three different climate scenarios produced from 15 global climate models (GCMs). The high (CH) global warming scenario came from the A1F1 scenario detailed in the IPCC Special Report on Emission Scenarios (SRES) (Nakicenovic and Swart, 2000), the low (CL) global warming scenario came from the B1 scenario in SRES, and the medium (CM) global warming scenario came from the A1T1 scenario in SRES. The CO_2 concentrations used in the WAVES modelling were 437, 446 and 455 ppm for the CL, CM and CH scenarios respectively. The outputs from the three scenarios from 15 GCMs produced a total of 45 climate scenarios for modelling. Each of the 45 scenarios produced climate modifiers that were applied to the historical climate sequence (Scenario A). Full details of the climate generation procedure can be found in Chiew et al. (2008a). Each GCM was assigned a code as shown in Table 3-2.

Table 3-2. Codes for the 45 climate scenarios representing combinations of 15 climate models and 3 global warming scenarios

GCM	Low global warming	Medium global warming	High global warming
cccma_t47	L01	M01	H01
cccma_t63	L02	M02	H02
cnrm	L03	M03	H03
csiro	L04	M04	H04
gfdl	L05	M05	H05
giss_aom	L06	M06	H06
iap	L07	M07	H07
inmcm	L08	M08	H08
ipsl	L09	M09	H09
miroc	L10	M10	H10
miub	L11	M11	H11
mpi	L12	M12	H12
mri	L13	M13	H13
ncar_ccsm	L14	M14	H14
ncar_pcm	L15	M15	H15

3.1.4 Soil

The Broadbridge-White equation (Broadbridge and White, 1998) for soil moisture retention is used in WAVES. To calculate hydraulic conductivity (K) and matric potential (Ψ) as a function of moisture content (θ) five parameters are required: saturated hydraulic conductivity (K_s, m/d), saturated moisture content (θ_s , cm^3/cm^3), residual moisture content (θ_r , cm^3/cm^3), inverse capillary length scale (α, m) and an empirical constant based on soil properties (C, unitless).

$$\Theta = \frac{\theta - \theta_r}{\theta_s - \theta_r} \tag{4}$$

where Θ is the relative moisture content (scaled between 0 and 1).

$$K(\Theta) = K_s \frac{(C-1)\Theta^2}{C-\Theta} \tag{5}$$

$$\psi(\Theta) = \frac{1}{\alpha}\left[\frac{1-\Theta}{\Theta} + \frac{1}{C}\ln\left(\frac{C-\Theta}{\Theta(C-1)}\right)\right] \tag{6}$$

The ASRIS 1 database (Johnston et al., 2003) is the best data set that covers the entire MDB. Some states have more detailed soil mapping but this was not used for consistency between different areas. ASRIS has data layers for soil type (Isbell, 2002) and K_s and plant available water capacity (PAWC) for two soil layers. The PAWC is defined as the difference in volumetric moisture content between matric potentials of 0.1 and 15 bar. A map of soil types is shown in Figure 3-1.

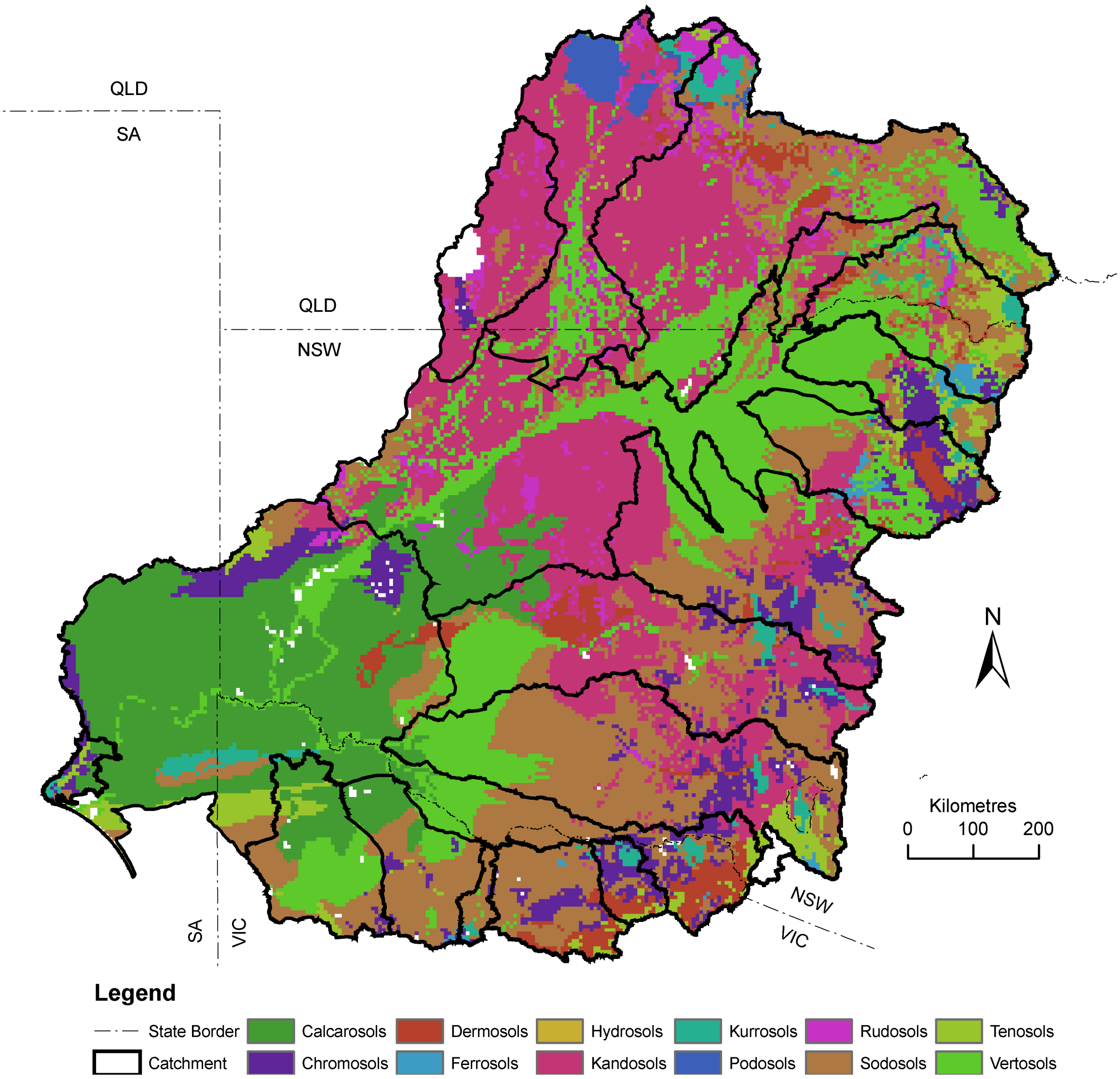

Figure 3-1. Soil types of the Murray-Darling Basin (Johnston et al., 2003)

The K_s and PAWC of the topsoils and subsoils were averaged across the MDB by soil type, and θ_s and θ_r were determined using equations and . The *C* and α parameters were estimated based on soil texture and K_s. The soil parameters used are shown in Table 3-3.

Table 3-3. Soil parameters used in the Broadbridge-White model for soil moisture retention and hydraulic conductivity in WAVES

Soil type	Topsoil					Subsoil				
	K_s (m/d)	C (unitless)	α (m)	θ_s (v/v)	θ_r (v/v)	K_s (m/d)	C (unitless)	α (m)	θ_s (v/v)	θ_r (v/v)
Calcarosols	2.3	1.01	0.04	0.21	0.07	0.12	1.5	0.2	0.33	0.2
Chromosols	1.6	1.02	0.05	0.24	0.1	0.08	1.3	0.2	0.34	0.2
Dermosols	1.5	1.05	0.05	0.26	0.1	0.4	1.45	0.15	0.28	0.15
Ferrosols	1.5	1.02	0.05	0.25	0.1	0.08	1.3	0.2	0.38	0.25
Hydrosols	1.4	1.02	0.05	0.22	0.1	0.18	1.5	0.18	0.32	0.18
Kandosols	3.6	1.01	0.02	0.21	0.06	0.42	1.45	0.15	0.29	0.15
Kurosols	2.4	1.02	0.03	0.22	0.08	0.20	1.48	0.15	0.28	0.18
Podosols	0.02	1.5	0.5	0.45	0.3	0.00002	0.2	0.2	0.28	0.05
Rudosols	2.0	1.02	0.03	0.23	0.08	0.24	1.48	0.18	0.30	0.18
Sodosols	0.75	1.4	0.13	0.28	0.13	0.02	1.5	0.5	0.45	0.35
Tenosols	0.25	1.01	0.04	0.23	0.07	1.3	1.02	0.05	0.22	0.1
Vertosols	0.04	1.4	0.35	0.45	0.3	0.01	1.5	0.5	0.47	0.35

The 12 soil types identified in Table 3-3 were run in WAVES with the same climate file and the same vegetation file to determine if the soil types could be grouped to less than 12. This process is detailed in Appendix I and resulted in a total of eight soil groups to be modelled. The Calcarosols, Chromosols and Hydrosols were found to be similar and so were combined and the Kandosols, Kurosols and Rudosols were also grouped.

3.1.5 Vegetation

Within the point scale modelling every point within the MDB was not going to be modelled and so not every vegetation type could be included. For simplicity, the Bureau of Rural Sciences land use map of the MDB was reclassified to three vegetation classes:

- annuals
- perennials
- trees.

The vegetation parameters required by WAVES were taken from the User Manual (Dawes et al., 2004). The annuals (including crops) were modelled as a C3 annual pasture, the perennials were modelled as a C3 perennial pasture and the trees were modelled as Eucalypts. The simplified vegetation groupings are shown in Figure 3-2.

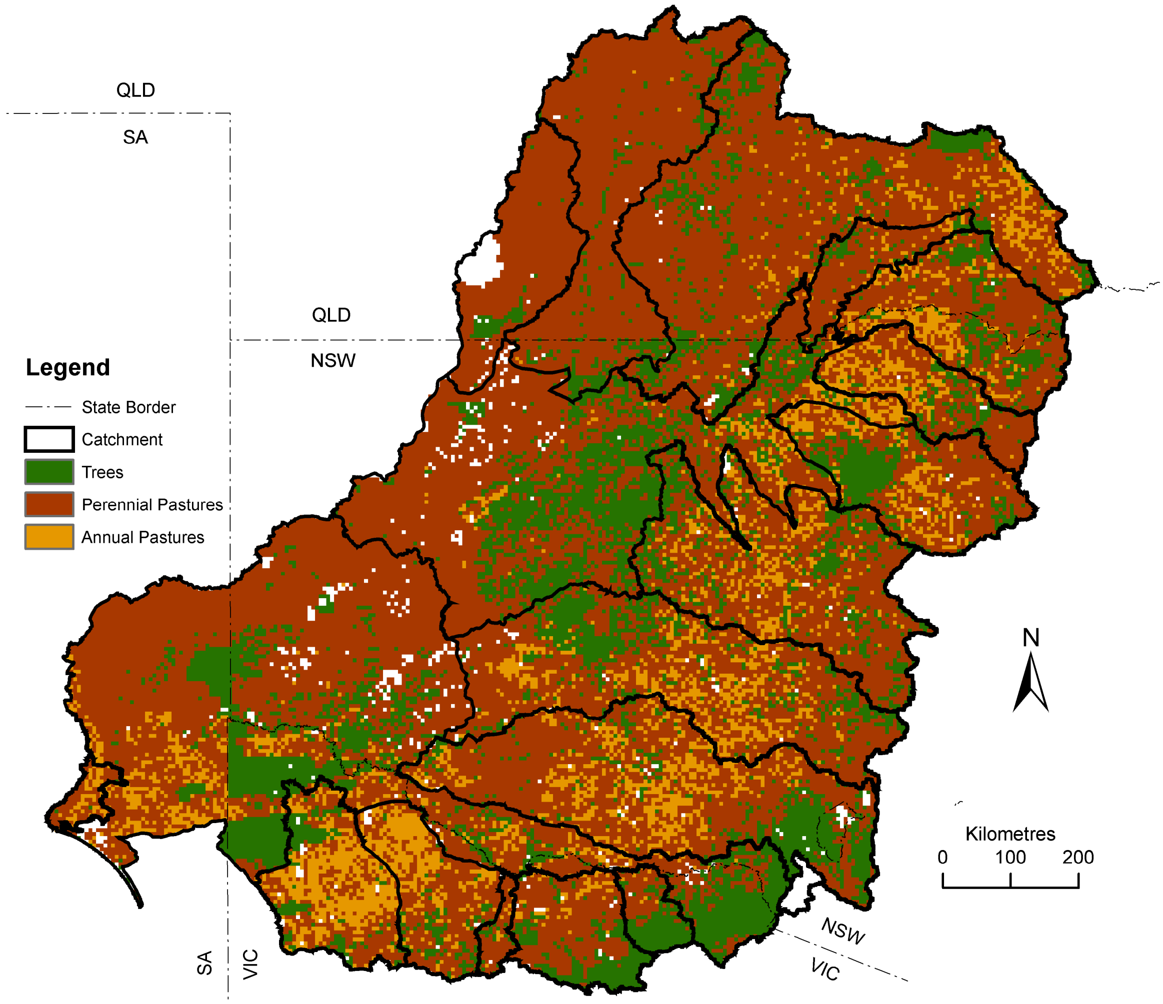

Figure 3-2. Simplified vegetation map of the Murray-Darling Basin

3.2 Upscaling

The output from the WAVES modelling was used to calculate a recharge scaling factor (RSF) for each model run under scenarios B and C. The RSF is defined as the ratio of the average annual recharge under the scenario under investigation (R_S) divided by the average annual recharge under Scenario A (R_A):

$$RSF = \frac{R_S}{R_A} \tag{7}$$

For the upscaling the RSFs were grouped by scenario (46), land use (3) and soil type (8). This gave 1104 groups each with 20 estimates of RSF, one from each of the 20 chosen locations throughout the MDB. A linear regression model was fitted for each group. RSF is estimated as $R\hat{S}F$ from the ratio of the annual average rainfall under the scenario under investigation (P_s) and the annual average historical rainfall (P_A) where a and b are fitting parameters:

$$R\hat{S}F = a\frac{P_S}{P_A} + b \tag{8}$$

Each linear regression model was assessed as to whether the parameters were statistically significant (P<0.1). If the slope parameter was not significant then the model was reduced to a single parameter model and the average RSF was applied as a constant for that combination of scenario, soil type and land use.

Together with the soil type raster and the land use raster, the known values of P_S and P_A on a ~5 km grid across the MDB enables the set of regression equations to be used to calculate $R\hat{S}F$ as a raster with a ~5 km pixel size for each scenario.

In a similar way to the RSF upscaling, a raster was created of the annual average recharge under Scenario A for use in the aggregation of results to the catchment and GMU level (see Section 3.3). A linear regression model was used for each combination of soil type and land use to estimate recharge as $\hat{R}_A$ from known values of average annual rainfall (P_A):

$$\ln(\hat{R}_A) = a * \ln(P_A) + b \tag{9}$$

The output from the upscaling procedure is:

- Scenario A – 1 R raster
- Scenario B – 1 RSF raster
- Scenario C – 45 RSF rasters.

3.3 Aggregation

The 45 different C Scenarios are used to investigate the differences between GCMs and their predictions of how the future climate will impact upon groundwater recharge. For further detailed groundwater modelling of the GMUs only three C Scenarios were modelled:

- 10th percentile of CH scenario (Cwet)
- 90th percentile of CH scenario (Cdry)
- 50th percentile of CM scenario (Cmid).

Scenario Cmid represents the 'best estimate' of climate change in this project. It is the median response of the GCMs under the medium global warming scenario. The greatest variability in estimates of recharge change come from the high global warming scenario. Therefore Scenario Cwet comes from the 10th percentile of the high global warming scenario and Scenario Cdry scenario comes from the 90th percentile of the high global warming scenario.

For internal consistency in the project, the same GCMs were used for scenarios Cwet, Cdry and Cmid for the catchment yield and groundwater recharge. The selection process is detailed in Chiew et al. (2008a). As different GCMs were ranked differently in each catchment, rasters were created for scenarios Cwet, Cdry and Cmid by stitching together the scenarios selected in each catchment.

The average RSFs were reported by region, GMU and groundwater model recharge region. The calculated recharge varied greatly depending upon soil type and land use but could give very similar RSFs. A weighted average was used in calculating average RSFs over an area to bias the average towards the pixels that had higher recharge ($\hat{R}_A$):

$$\overline{RSF}_{S,R} = \frac{\sum_{i=1}^{n} \hat{R}_{A,i} . R\hat{S}F_{S,i}}{\sum_{i=1}^{n} \hat{R}_{A,i}} \qquad (10)$$

where $\overline{RSF}_{S,R}$ is the average RSF for Scenario S and Region R and *n* is the number of pixels in R.

The outcomes of this section are:

- RSF rasters (3 for Scenario C)
- table of average RSF by catchment (1 for Scenario B, 3 for Scenario C)
- table of average RSF by GMU (1 for Scenario B, 3 for Scenario C)
- table of average RSF by region (1 for Scenario B, 3 for Scenario C).

4 Results

4.1 Point scale modelling

WAVES was run a total of 22,560 times with an approximate run time of 1.5 minutes. This equates to 26 days of computing time on a PC but utilising a more powerful computer this task was completed in less than four days. For each model run undertaken, WAVES produced water balance outputs that detailed the processes occurring in the modelled soil profiles. Each model run produced over 70 MB of output resulting in 1.6 TB of output in total.

Of the total WAVES model runs, 88% ran successfully to completion. The results from the 12% that did not run successfully were filtered out and removed from further consideration. The missing results had some impact upon the upscaling where there were less than 20 results available for generating the regression equations (see Section 4.2). The minimum number of points in any regression equation was eight, and this was deemed acceptable.

An example of the model outputs for the rainfall and recharge in the Ovens region for perennial pastures on a Sodosol soil is shown in Figure 4-1. This shows 100 mm of recharge from 38,000 mm of rainfall in a 112-year period.

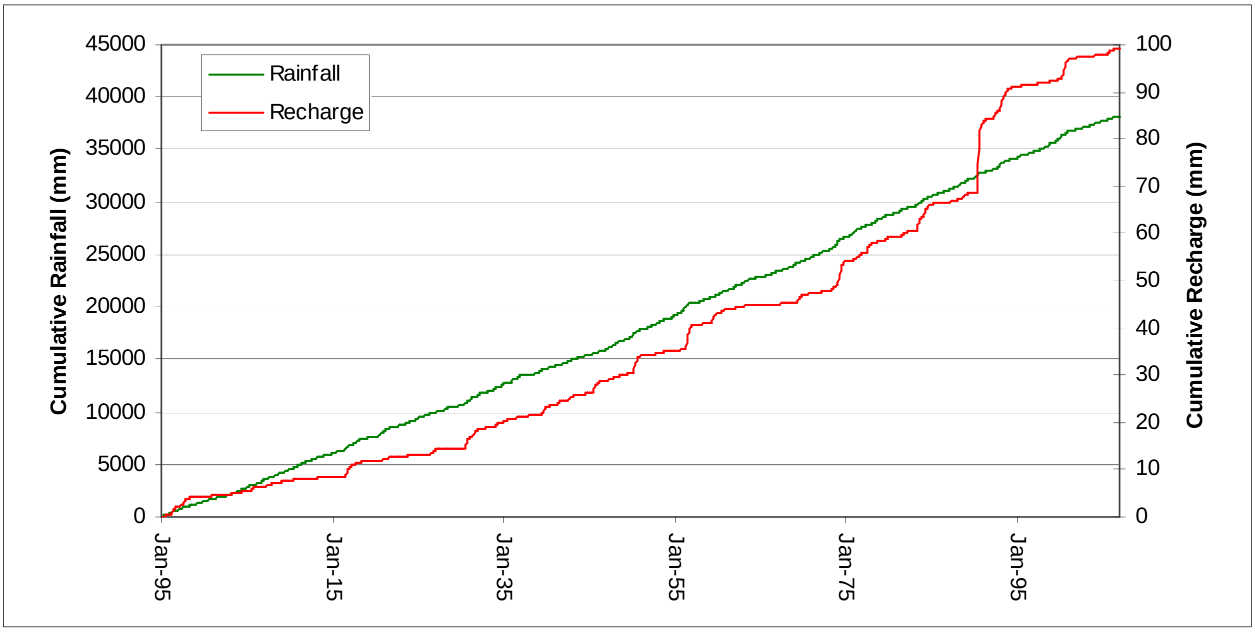

Figure 4-1. An example of WAVES model output for vegetation type C3PP on Sodosol soils in the Ovens region

4.2 Upscaling

To determine the change in recharge occurring across the MDB, the modelling undertaken at 20 points across the MDB was upscaled to basin level. The first step of the upscaling process involved creating a baseline recharge map of the MDB. Due to the assumption of no slope in the WAVES modelling, the unsaturated lateral flow and runoff were under estimated leading to recharge being over estimated. Regressions were undertaken as described in the methodology (Equation) to determine relationships between rainfall and recharge for each combination of soil and vegetation.

Examples of a good and moderate fitting regression between rainfall and recharge can be seen in Figure 4-2, with regression parameters presented in Table 4-1. It was found that for all relationships, the slope of the rainfall-recharge relationship was significant and regression equations could be used in upscaling.

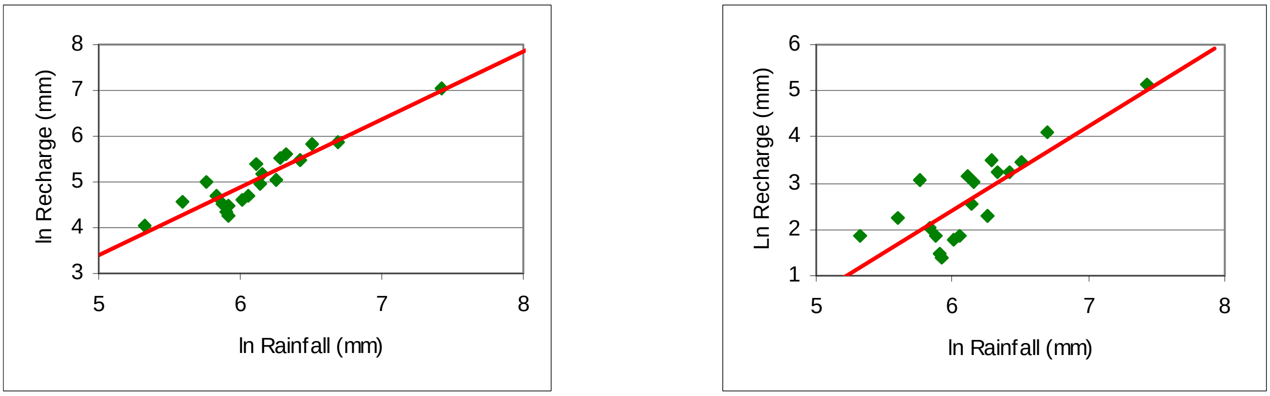

Figure 4-2. Modelled data points and a regression fit line for baseline recharge scaling, for vegetation type C3AP on Calcarosol soils (left) and for vegetation type C3PP on Kandosol soils (right).

Table 4-1. Parameters obtained from the regressions presented in Figure 4-2

Soil type	Vegetation type	Calculated		r^2	P value
		Slope	Intercept		
Calcarosols	C3AP	1.48	-4.04	0.86	0.00
Kandosols	C3PP	1.83	-8.55	0.66	0.00

Once the relationships had been determined, baseline recharge was scaled across the MDB using maps of soil, vegetation and average annual rainfall. The resulting map of average annual recharge is presented in Figure 4-3. Although the results of the recharge map look plausible they cannot be relied upon because no attempt has been made at validating the results. The scope of this work has been investigating the change in recharge, not attempting to estimate recharge itself.

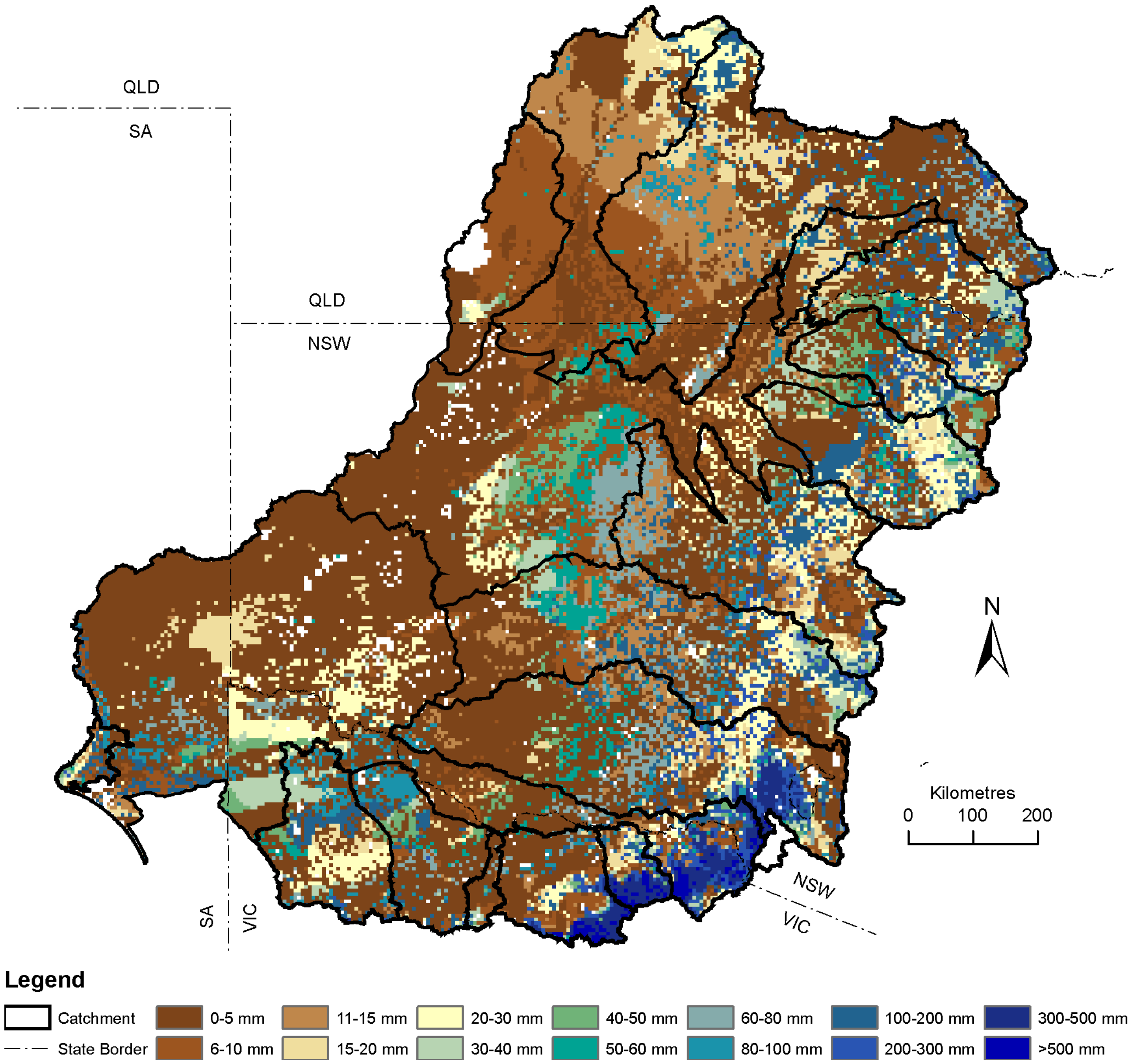

Figure 4-3. Modelled annual average (1895 to 2006) dryland diffuse recharge in the Murray-Darling Basin (Note: recharge is likely to be over estimated in parts of this figure due to lack of consideration of runoff-producing mechanisms.)

To determine the change in recharge occurring under each scenario, the point scale measurements of recharge obtained from the 22,560 model runs were used to create linear regressions (Equation). The linear regressions were undertaken for each scenario using the change in rainfall under Scenario A and change in recharge under Scenario A using data modelled at 20 points. The regressions were undertaken for each unique combination of soil type and vegetation type. Regressions were assessed based on the criteria specified in the methodology.

Examples of regressions that did and did not meet the criteria are presented in Figure 4-4. Table 4-2 presents the parameters obtained from each regression, and the values used in upscaling. The full list of regression equations is presented as an appendix (*Appendix II – Regression equations used in upscaling*). Of all the regressions undertaken, 60% were found to have a slope significantly different from zero (P<0.1) and could be applied for upscaling as linear models. The other 40% did not have a significant slope and used an average of the RSFs for that particular combination of scenario, soil type and veg type. When looking closer at which regressions failed to be statistically significant it was found that the annual pastures had 93% of combinations successful whereas the perennial pastures only had 31% successful. Further investigations of the perennial pastures revealed that the soils with higher conductivities had slightly higher success rates (36% for Kandosols versus 31% for Sodosols).

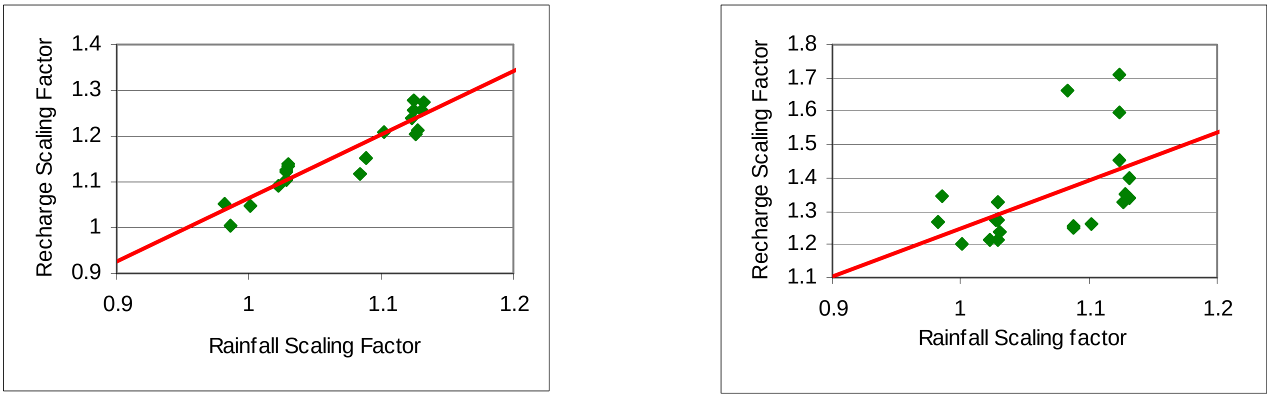

Figure 4-4. Modelled data points and a regression fit line for recharge scaling factor scaling for vegetation type C3AP on Calcarosol soils (left) and for vegetation type C3PP on Kandosol soils, using the high global warming global climate model cccma t47

Table 4-2. Parameters obtained from the regressions presented in Figure 4-4

Soil type	Vegetation type	Calculated		r^2	P value	Adopted for upscaling	
		Slope	Intercept			Slope	Intercept
Calcarosols	C3AP	1.38	-0.32	0.86	0.01	1.38	-0.32
Kandosols	C3PP	1.44	-0.19	0.27	0.12	0.00	1.35

The Podosols as a soil group presented a unique case in the upscaling. The subsoil conductivity was extremely low (Table 3-3) and so there was no recharge calculated under Scenario A by WAVES. Dividing by zero in Equation results in an undefined result and the scaling method fails. To overcome this, the RSF for all scenarios and vegetation types on Podosol soils were set to 1.

Once relationships had been determined for scaling factors at point scales, they were used in conjunction with rasters of rainfall scaling factors, soils and vegetation to determine the recharge scaling factors across the MDB. Where regression criteria were met, the RSF was determined as a linear function of rainfall scaling factor (Equation). Where regression criteria were not met, the RSF was determined to be the average RSF of the 20 point scale measurements. The upscaled RSF map under Scenario B is presented in Figure 4-5, and a map containing the observed annual average rainfall in the period 1997 to 2006 as a proportion of the average annual rainfall from 1895 to 2006 is presented in Figure 4-6 for comparison. The 45 RSF maps under Scenario C are presented in Appendix III.

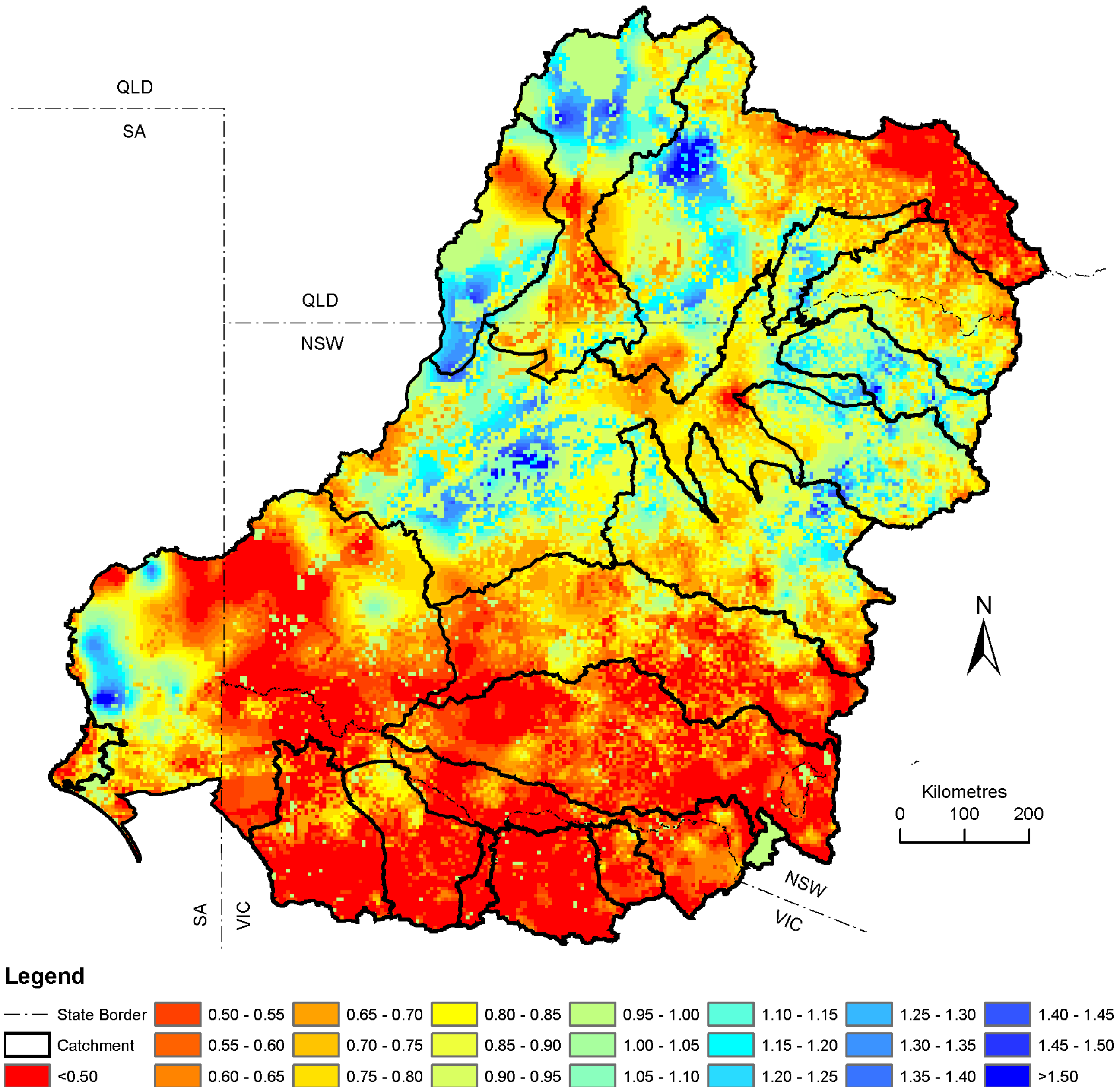

Figure 4-5. Upscaled recharge scaling factors for the Murray-Darling Basin under Scenario B

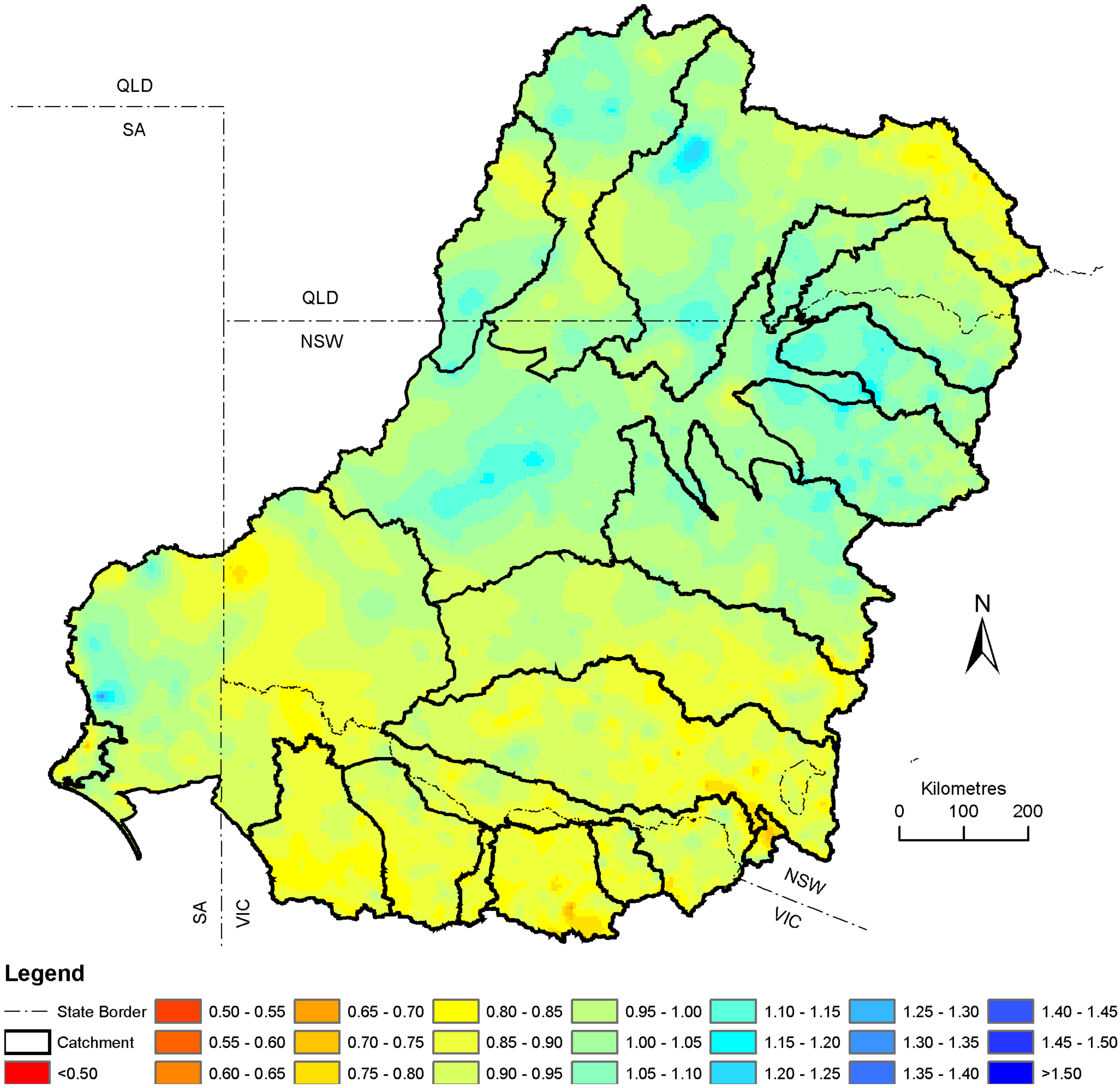

Figure 4-6. Observed annual average rainfall in the period 1997 to 2006 as a proportion of the average annual rainfall in the period 1895 to 2006

.

4.3 Aggregation

Once baseline recharge (Figure 4-3) and scaling factors had been upscaled to the whole MDB, average RSFs were determined at the region level. This was undertaken for Scenario B and 45 C scenarios. The Scenario C results are presented in Appendix IV.

Three variants were chosen from the 45 C scenarios: a wet, mid and dry scenario. The 'mid' scenario was assessed as being the 'best estimate' of climate change upon recharge, the 'wet' scenario was assessed as being at the extreme end of projections for a wetter climate, and the 'dry' scenario was assessed as being at the extreme end of projections for a drier climate. These were selected based on the 10th percentile of the high global warming scenario, the 50th percentile of the medium global warming scenario, and the 90th percentile of the high global warming scenario for mean annual runoff at a region level as described in Chiew et al. (2008b). There were some differences in the selected GCMs for the individual catchments as can be seen in Appendix IV. The RSF values for scenarios B and C are presented in Table 4-3.

Table 4-3. Recharge scaling factors for each region, with rainfall scaling factors (RaSF) shown for comparison

Region	Scenario B		Scenario C					
			Scenario Cdry		Scenario Cmid		Scenario Cwet	
	RaSF	RSF	RaSF	RSF	RaSF	RSF	RaSF	RSF
Warrego	101%	107%	92%	88%	96%	99%	111%	141%
Condamine-Balonne	98%	98%	91%	95%	97%	94%	110%	128%
Paroo	100%	102%	93%	91%	96%	100%	113%	155%
Moonie	103%	109%	91%	85%	94%	91%	109%	127%
Border Rivers	100%	102%	90%	94%	100%	99%	109%	128%
Barwon-Darling	103%	113%	87%	86%	97%	93%	114%	129%
Gwydir	107%	122%	90%	94%	100%	101%	111%	132%
Namoi	105%	114%	90%	93%	98%	101%	113%	133%
Macquarie-Castlereagh	101%	103%	87%	87%	98%	97%	112%	135%
Murray	92%	81%	81%	69%	97%	97%	108%	108%
Lachlan	92%	83%	82%	66%	96%	98%	107%	121%
Murrumbidgee	89%	73%	81%	70%	98%	96%	106%	115%
Eastern Mt Lofty Ranges	93%	83%	81%	64%	95%	95%	101%	113%
Wimmera	87%	72%	80%	63%	94%	97%	100%	110%
Loddon-Avoca	89%	78%	80%	64%	96%	98%	103%	110%
Ovens	89%	78%	82%	78%	96%	93%	103%	104%
Goulburn-Broken	85%	64%	82%	78%	96%	94%	100%	106%
Campaspe	87%	63%	82%	80%	96%	96%	100%	114%

Composite C scenario RSF rasters were created for the wet, mid and dry scenarios. These rasters were created using the climate scenario specific to each region. This was necessary as some model boundaries and GMU boundaries crossed multiple regions. The composite maps are presented in Figure 4-7 for Scenario Cdry, Figure 4-8 for Scenario Cmid and Figure 4-9 for Scenario Cwet.

Under Scenario Cdry all of the regions of the MDB are predicted to have less recharge (Table 4-3), with the greatest reductions being those regions that flow to the Murray with less severe reductions in the regions that flow to the Darling (Figure 4-7). However, recharge reduction is more severe under Scenario B compared to Scenario Cdry (Figure 4-5). Under Scenario B, the previous ten years produced less recharge than that predicted by the climate change scenarios of 2030. The apparent discrepancy between the numbers in Table 4-3 and the colours in Figure 4-5 and Figure 4-7 is due to the way the weighted averages are calculated in Table 4-3 (Equation). As the average is weighted by the recharge under Scenario A (Figure 4-3), a pixel in a high recharge area may have 1000 times more influence over the average as a pixel in a low recharge area.

Under Scenario Cmid little change in recharge over the MDB as a whole is observed (Figure 4-8) with a slight decrease in most regions (Table 4-3). The modelling has predicted an increase in recharge for the western part of the Murray region.

Under Scenario Cwet the entire MDB is predicted to have an increase in recharge (Table 4-3). This is particularly so for the regions that flow to the Darling (Figure 4-9).

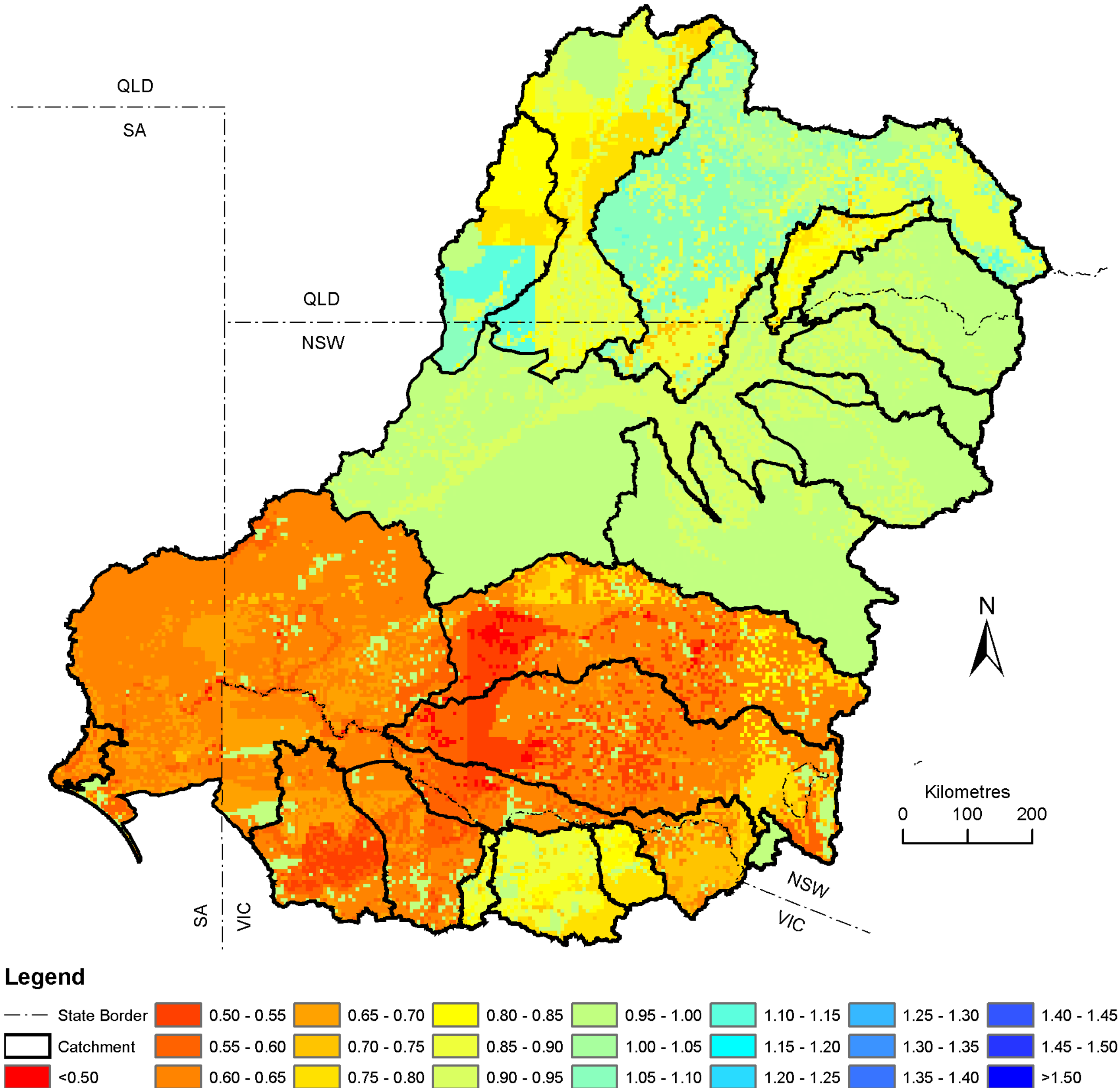

Figure 4-7. Recharge scaling factors for the Murray-Darling Basin under Scenario Cdry

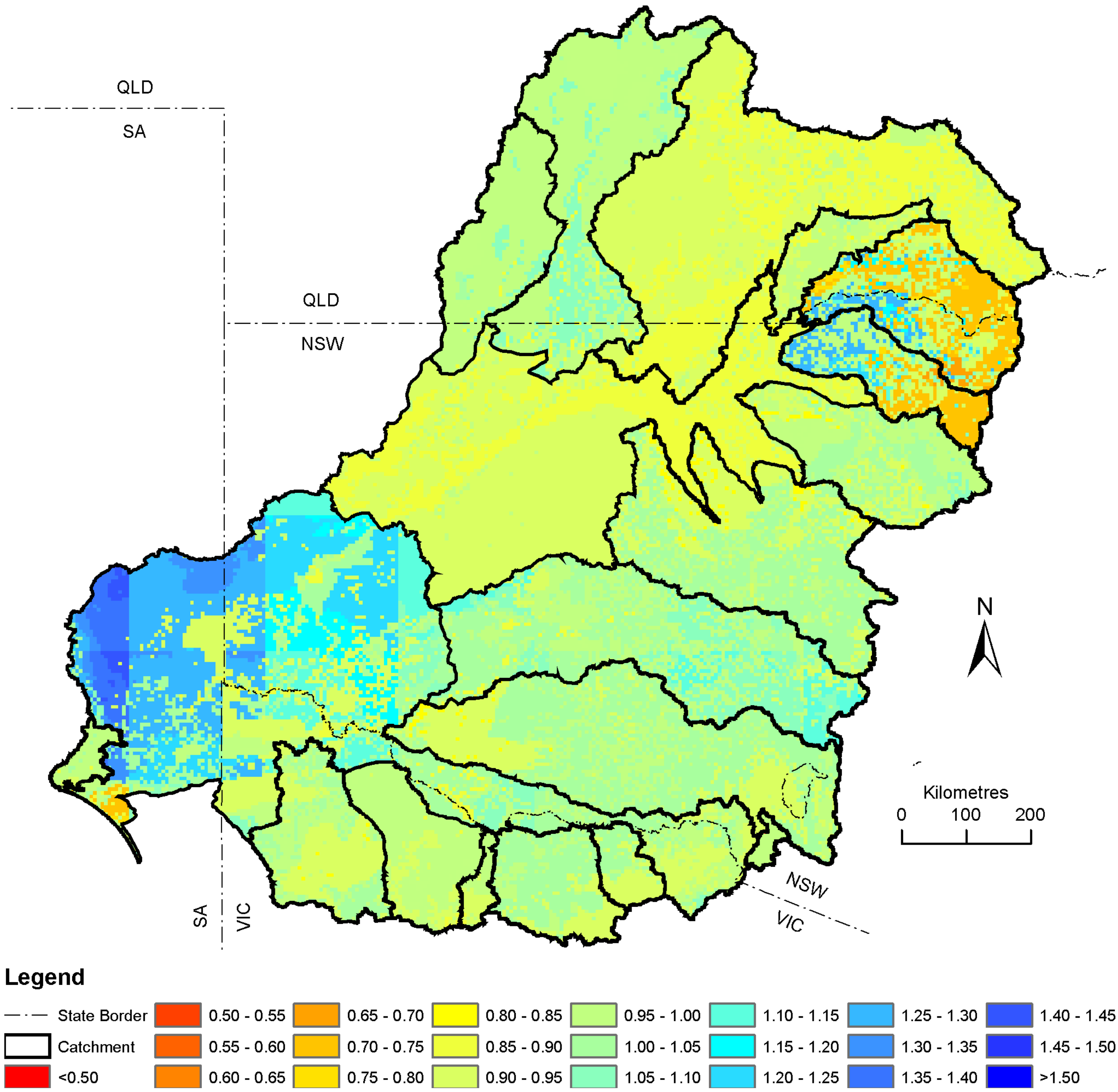

Figure 4-8. Recharge scaling factors for the Murray-Darling Basin under Scenario Cmid

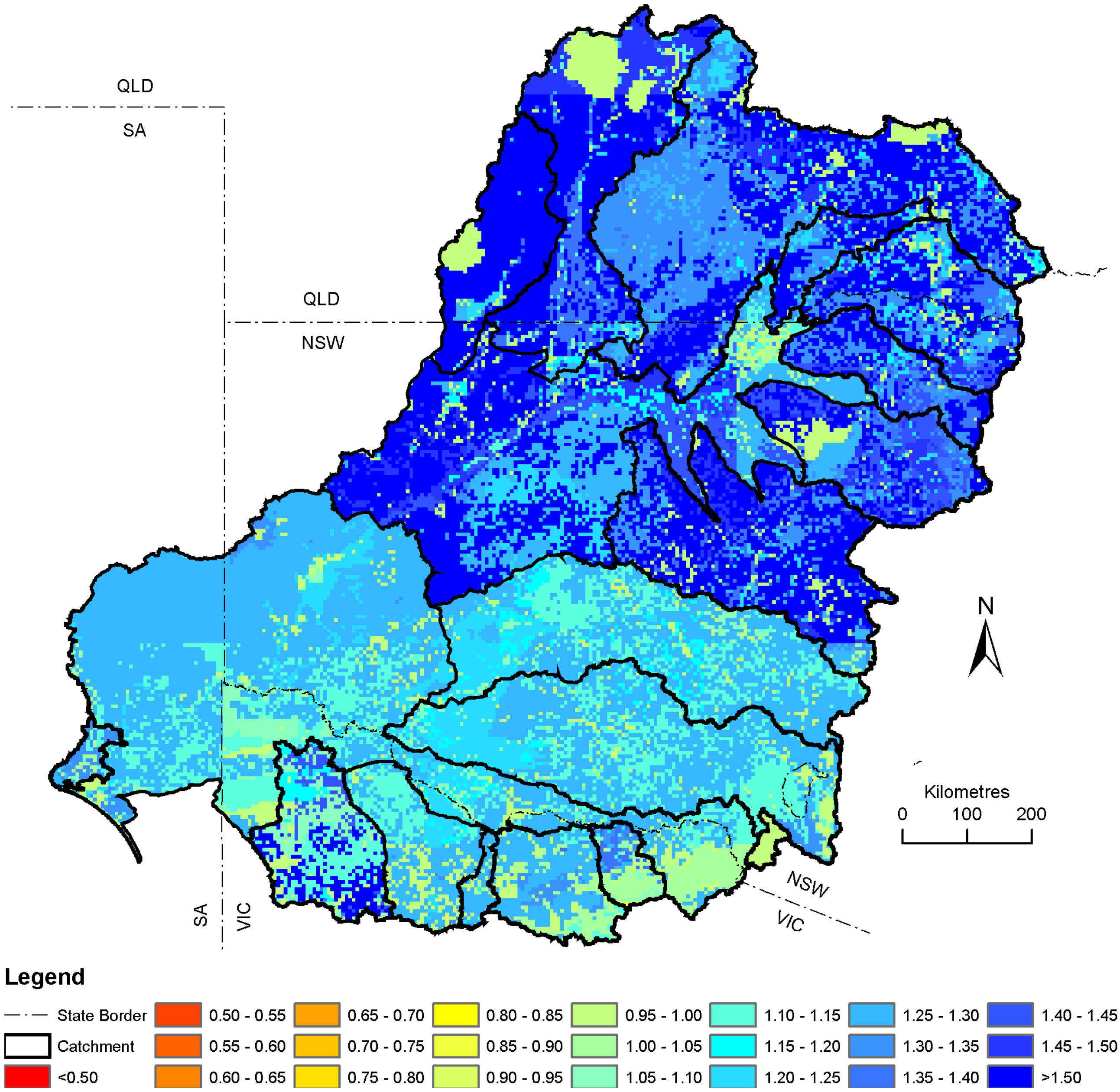

Figure 4-9. Recharge scaling factors for the Murray-Darling Basin under Scenario Cwet

Once the C scenario maps were produced, RSFs for GMUs and model domains were determined, as presented in Appendix V. These results are highly variable with little consistency between GCMs. This is especially evident in that the scenarios Cwet and Cdry come from the same emission scenario (CH) from different GCMs.

Under Scenario B, recharge was reduced on average by 13%. The greatest decrease in recharge under Scenario B was observed in the Toowoomba City Basalt GMU in the Condamine-Balonne region, with a 60% decrease in recharge. The greatest increase in recharge under Scenario B was observed in both the Lower Gwydir Alluvium GMU in the Gwydir Catchment and Gulargambone Tertiary Basalt GMU, with an increase of 25%.

Under Scenario Cdry, recharge was reduced on average by 16%. The greatest decrease in recharge under Scenario Cdry was observed in the Lower Murrumbidgee Alluvium GMU in the Murrumbidgee catchment, with a 44% decrease in recharge. The greatest increase in recharge under Scenario Cdry was observed in the Toowoomba City Basalt GMU in the Condamine-Balonne region with an increase of 8%.

Under Scenario Cmid, recharge was reduced on average by 2%. The greatest decrease in recharge under Scenario Cmid was observed in the Swan Creek Alluvium GMU in the Condamine-Balonne region, with a 10% decrease in recharge. The greatest increase in recharge under Scenario Cmid was observed in the Lower Gwydir Alluvium GMU in the Gwydir region with an increase of 22%.

Under Scenario Cwet, recharge was increased on average by 26%. The only decrease in recharge under Scenario Cwet was observed in the Spring Hill WSPA GMU in the Loddon-Avoca region, with a 1% decrease in recharge. The greatest increase in recharge under Scenario Cwet was observed in the Cudgegong Valley Alluvium GMU in the Macquarie-Castlereagh region with an increase of 73%.

5 Discussion

5.1 Guidance on interpreting results

There is a great deal of uncertainty when predicting the impact of climate change upon groundwater recharge in the MDB. The first source of uncertainty is in climate change itself; this has been addressed through modelling three global warming scenarios – high, medium and low. The second source of uncertainty is in the impact of increased global temperatures upon climate; this has been addressed through the use of 15 different GCMs. The third source of uncertainty is in our ability to determine groundwater recharge; this has been addressed by not estimating recharge directly but by estimating the change in recharge.

The approach taken by this project for reporting this uncertainty is to report on the best estimate of the impact of climate change upon recharge and then to present bounds on this estimate representing the likely extremes in a wet future climate and a dry future climate. This report concludes that the recharge for a future climate in ~2030 will be within the bounds set by scenarios Cwet and Cdry and that the best estimate of the recharge is obtained from Scenario Cmid.

5.2 Sensitivity analysis

Some sensitivity analysis was performed on assumptions used in this work:

- The upscaling procedure was examined by testing the RSF calculated from the output from WAVES at a point against the upscaled estimate of RSF based on the change in rainfall and using soil and vegetation type as covariates.
- An alternate upscaling methodology was tested.
- An alternate definition for Scenario B was tested.

5.2.1 Appropriateness of upscaling methodology

To test the validity of the upscaling methods used in modelling, including the use of bulk soil parameters, RSFs obtained using point data from the 20 points across the MDB under scenarios B and C were compared to the upscaled RSFs for the points. A comparison of upscaled and point data can be seen in Figure 5-1. Whilst there is significant scatter, the slope is close to 1 indicating that upscaling is appropriate.

The scatter means that an individual pixel in an RSF raster may deviate from the correct value had it been modelled in WAVES. The overall slope of the line with a gradient of 1 means that the upscaling model is a good fit on average. The implication is that where small groups of pixels are aggregated, such as in small GMUs, there is the opportunity for erroneous results to be reported. As the number of pixels that are used in the aggregation increases, so does the certainty in the result.

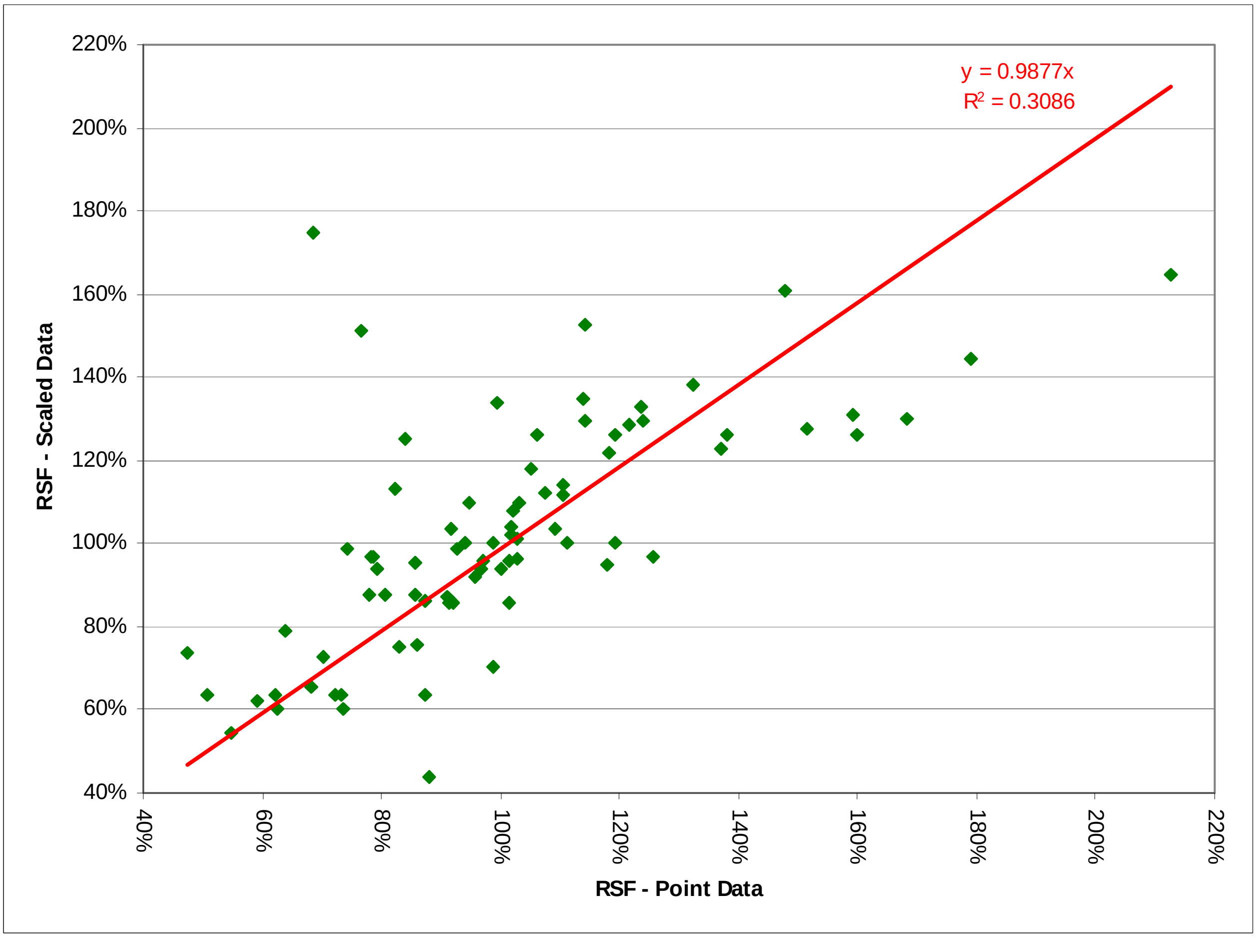

Figure 5-1. Recharge scaling factors obtained from upscaling plotted against those obtained from point data

5.2.2 Alternate upscaling methodology

The original methodology used for the upscaling was based upon predicting the RSF from the ratio of rainfall in the scenario (P_S) and the historical rainfall (P_a) (Equation). An alternative method of upscaling RSF is by estimating the recharge ($\hat{R}$) from a linear regression with P:

$$R\hat{S}F = \frac{\hat{R}_B}{\hat{R}_A} = \frac{a_S P_S + b_S}{a_A P_A + b_A} \qquad (11)$$

where *a* and *b* are fitting parameters.

Three examples have been used to evaluate the difference between the two methodologies. The three examples are under Scenario B: annual pastures on Calcarosols; trees on Ferrosols; and perennial pastures on Vertosols.

In all three cases the original methodology produced superior results as seen by plotting the observed RSF against the estimated $R\hat{S}F$ (Figure 5-2, Figure 5-3 and Figure 5-4). A perfect scaling method would have an r^2 of 1 and a regression line of y=x.

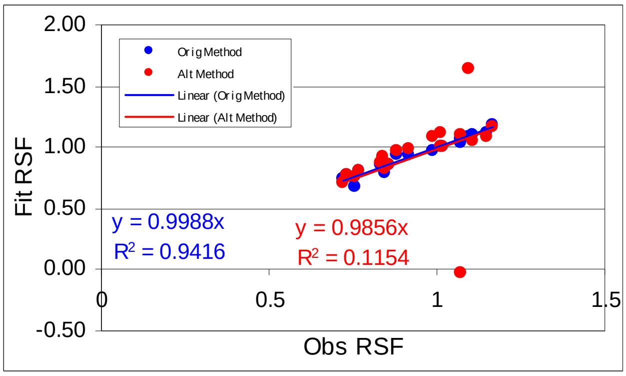

Figure 5-2. A comparison of the original and alternate upscaling methodologies for annual pastures on Calcarosol soils under Scenario B. The fitted recharge scaling factor is plotted against the observed recharge scaling factor and a regression line is fitted to the data points. The slope and r^2 of the regression line determine the goodness of fit

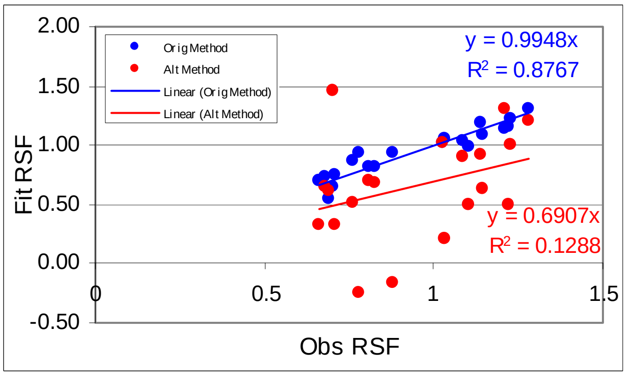

Figure 5-3. A comparison of the original and alternate upscaling methodologies for trees on Ferrosol soils under Scenario B. The fitted recharge scaling factor is plotted against the observed recharge scaling factor and a regression line is fitted to the data points. The slope and r^2 of the regression line determine the goodness of fit

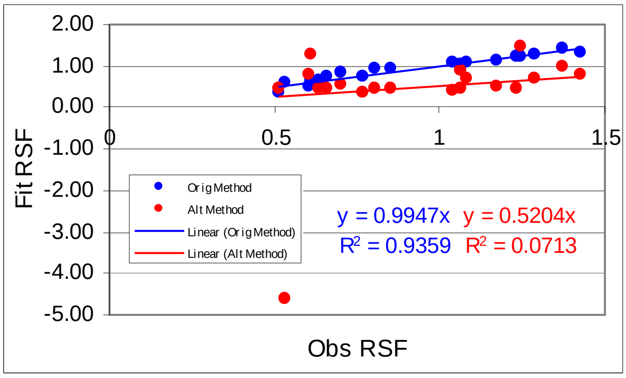

Figure 5-4. A comparison of the original and alternate upscaling methodologies for perennial pastures on Vertosol soils under Scenario B. The fitted recharge scaling factor is plotted against the observed recharge scaling factor and a regression line is fitted to the data points. The slope and r^2 of the regression line determine the goodness of fit

5.2.3 Alternate definition for Scenario B

The original Scenario B consists of the historical (1895 to 2006) climate sequence scaled for the averages of the past ten years to create a climate sequence intended to simulate the scenario where the climate of the past ten years is the new normal. The alternative to scaling the historical sequence is to just use the past ten years' climate sequence as Scenario

B. The difference between these two alternate definitions for Scenario B are shown in Table 5-1 for RSFs averaged over each region. The alternate RSF with only ten years of data is smaller in every case.

Table 5-1. Comparison between recharge scaling factors calculated for each region for the original and alternate definition of Scenario B

Catchment	Original RSF	Alternate RSF
Warrego	107%	96%
Condamine-Balonne	98%	82%
Paroo	103%	94%
Moonie	109%	94%
Border Rivers	102%	85%
Barwon-Darling	113%	93%
Gwydir	122%	106%
Namoi	114%	97%
Macquarie-Castlereagh	103%	89%
Murray	81%	60%
Lachlan	83%	70%
Murrumbidgee	73%	54%
Eastern Mt Lofty Ranges	83%	76%
Wimmera	72%	58%
Loddon-Avoca	78%	67%
Ovens	78%	53%
Goulburn-Broken	64%	41%
Campaspe	63%	42%

5.3 Episodic recharge events

For some catchments in the MDB, a disproportionately large change in recharge was observed for a relatively small or no change in rainfall. This may be explained by episodic recharge. Episodic recharge is a term used to describe infrequent or irregular pulses of recharge to groundwater (Lewis, 2000). Figure 5-5 presents relationships between rainfall and recharge on a clayey soil for perennial and annual pastures. For annual pastures, there is strong correlation between an increase in rainfall and an increase in recharge. For perennial pastures, however, recharge is not as strongly related to rainfall, with constant increases interrupted by large steps. This would suggest that episodic recharge is occurring on such combinations of vegetation and soils.

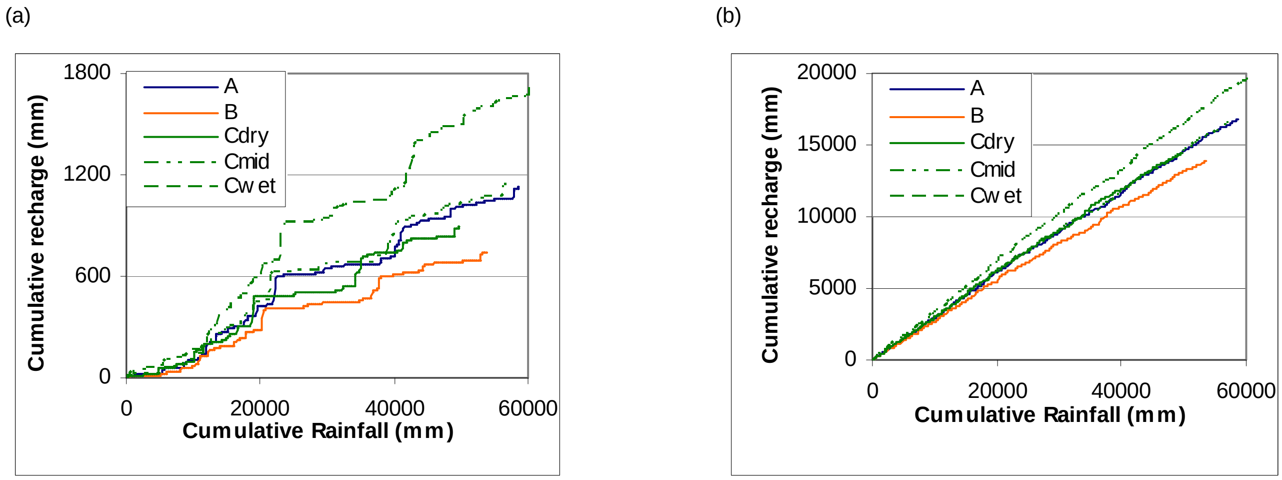

Figure 5-5. Double mass plots of rainfall and recharge for Tenosol soils in the Ovens regions under scenarios A, B and C with (a) perennial pastures and (b) annual pastures

If large percentages of a time series of recharge are occurring in a small percentage of events, then small changes in the water balance during these events may become significant. Given the relative equivalent depths of rainfall and recharge in some areas in such environments (rainfall is much greater than recharge), and the threshold process of recharge, a small increase in rainfall may translate to a significant increase in recharge.

Episodic recharge also played a role in the scaling of recharge. Of the 382 C scenario regression equations that did not have a significant slope, 57% were perennial pastures, 38% were trees and only 6% were annual pastures. This is consistent with the correlation between rainfall and recharge associated with each vegetation type.

6 Conclusions

This report has provided a methodology for estimating the change in dryland diffuse recharge under different climate scenarios. This methodology was used to estimate the impact of climate change on groundwater recharge in the MDB.

The results generally followed the IPCC general predictions for Australia with less rainfall in the south producing less recharge and little change in the rainfall in the north producing little change in the recharge. However, there were considerable inconsistencies between GCMs where for the same climate scenario different GCMs could produce recharge estimates that were as different as a plus or minus 50% change in recharge. This uncertainty has highlighted the value in undertaking such a rigorous investigation with so many scenarios.

Under Scenario B, the modelling predicts that recharge decreases by up to 50% in the southern parts of the MDB and in the Condamine, while in the remainder of the northern parts of the MDB recharge increases by up to 20%. Under Scenario Cdry, recharge reduces in all parts of the MDB though not as extremely as under Scenario B. Under Scenario Cmid, little change in recharge is observed throughout the MDB with small decreases in the south and small increases in the north. Under Scenario Cwet, recharge increases in all regions of the MDB with up to a 50% increase in the north and down to a 5% increase in the south.

7 References

ABS (2003) Year Book Australia 2003, Australian Bureau of Statistics, Canberra.

Allen DM, Mackie DC, Wei M (2004) Groundwater and climate change: a sensitivity analysis for the Grand Forks aquifer, southern British Columbia, Canada. Hydrogeol. J., 12(3): 270-290.

Beverly C, Bari M, Christy B, Hocking M, Smettem K (2005) Predicted salinity impacts from land use change: comparison between rapid assessment approaches and a detailed modelling framework. Aust. J. Exp. Agric, 45(11): 17.

Broadbridge P, White I (1998) Constant rate rainfall infiltration: A versatile non-linear model: I. Analytical solution. Water Resour. Res., 24: 145-154.

Brunner P, Bauer P, Eugster M, Kinzelbach W (2004) Using remote sensing to regionalize local precipitation recharge rates obtained from the Chloride Method. J. Hydrol., 294(4): 241-250.

Chiew FHS, Teng J, Kirono D, Frost A, Bathols J, Vaze J, Viney N, Hennessy KJ, Cai W (2008a) Climate data for hydrologic scenario modelling across the Murray-Darling Basin. A report to the Australian government from CSIRO Murray-darling Basin Sustainable Yields Project, CSIRO, Australia, In Prep.

Chiew FHS, Vaze J, Viney NR, Jordan PW, Perraud J-M, Zhang L, Teng J, Young WJ, Pena Arancibia J, Morden RA, Freebairn A, Austin J, Hill PI, Wiesenfeld CR and Murphy R (2008b) Rainfall-runoff modelling across the Murray-Darling Basin. A report to the Australian Government from the CSIRO Murray-Darling Basin Sustainable Yields Project. CSIRO, Australia.

Christensen JH, Hewitson B, Busuloc A, Chen A, Gao X, Held I, Jones R, Kolli RK, Kwon WT, Laprise R, Magana Rueda V, Mearns L, Menendez CG, Ralsanen J, Rinke A, Sarr A, Whetton P (2007) Regional Climate Projections. In: S. Solomon et al. (Editors), Climate Change 2007: The Physical Science Basis. Contribution of Working Group I to the Fourth Assessment Report of the Intergovernmental Panel on Climate Change. Cambridge University Press, Cambridge.

Cook PG, Walker GR, Jolly ID (1989) Spatial Variability of Groundwater Recharge in a Semiarid Region. J. Hydrol., 111: 195-212.

CSIRO and BOM (2007) Climate change in Australia, CSIRO and BOM.

Dawes W, Zhang L, Dyce P (2004) WAVES v3.5 User Manual, CSIRO Land and Water, Canberra.

DFA (1974) Agreement between the Government of Australia and the Government of Japan for the Protection of Migratory Birds in Danger of Extinction and their Environment. Australian Treaty Series 1981 No. 6, Department of Foreign Affairs, Canberra.

DFAT (1986) Agreement between the Government of Australia and the Government of the People's Republic of China for the Protection of Migratory Birds and their Environment. Australian Treaty Series 1988 No. 22, Department of Foreign Affairs and Trade, Canberra.

Eckhardt K, Ulbrich U (2003) Potential impacts of climate change on groundwater recharge and streamflow in a central European low mountain range. J. Hydrol., 284(1-4): 244-252.

Hatton TJ, Walker J, Dawes WR, Dunin FX (1992) Simulations of Hydroecological Responses to Elevated CO_2 at the Catchment Scale. Aust. J. Bot., 40: 679-696.

Hsu KC, Wang CH, Chen KC, Chen CT, Ma KW (2007) Climate-induced hydrological impacts on the groundwater system of the Pingtung Plain, Taiwan. Hydrogeol. J., 15(5): 903-913.

IPCC (2001) IPCC Third Assessment Report - Climate Change 2001: The Scientific Basis. Cambridge University Press, Cambridge, UK.

IPCC (2007) Climate Change 2007: The Physical Science Basis. Contribution of Working Group 1 to the Fourth Assessment Report of the Intergovernmental Panel on Climate Change. Cambridge University Press, Cambridge UK, 996 pp.

Isbell RF (2002) Australian Soils Classification. CSIRO, Collingwood, Victoria, 144 pp.

Jeffrey SJ, Carter JO, Moodie KB, Beswick AR (2001) Using spatial interpolation to construct a comprehensive archive of Australian climate data. Environ. Modell. Softw., 16(4): 309-330.

Johnston RM, Barry SJ, Bleys E, Bui EN, Moran CJ, Simon DAP, Carlile P, McKenzie NJ, Henderson BL, Chapman G, Imhoff M, Maschmedt D, Howe D, Grose C, Schoknecht N, Powell B, Grundy M (2003) ASRIS: the database. Aust. J. Soil Res, 41(6): 1021-1036.

Jyrkama MI, Sykes JF (2007) The impact of climate change on spatially varying groundwater recharge in the grand river watershed (Ontario). J. Hydrol., 338(3-4): 237-250.

Kirshen PH (2002) Potential Impacts of Global Warming on Groundwater in Eastern Massachusetts. Journal of Water Resources Planning and Management, 128(3): 216-226.

Lewis MF (2000) Episodic recharge in the western Australian wheatbelt. PhD Thesis, University of Melbourne, Melbourne.

Littleboy M, Herron N, Barnett P (2003) Applying unsaturated zone modelling to develop recharge maps for the Murray-Darling Basin in New South Wales, Australia, MODSIM 2003.

Loáiciga HA, Maidment DR, Valdes JB (2000) Climate-change impacts in a regional karst aquifer, Texas, USA. J. Hydrol., 227(1-4): 173-194.

Nakicenovic N, Swart R (2000) Special Report on Emission Scenarios, Intergovernmental Panel on Climate Change.

Neitsch S, Arnold JG, Kiniry J, Williams J (2000) Soil and water assessment tool theoretical documentation 2000, Grassland, soil and water research laboratory, Agricultural Research Service, Temple, Texas.

Ramsar Convention Bureau (1971) Convention on Wetlands of International Importance especially as Waterfowl Habitat. Ramsar (Iran), 2 February 1971. UN Treaty Series No. 14583. As amended by the Paris Protocol, 3 December 1982, and Regina Amendments, 28 May 1987.

Rosenberg NJ, Epstein DJ, Wang D, Vail L, Srinivasan R, Arnold JG (1999) Possible Impacts of Global Warming on the Hydrology of the Ogallala Aquifer Region. Climatic Change, 42(4): 677-692.

Salama R, Hatton T, Dawes W (1999) Predicting land use impacts on regional scale groundwater recharge and discharge. Journal of Environmental Quality, 28(2): 446-460.

Schroeder PR, Dozier TS, Zappi PA, McEnroe BM, Sjostrom JW, Peyton RL (1994) The hydrologic evaluation of landfill performance (HELP) model: Engineering documentation for version 3., US Environmental Protection Agency, Office of Research and Development, Washington, DC.

Scibek J, Allen DM (2006) Comparing modelled responses of two high-permeability, unconfined aquifers to predicted climate change. Global and Planetary Change, 50(1-2): 50-62.

Sophocleous M (1992) Groundwater recharge estimation and regionalization: the Great Bend Prairie of central Kansas and its recharge statistics. J. Hydrol., 137: 113-140.

Tuteja NK, Vaze J, Teng J (2005) The CLASS Modelling Framework: A platform for distributed eco-hydrological modelling, MODSIM 2005, Melbourne.

UNFCCC (1992) United Nations Framework Convention on CLimate Change, UN, New York.

Zhang L, Dawes W (1998) WAVES - An Integrated Energy and Water Balance Model. Technical Report No. 31/98, CSIRO Land and Water.

Zhang L, Dawes WR, Hatton TJ, Hume IH, O'Connell MG, Mitchell DC, Milthorp PL, Yee M (1999) Estimating episodic recharge under different crop/pasture rotations in the Mallee region. Part 2. Recharge control by agronomic practices. Agric. Water Manage., 42(2): 237-249.

8 Appendix I – Soils simplification

To determine if the number of model runs could be reduced, statistical analysis was undertaken on soil types across the MDB to see which behaved similarly. This was done by comparing the recharge obtained across the rainfall range observed in the MDB for all 12 soil types. The climate sequences were taken from seven points located in either the Namoi or Campaspe region. The recharge obtained for different rainfall amounts was compared for combinations of soils visually and statistically using a T-test, F-test and a slope test. The T-test was used to determine whether the means of two data sets are the same. The criterion used to determine that the two soils had a similar mean across a range of data was a T-test returning a value <0.1. Results of T-tests are presented in Table 8-1. An F-test was used to determine if the standard deviation of the two data sets was similar. The criterion set for this was an F-test returning a value >0.9. Results of F-tests are presented in Table 8-2. The slope test was to determine how similar the slope of the two data sets plotted against one another was to 1 (1 being a perfect relationship). The criterion set for this was 0.95 < slope <1.05. Results of slope tests are presented in Table 8-3. If two soil types, or a group of soil types, met two or more of these criteria, then they were visually inspected to check their validity. For example, Tenosols and Podosols were statistically similar to most other soil types; however, on visual inspection were significantly different. The visual plotting of the soil types is presented in Figure 8-1.

Table 8-1. Results of T-tests undertaken to determine the similarity of soil types. Soil pairs that meet criterion for similarity are in bold

	Calc	Chrom	Derm	Ferr	Hydr	Kand	Kuro	Podo	Rudo	Sodo	Teno	Vert
Calc		**0.07**	0.59	0.13	0.33	0.28	0.32	**0.03**	0.27	**0.08**	0.23	0.35
Chrom	**0.07**		0.79	0.23	**0.06**	0.16	0.21	**0.03**	0.13	**0.10**	0.35	0.38
Derm	0.59	0.79		0.69	0.34	**0.02**	**0.01**	**0.02**	**0.06**	0.26	0.78	0.46
Ferr	0.13	0.23	0.69		0.15	0.19	0.21	**0.04**	0.17	**0.07**	0.73	0.40
Hydr	0.33	**0.06**	0.34	0.15		0.29	0.34	**0.03**	**0.09**	**0.09**	**0.04**	0.35
Kand	0.28	0.16	**0.02**	0.19	0.29		0.65	**0.03**	0.38	0.11	**0.02**	0.34
Kuro	0.32	0.21	**0.01**	0.21	0.34	0.65		**0.03**	0.48	0.12	**0.05**	0.35
Podo	**0.03**	**0.03**	**0.02**	0.04	**0.03**	**0.03**	**0.03**		**0.03**	**0.04**	**0.02**	**0.08**
Rudo	0.27	0.13	**0.06**	0.17	**0.09**	0.38	0.48	**0.03**		**0.10**	**0.01**	0.34
Sodo	**0.08**	**0.10**	0.26	**0.07**	**0.09**	0.11	0.12	**0.04**	**0.10**		0.19	0.74
Teno	0.23	0.35	0.78	0.73	**0.04**	**0.02**	**0.05**	**0.02**	**0.01**	0.19		0.45
Vert	0.35	0.38	0.46	0.40	0.35	0.34	0.35	**0.08**	0.34	0.74	0.45	

Table 8-2. Results of F-tests undertaken to determine the similarity of soil types. Soil pairs that meet criterion for similarity are in bold

	Calc	Chrom	Derm	Ferr	Hydr	Kand	Kuro	Podo	Rudo	Sodo	Teno	Vert
Calc		**0.99**	0.80	0.82	**0.94**	0.79	0.76	0.00	0.84	0.53	**0.91**	0.13
Chrom	**0.99**		0.81	0.81	**0.95**	0.80	0.76	0.00	0.85	0.52	**0.92**	0.13
Derm	0.80	0.81		0.63	0.86	**0.99**	**0.95**	0.00	**0.96**	0.38	0.89	0.08
Ferr	0.82	0.81	0.63		0.76	0.63	0.59	0.00	0.67	0.68	0.73	0.20
Hydr	**0.94**	**0.95**	0.86	0.76		0.85	0.82	0.00	**0.90**	0.48	**0.97**	0.12
Kand	0.79	0.80	**0.99**	0.63	0.85		**0.96**	0.00	**0.95**	0.37	0.88	0.08
Kuro	0.76	0.76	**0.95**	0.59	0.82	**0.96**		0.00	**0.91**	0.35	0.84	0.07
Podo	0.00	0.00	0.00	0.00	0.00	0.00	0.00		0.00	0.00	0.00	0.00
Rudo	0.84	0.85	**0.96**	0.67	**0.90**	**0.95**	**0.91**	0.00		0.40	**0.93**	0.09
Sodo	0.53	0.52	0.38	0.68	0.48	0.37	0.35	0.00	0.40		0.46	0.38
Teno	**0.91**	**0.92**	0.89	0.73	**0.97**	0.88	0.84	0.00	**0.93**	0.46		0.11
Vert	0.13	0.13	0.08	0.20	0.12	0.08	0.07	0.00	0.09	0.38	0.11	

Table 8-3. Results of slope tests undertaken to determine similarity of soil types. Soil pairs that meet criterion for similarity are in bold

	Calc	Chrom	Derm	Ferr	Hydr	Kand	Kuro	Podo	Rudo	Sodo	Teno	Vert
Calc		**1.00**	1.07	0.94	**1.02**	1.08	1.09	97.9	1.06	0.83	**1.03**	0.65
Chrom	**1.00**		1.07	0.93	**1.02**	1.07	1.09	97.6	**1.05**	0.83	**1.03**	0.65
Derm	1.07	1.07		0.87	**0.95**	**1.00**	**1.02**	92.5	**0.98**	0.77	**0.96**	0.60
Ferr	0.94	0.93	0.87		1.09	1.15	1.16	103.5	1.13	0.89	1.10	0.69
Hydr	**1.02**	**1.02**	**0.95**	1.09		**1.05**	1.07	96.1	**1.04**	0.81	**1.01**	0.63
Kand	1.08	1.07	**1.00**	1.15	**1.05**		**1.01**	91.7	**0.98**	0.77	**0.96**	0.60
Kuro	1.09	1.09	**1.02**	1.16	1.07	**1.01**		90.6	**0.97**	0.76	0.94	0.59
Podo	97.9	97.6	92.5	103.5	96.1	91.7	90.6		0.01	0.01	0.01	0.00
Rudo	1.06	**1.05**	0.98	1.13	**1.04**	**0.98**	**0.97**	0.01		0.79	**0.97**	0.61
Sodo	0.83	0.83	0.77	0.89	0.81	0.77	0.76	0.01	0.79		1.23	0.77
Teno	**1.03**	**1.03**	**0.96**	1.10	**1.01**	**0.96**	0.94	0.01	**0.97**	1.23		0.63
Vert	0.65	0.65	0.60	0.69	0.63	0.60	0.59	0.00	0.61	0.77	0.63	

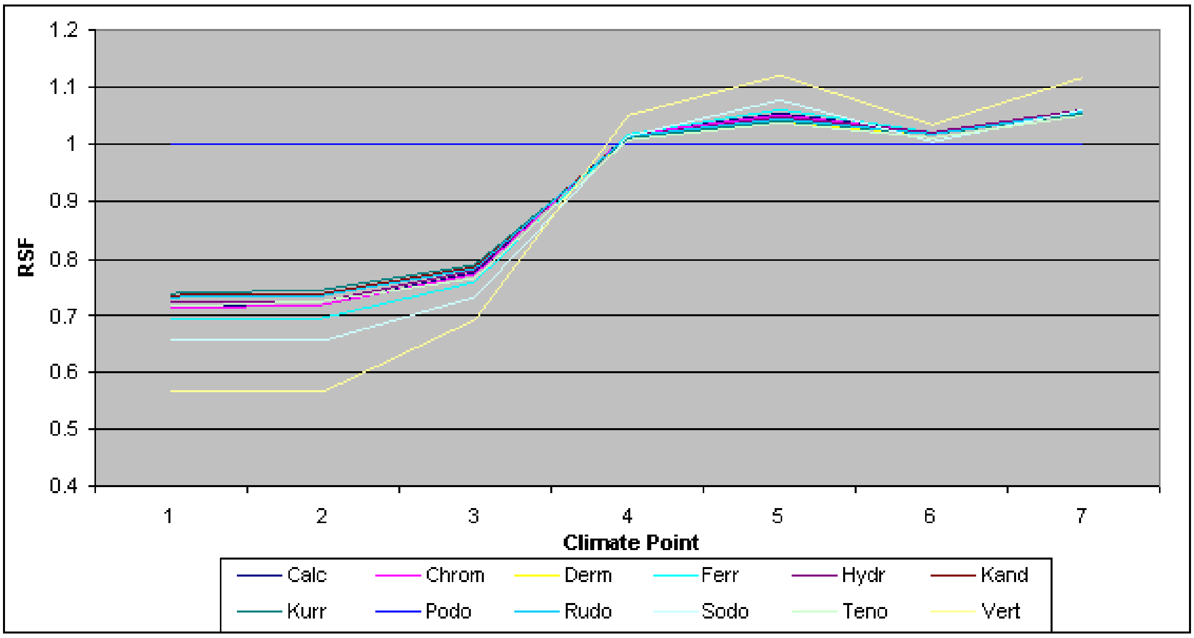

Figure 8-1. Recharge scaling factors for different soil types at seven points throughout the Murray-Darling Basin for vegetation type C3AP under Scenario B

9 Appendix II – Regression equations used in upscaling

Scenario	Soil type	Vegetation type	Calculated slope	Calculated intercept	r^2	Average RSF	p	Adopted slope	Adopted intercept
h01	calc	tree	1.34	-0.18	0.57	1.25	0.04	1.34	-0.18
h01	calc	C3pp	1.89	-0.61	0.29	1.40	0.11	0.00	1.40
h01	calc	C3ap	1.38	-0.32	0.86	1.16	0.01	1.38	-0.32
h01	derm	tree	1.08	0.08	0.53	1.24	0.05	1.08	0.08
h01	derm	C3pp	0.44	1.00	0.00	1.47	0.88	0.00	1.47
h01	derm	C3ap	1.33	-0.27	0.90	1.15	0.01	1.33	-0.27
h01	ferr	tree	1.71	-0.54	0.52	1.29	0.05	1.71	-0.54
h01	ferr	C3pp	2.07	-0.75	0.23	1.47	0.15	0.00	1.47
h01	ferr	C3ap	1.42	-0.35	0.81	1.17	0.01	1.42	-0.35
h01	kand	tree	1.09	0.06	0.48	1.23	0.05	1.09	0.06
h01	kand	C3pp	1.44	-0.19	0.27	1.35	0.12	0.00	1.35
h01	kand	C3ap	1.29	-0.23	0.89	1.15	0.01	1.29	-0.23
h01	sodo	tree	1.91	-0.74	0.54	1.30	0.04	1.91	-0.74
h01	sodo	C3pp	1.99	-0.60	0.16	1.53	0.20	0.00	1.53
h01	sodo	C3ap	1.71	-0.62	0.71	1.21	0.02	1.71	-0.62
h01	teno	tree	1.24	-0.07	0.48	1.26	0.06	1.24	-0.07
h01	teno	C3pp	1.53	-0.25	0.24	1.38	0.14	0.00	1.38
h01	teno	C3ap	1.23	-0.15	0.81	1.17	0.01	1.23	-0.15
h01	vert	tree	2.44	-1.31	0.61	1.30	0.03	2.44	-1.31
h01	vert	C3pp	2.07	-0.60	0.14	1.61	0.23	0.00	1.61
h01	vert	C3ap	2.27	-1.14	0.63	1.28	0.03	2.27	-1.14
h02	calc	tree	2.29	-1.26	0.33	1.15	0.10	2.29	-1.26
h02	calc	C3pp	5.06	-4.01	0.14	1.33	0.23	0.00	1.33
h02	calc	C3ap	1.69	-0.65	0.38	1.14	0.08	1.69	-0.65
h02	derm	tree	2.21	-1.18	0.33	1.15	0.10	2.21	-1.18
h02	derm	C3pp	3.97	-2.88	0.03	1.28	0.63	0.00	1.28
h02	derm	C3ap	1.61	-0.58	0.46	1.12	0.06	1.61	-0.58
h02	ferr	tree	2.03	-0.99	0.22	1.16	0.15	0.00	1.16
h02	ferr	C3pp	5.59	-4.55	0.15	1.35	0.21	0.00	1.35
h02	ferr	C3ap	1.82	-0.77	0.34	1.15	0.09	1.82	-0.77
h02	kand	tree	1.56	-0.51	0.18	1.14	0.18	0.00	1.14
h02	kand	C3pp	3.96	-2.88	0.11	1.29	0.28	0.00	1.29
h02	kand	C3ap	1.52	-0.48	0.38	1.13	0.08	1.52	-0.48
h02	sodo	tree	1.50	-0.44	0.14	1.14	0.23	0.00	1.14
h02	sodo	C3pp	3.39	-2.27	0.14	1.30	0.23	0.00	1.30
h02	sodo	C3ap	1.89	-0.84	0.38	1.16	0.08	1.89	-0.84
h02	teno	tree	1.53	-0.46	0.13	1.14	0.24	0.00	1.14
h02	teno	C3pp	4.42	-3.33	0.10	1.33	0.29	0.00	1.33
h02	teno	C3ap	1.70	-0.65	0.32	1.14	0.10	0.00	1.14
h02	vert	tree	-0.82	1.99	0.04	1.12	0.49	0.00	1.12
h02	vert	C3pp	1.52	-0.34	0.11	1.26	0.28	0.00	1.26
h02	vert	C3ap	1.90	-0.81	0.23	1.19	0.15	0.00	1.19
h03	calc	tree	2.30	-1.24	0.22	0.78	0.15	0.00	0.78
h03	calc	C3pp	-0.36	1.15	0.00	0.83	0.82	0.00	0.83
h03	calc	C3ap	1.14	-0.09	0.33	0.91	0.10	1.14	-0.09
h03	derm	tree	2.05	-1.03	0.28	0.77	0.12	0.00	0.77
h03	derm	C3pp	1.50	-0.59	0.05	0.74	0.66	0.00	0.74

Scenario	Soil type	Vegetation type	Calculated slope	Calculated intercept	r^2	Average RSF	p	Adopted slope	Adopted intercept
h03	derm	C3ap	1.11	-0.08	0.38	0.90	0.08	1.11	-0.08
h03	ferr	tree	2.55	-1.46	0.30	0.78	0.11	0.00	0.78
h03	ferr	C3pp	-0.48	1.26	0.01	0.85	0.79	0.00	0.85
h03	ferr	C3ap	1.18	-0.13	0.32	0.91	0.10	0.00	0.91
h03	kand	tree	2.18	-1.14	0.30	0.78	0.11	0.00	0.78
h03	kand	C3pp	0.10	0.75	0.00	0.84	0.94	0.00	0.84
h03	kand	C3ap	1.06	-0.02	0.32	0.91	0.10	0.00	0.91
h03	sodo	tree	2.27	-1.24	0.21	0.75	0.16	0.00	0.75
h03	sodo	C3pp	0.54	0.38	0.00	0.86	0.81	0.00	0.86
h03	sodo	C3ap	1.84	-0.71	0.64	0.90	0.03	1.84	-0.71
h03	teno	tree	2.51	-1.41	0.32	0.79	0.10	0.00	0.79
h03	teno	C3pp	-0.16	0.98	0.00	0.83	0.91	0.00	0.83
h03	teno	C3ap	0.93	0.09	0.21	0.91	0.16	0.00	0.91
h03	vert	tree	2.62	-1.57	0.24	0.73	0.14	0.00	0.73
h03	vert	C3pp	2.60	-1.45	0.09	0.83	0.32	0.00	0.83
h03	vert	C3ap	2.41	-1.23	0.48	0.89	0.06	2.41	-1.23
h04	calc	tree	2.88	-1.77	0.51	0.86	0.05	2.88	-1.77
h04	calc	C3pp	1.96	-0.79	0.21	1.00	0.16	0.00	1.00
h04	calc	C3ap	1.61	-0.55	0.82	0.92	0.01	1.61	-0.55
h04	derm	tree	2.78	-1.67	0.61	0.87	0.03	2.78	-1.67
h04	derm	C3pp	1.42	-0.30	0.29	1.03	0.24	0.00	1.03
h04	derm	C3ap	1.63	-0.58	0.85	0.92	0.01	1.63	-0.58
h04	ferr	tree	2.86	-1.75	0.40	0.86	0.07	2.86	-1.75
h04	ferr	C3pp	1.96	-0.78	0.18	1.01	0.18	0.00	1.01
h04	ferr	C3ap	1.74	-0.67	0.81	0.92	0.01	1.74	-0.67
h04	kand	tree	2.74	-1.63	0.54	0.88	0.04	2.74	-1.63
h04	kand	C3pp	1.87	-0.72	0.24	0.99	0.14	0.00	0.99
h04	kand	C3ap	1.50	-0.45	0.82	0.93	0.01	1.50	-0.45
h04	sodo	tree	2.49	-1.49	0.39	0.78	0.08	2.49	-1.49
h04	sodo	C3pp	1.67	-0.53	0.15	0.99	0.22	0.00	0.99
h04	sodo	C3ap	2.24	-1.16	0.88	0.89	0.01	2.24	-1.16
h04	teno	tree	2.96	-1.83	0.45	0.87	0.06	2.96	-1.83
h04	teno	C3pp	1.70	-0.55	0.16	1.01	0.21	0.00	1.01
h04	teno	C3ap	1.68	-0.62	0.81	0.92	0.01	1.68	-0.62
h04	vert	tree	2.72	-1.76	0.32	0.73	0.10	2.72	-1.76
h04	vert	C3pp	1.70	-0.64	0.12	0.91	0.26	0.00	0.91
h04	vert	C3ap	3.00	-1.90	0.80	0.85	0.01	3.00	-1.90
h05	calc	tree	1.10	-0.06	0.21	0.95	0.16	0.00	0.95
h05	calc	C3pp	1.76	-0.59	0.09	1.04	0.31	0.00	1.04
h05	calc	C3ap	2.17	-1.02	0.81	0.98	0.01	2.17	-1.02
h05	derm	tree	1.26	-0.21	0.30	0.96	0.11	0.00	0.96
h05	derm	C3pp	-5.58	6.33	0.23	1.06	0.29	0.00	1.06
h05	derm	C3ap	2.05	-0.92	0.81	0.97	0.01	2.05	-0.92
h05	ferr	tree	1.73	-0.64	0.43	0.96	0.07	1.73	-0.64
h05	ferr	C3pp	1.94	-0.73	0.09	1.07	0.31	0.00	1.07
h05	ferr	C3ap	2.33	-1.16	0.79	0.99	0.01	2.33	-1.16
h05	kand	tree	1.26	-0.21	0.35	0.96	0.09	1.26	-0.21
h05	kand	C3pp	1.56	-0.42	0.09	1.02	0.32	0.00	1.02
h05	kand	C3ap	1.98	-0.84	0.79	0.98	0.01	1.98	-0.84
h05	sodo	tree	1.61	-0.59	0.42	0.90	0.07	1.61	-0.59
h05	sodo	C3pp	2.15	-0.88	0.13	1.11	0.24	0.00	1.11
h05	sodo	C3ap	2.92	-1.71	0.86	0.99	0.01	2.92	-1.71
h05	teno	tree	1.60	-0.54	0.43	0.94	0.07	1.60	-0.54
h05	teno	C3pp	1.73	-0.56	0.08	1.05	0.33	0.00	1.05
h05	teno	C3ap	2.05	-0.91	0.72	0.99	0.02	2.05	-0.91

Scenario	Soil type	Vegetation type	Calculated slope	Calculated intercept	r^2	Average RSF	p	Adopted slope	Adopted intercept
h05	vert	tree	1.37	-0.42	0.35	0.85	0.09	1.37	-0.42
h05	vert	C3pp	2.87	-1.53	0.25	1.12	0.14	0.00	1.12
h05	vert	C3ap	3.72	-2.43	0.87	1.00	0.01	3.72	-2.43
h06	calc	tree	2.70	-1.49	0.63	0.78	0.03	2.70	-1.49
h06	calc	C3pp	3.41	-2.10	0.41	0.76	0.07	3.41	-2.10
h06	calc	C3ap	2.53	-1.36	0.93	0.77	0.00	2.53	-1.36
h06	derm	tree	2.39	-1.21	0.67	0.79	0.03	2.39	-1.21
h06	derm	C3pp	-3.74	4.20	0.18	0.88	0.38	0.00	0.88
h06	derm	C3ap	2.30	-1.16	0.92	0.78	0.00	2.30	-1.16
h06	ferr	tree	2.98	-1.75	0.67	0.76	0.03	2.98	-1.75
h06	ferr	C3pp	3.74	-2.39	0.40	0.76	0.07	3.74	-2.39
h06	ferr	C3ap	2.78	-1.58	0.93	0.76	0.00	2.78	-1.58
h06	kand	tree	2.63	-1.41	0.67	0.79	0.03	2.63	-1.41
h06	kand	C3pp	3.28	-1.99	0.46	0.77	0.06	3.28	-1.99
h06	kand	C3ap	2.32	-1.17	0.91	0.78	0.01	2.32	-1.17
h06	sodo	tree	3.16	-1.92	0.75	0.73	0.02	3.16	-1.92
h06	sodo	C3pp	3.24	-1.92	0.28	0.80	0.12	0.00	0.80
h06	sodo	C3ap	3.08	-1.86	0.94	0.73	0.00	3.08	-1.86
h06	teno	tree	2.88	-1.66	0.68	0.76	0.03	2.88	-1.66
h06	teno	C3pp	4.07	-2.68	0.50	0.74	0.05	4.07	-2.68
h06	teno	C3ap	2.56	-1.38	0.89	0.77	0.01	2.56	-1.38
h06	vert	tree	4.06	-2.71	0.75	0.70	0.02	4.06	-2.71
h06	vert	C3pp	3.13	-1.84	0.35	0.79	0.09	3.13	-1.84
h06	vert	C3ap	3.56	-2.30	0.93	0.69	0.00	3.56	-2.30
h07	calc	tree	0.26	0.64	0.00	0.89	0.80	0.00	0.89
h07	calc	C3pp	3.07	-2.05	0.04	0.90	0.48	0.00	0.90
h07	calc	C3ap	1.37	-0.37	0.37	0.95	0.08	1.37	-0.37
h07	derm	tree	0.85	0.10	0.04	0.91	0.48	0.00	0.91
h07	derm	C3pp	7.42	-6.27	0.23	0.89	0.26	0.00	0.89
h07	derm	C3ap	1.40	-0.40	0.47	0.95	0.06	1.40	-0.40
h07	ferr	tree	1.47	-0.54	0.07	0.87	0.38	0.00	0.87
h07	ferr	C3pp	2.80	-1.82	0.03	0.87	0.56	0.00	0.87
h07	ferr	C3ap	1.47	-0.47	0.30	0.94	0.11	0.00	0.94
h07	kand	tree	0.87	0.07	0.05	0.91	0.43	0.00	0.91
h07	kand	C3pp	0.74	0.20	0.00	0.91	0.85	0.00	0.91
h07	kand	C3ap	1.29	-0.29	0.39	0.95	0.08	1.29	-0.29
h07	sodo	tree	-0.43	1.25	0.01	0.83	0.77	0.00	0.83
h07	sodo	C3pp	1.05	-0.16	0.00	0.85	0.81	0.00	0.85
h07	sodo	C3ap	1.65	-0.66	0.15	0.92	0.21	0.00	0.92
h07	teno	tree	2.28	-1.31	0.16	0.89	0.21	0.00	0.89
h07	teno	C3pp	3.48	-2.44	0.05	0.91	0.45	0.00	0.91
h07	teno	C3ap	1.62	-0.61	0.36	0.95	0.09	1.62	-0.61
h07	vert	tree	-1.12	1.89	0.03	0.82	0.51	0.00	0.82
h07	vert	C3pp	-0.59	1.39	0.00	0.82	0.85	0.00	0.82
h07	vert	C3ap	1.02	-0.09	0.03	0.89	0.55	0.00	0.89
h08	calc	tree	3.37	-2.30	0.71	0.87	0.02	3.37	-2.30
h08	calc	C3pp	5.00	-3.76	0.45	0.95	0.06	5.00	-3.76
h08	calc	C3ap	1.86	-0.79	0.82	0.97	0.01	1.86	-0.79
h08	derm	tree	3.01	-1.96	0.83	0.88	0.01	3.01	-1.96
h08	derm	C3pp	4.17	-3.10	0.40	0.80	0.18	0.00	0.80
h08	derm	C3ap	1.78	-0.72	0.85	0.96	0.01	1.78	-0.72
h08	ferr	tree	3.63	-2.54	0.71	0.88	0.02	3.63	-2.54
h08	ferr	C3pp	5.44	-4.17	0.44	0.97	0.06	5.44	-4.17
h08	ferr	C3ap	2.00	-0.91	0.81	0.97	0.01	2.00	-0.91
h08	kand	tree	2.87	-1.83	0.83	0.88	0.01	2.87	-1.83

Scenario	Soil type	Vegetation type	Calculated slope	Calculated intercept	r^2	Average RSF	p	Adopted slope	Adopted intercept
h08	kand	C3pp	4.29	-3.09	0.46	0.96	0.06	4.29	-3.09
h08	kand	C3ap	1.74	-0.67	0.80	0.96	0.01	1.74	-0.67
h08	sodo	tree	3.41	-2.39	0.71	0.82	0.02	3.41	-2.39
h08	sodo	C3pp	5.55	-4.27	0.40	0.96	0.08	5.55	-4.27
h08	sodo	C3ap	2.20	-1.11	0.86	0.96	0.01	2.20	-1.11
h08	teno	tree	3.22	-2.15	0.75	0.88	0.02	3.22	-2.15
h08	teno	C3pp	4.53	-3.30	0.41	0.97	0.07	4.53	-3.30
h08	teno	C3ap	1.93	-0.86	0.79	0.96	0.01	1.93	-0.86
h08	vert	tree	3.25	-2.27	0.62	0.80	0.03	3.25	-2.27
h08	vert	C3pp	5.40	-4.16	0.43	0.94	0.07	5.40	-4.16
h08	vert	C3ap	2.72	-1.63	0.79	0.94	0.01	2.72	-1.63
h09	calc	tree	1.23	-0.30	0.69	0.77	0.02	1.23	-0.30
h09	calc	C3pp	0.76	-0.06	0.16	0.60	0.20	0.00	0.60
h09	calc	C3ap	2.25	-1.14	0.92	0.79	0.00	2.25	-1.14
h09	derm	tree	1.09	-0.16	0.72	0.78	0.02	1.09	-0.16
h09	derm	C3pp	-0.53	1.16	0.04	0.67	0.63	0.00	0.67
h09	derm	C3ap	2.03	-0.95	0.92	0.80	0.00	2.03	-0.95
h09	ferr	tree	1.44	-0.49	0.78	0.76	0.01	1.44	-0.49
h09	ferr	C3pp	0.94	-0.22	0.20	0.58	0.16	0.00	0.58
h09	ferr	C3ap	2.45	-1.33	0.92	0.78	0.01	2.45	-1.33
h09	kand	tree	1.20	-0.26	0.77	0.77	0.02	1.20	-0.26
h09	kand	C3pp	0.73	0.00	0.16	0.63	0.21	0.00	0.63
h09	kand	C3ap	2.03	-0.95	0.92	0.81	0.00	2.03	-0.95
h09	sodo	tree	2.05	-1.02	0.75	0.74	0.02	2.05	-1.02
h09	sodo	C3pp	0.85	-0.10	0.21	0.63	0.16	0.00	0.63
h09	sodo	C3ap	3.18	-1.97	0.94	0.78	0.00	3.18	-1.97
h09	teno	tree	1.34	-0.41	0.75	0.75	0.02	1.34	-0.41
h09	teno	C3pp	1.06	-0.32	0.20	0.59	0.17	0.00	0.59
h09	teno	C3ap	2.11	-1.03	0.90	0.79	0.01	2.11	-1.03
h09	vert	tree	2.57	-1.47	0.66	0.75	0.03	2.57	-1.47
h09	vert	C3pp	1.96	-0.99	0.58	0.70	0.04	1.96	-0.99
h09	vert	C3ap	4.24	-2.88	0.94	0.78	0.00	4.24	-2.88
h10	calc	tree	3.33	-2.37	0.83	1.26	0.01	3.33	-2.37
h10	calc	C3pp	2.78	-1.53	0.70	1.51	0.02	2.78	-1.53
h10	calc	C3ap	1.33	-0.23	0.65	1.23	0.03	1.33	-0.23
h10	derm	tree	2.65	-1.65	0.84	1.24	0.01	2.65	-1.65
h10	derm	C3pp	2.58	-1.37	0.68	1.48	0.05	2.58	-1.37
h10	derm	C3ap	1.39	-0.31	0.77	1.21	0.02	1.39	-0.31
h10	ferr	tree	3.73	-2.77	0.77	1.30	0.02	3.73	-2.77
h10	ferr	C3pp	3.26	-1.96	0.65	1.59	0.03	3.26	-1.96
h10	ferr	C3ap	1.39	-0.26	0.59	1.25	0.04	1.39	-0.26
h10	kand	tree	2.66	-1.67	0.83	1.23	0.01	2.66	-1.67
h10	kand	C3pp	2.34	-1.11	0.69	1.44	0.03	2.34	-1.11
h10	kand	C3ap	1.26	-0.16	0.69	1.21	0.02	1.26	-0.16
h10	sodo	tree	4.40	-3.49	0.71	1.31	0.02	4.40	-3.49
h10	sodo	C3pp	4.59	-3.40	0.86	1.60	0.01	4.59	-3.40
h10	sodo	C3ap	2.29	-1.19	0.78	1.31	0.02	2.29	-1.19
h10	teno	tree	3.14	-2.16	0.78	1.26	0.02	3.14	-2.16
h10	teno	C3pp	2.27	-0.96	0.46	1.51	0.06	2.27	-0.96
h10	teno	C3ap	1.34	-0.23	0.65	1.23	0.03	1.34	-0.23
h10	vert	tree	4.79	-3.91	0.64	1.31	0.03	4.79	-3.91
h10	vert	C3pp	6.85	-5.80	0.90	1.67	0.01	6.85	-5.80
h10	vert	C3ap	3.41	-2.33	0.83	1.39	0.01	3.41	-2.33
h11	calc	tree	2.18	-1.21	0.87	1.11	0.01	2.18	-1.21
h11	calc	C3pp	3.71	-2.47	0.59	1.48	0.04	3.71	-2.47

Scenario	Soil type	Vegetation type	Calculated slope	Calculated intercept	r^2	Average RSF	p	Adopted slope	Adopted intercept
h11	calc	C3ap	1.75	-0.67	0.74	1.19	0.02	1.75	-0.67
h11	derm	tree	2.06	-1.08	0.94	1.12	0.00	2.06	-1.08
h11	derm	C3pp	2.83	-1.58	0.29	1.44	0.19	0.00	1.44
h11	derm	C3ap	1.70	-0.64	0.82	1.18	0.01	1.70	-0.64
h11	ferr	tree	2.50	-1.53	0.78	1.13	0.02	2.50	-1.53
h11	ferr	C3pp	4.07	-2.80	0.53	1.53	0.05	4.07	-2.80
h11	ferr	C3ap	1.90	-0.81	0.71	1.21	0.02	1.90	-0.81
h11	kand	tree	1.86	-0.87	0.86	1.10	0.01	1.86	-0.87
h11	kand	C3pp	3.17	-1.95	0.62	1.43	0.03	3.17	-1.95
h11	kand	C3ap	1.61	-0.54	0.77	1.18	0.02	1.61	-0.54
h11	sodo	tree	2.04	-1.11	0.80	1.06	0.01	2.04	-1.11
h11	sodo	C3pp	3.45	-2.29	0.68	1.39	0.03	3.45	-2.29
h11	sodo	C3ap	2.27	-1.19	0.79	1.23	0.01	2.27	-1.19
h11	teno	tree	2.19	-1.20	0.88	1.14	0.01	2.19	-1.20
h11	teno	C3pp	3.45	-2.18	0.47	1.50	0.06	3.45	-2.18
h11	teno	C3ap	1.78	-0.69	0.75	1.20	0.02	1.78	-0.69
h11	vert	tree	1.57	-0.65	0.70	1.01	0.02	1.57	-0.65
h11	vert	C3pp	2.41	-1.33	0.60	1.23	0.04	2.41	-1.33
h11	vert	C3ap	2.74	-1.67	0.83	1.24	0.01	2.74	-1.67
h12	calc	tree	1.34	-0.33	0.08	0.92	0.34	0.00	0.92
h12	calc	C3pp	16.46	-14.34	0.55	1.12	0.04	16.46	-14.34
h12	calc	C3ap	3.69	-2.48	0.69	0.98	0.02	3.69	-2.48
h12	derm	tree	2.45	-1.36	0.34	0.95	0.09	2.45	-1.36
h12	derm	C3pp	10.20	-8.47	0.32	1.05	0.17	0.00	1.05
h12	derm	C3ap	3.43	-2.24	0.73	0.98	0.02	3.43	-2.24
h12	ferr	tree	1.34	-0.34	0.05	0.92	0.43	0.00	0.92
h12	ferr	C3pp	19.26	-16.95	0.54	1.14	0.04	19.26	-16.95
h12	ferr	C3ap	4.13	-2.89	0.66	0.99	0.03	4.13	-2.89
h12	kand	tree	1.32	-0.31	0.10	0.94	0.29	0.00	0.94
h12	kand	C3pp	13.92	-11.97	0.53	1.10	0.05	13.92	-11.97
h12	kand	C3ap	3.59	-2.39	0.70	0.99	0.02	3.59	-2.39
h12	sodo	tree	-0.45	1.29	0.01	0.87	0.73	0.00	0.87
h12	sodo	C3pp	13.69	-11.74	0.57	1.12	0.04	13.69	-11.74
h12	sodo	C3ap	3.60	-2.42	0.60	0.96	0.03	3.60	-2.42
h12	teno	tree	1.69	-0.66	0.10	0.93	0.29	0.00	0.93
h12	teno	C3pp	16.18	-14.06	0.53	1.13	0.05	16.18	-14.06
h12	teno	C3ap	4.65	-3.37	0.70	1.00	0.02	4.65	-3.37
h12	vert	tree	-1.73	2.44	0.05	0.81	0.43	0.00	0.81
h12	vert	C3pp	6.88	-5.44	0.41	1.03	0.07	6.88	-5.44
h12	vert	C3ap	2.22	-1.15	0.23	0.93	0.14	0.00	0.93
h13	calc	tree	1.11	-0.17	0.13	0.88	0.25	0.00	0.88
h13	calc	C3pp	2.25	-1.02	0.10	1.10	0.30	0.00	1.10
h13	calc	C3ap	1.45	-0.39	0.56	0.98	0.04	1.45	-0.39
h13	derm	tree	1.40	-0.41	0.23	0.91	0.14	0.00	0.91
h13	derm	C3pp	3.74	-2.45	0.55	1.07	0.09	3.74	-2.45
h13	derm	C3ap	1.41	-0.36	0.60	0.98	0.03	1.41	-0.36
h13	ferr	tree	0.98	-0.06	0.08	0.87	0.34	0.00	0.87
h13	ferr	C3pp	2.09	-0.88	0.07	1.09	0.35	0.00	1.09
h13	ferr	C3ap	1.53	-0.46	0.53	0.99	0.05	1.53	-0.46
h13	kand	tree	1.32	-0.34	0.21	0.91	0.16	0.00	0.91
h13	kand	C3pp	2.16	-0.95	0.12	1.10	0.26	0.00	1.10
h13	kand	C3ap	1.36	-0.30	0.54	0.98	0.04	1.36	-0.30
h13	sodo	tree	0.68	0.13	0.05	0.77	0.42	0.00	0.77
h13	sodo	C3pp	1.12	-0.02	0.03	1.04	0.55	0.00	1.04
h13	sodo	C3ap	1.62	-0.58	0.60	0.95	0.04	1.62	-0.58

Scenario	Soil type	Vegetation type	Calculated slope	Calculated intercept	r^2	Average RSF	p	Adopted slope	Adopted intercept
h13	teno	tree	1.03	-0.08	0.09	0.89	0.30	0.00	0.89
h13	teno	C3pp	2.59	-1.34	0.13	1.11	0.25	0.00	1.11
h13	teno	C3ap	1.55	-0.48	0.50	0.99	0.05	1.55	-0.48
h13	vert	tree	0.75	0.01	0.05	0.72	0.44	0.00	0.72
h13	vert	C3pp	0.27	0.62	0.00	0.87	0.86	0.00	0.87
h13	vert	C3ap	1.74	-0.74	0.47	0.90	0.06	1.74	-0.74
h14	calc	tree	1.30	-0.36	0.16	0.96	0.20	0.00	0.96
h14	calc	C3pp	2.18	-1.03	0.08	1.20	0.34	0.00	1.20
h14	calc	C3ap	1.80	-0.77	0.67	1.07	0.03	1.80	-0.77
h14	derm	tree	1.04	-0.07	0.23	0.99	0.14	0.00	0.99
h14	derm	C3pp	1.08	0.00	0.01	1.09	0.78	0.00	1.09
h14	derm	C3ap	1.71	-0.69	0.71	1.06	0.02	1.71	-0.69
h14	ferr	tree	1.34	-0.41	0.12	0.95	0.26	0.00	0.95
h14	ferr	C3pp	2.08	-0.92	0.07	1.19	0.37	0.00	1.19
h14	ferr	C3ap	1.95	-0.91	0.64	1.07	0.03	1.95	-0.91
h14	kand	tree	1.27	-0.31	0.24	0.99	0.14	0.00	0.99
h14	kand	C3pp	1.88	-0.73	0.08	1.19	0.35	0.00	1.19
h14	kand	C3ap	1.58	-0.55	0.63	1.06	0.03	1.58	-0.55
h14	sodo	tree	-0.28	1.15	0.01	0.86	0.77	0.00	0.86
h14	sodo	C3pp	1.38	-0.31	0.05	1.10	0.44	0.00	1.10
h14	sodo	C3ap	2.28	-1.27	0.73	1.06	0.02	2.28	-1.27
h14	teno	tree	1.57	-0.63	0.22	0.97	0.16	0.00	0.97
h14	teno	C3pp	1.89	-0.73	0.05	1.20	0.43	0.00	1.20
h14	teno	C3ap	1.70	-0.67	0.56	1.07	0.04	1.70	-0.67
h14	vert	tree	-0.36	1.18	0.01	0.82	0.76	0.00	0.82
h14	vert	C3pp	-0.64	1.61	0.02	0.95	0.63	0.00	0.95
h14	vert	C3ap	2.63	-1.66	0.46	1.02	0.06	2.63	-1.66
h15	calc	tree	3.01	-2.07	0.56	1.13	0.04	3.01	-2.07
h15	calc	C3pp	3.60	-2.54	0.23	1.30	0.14	0.00	1.30
h15	calc	C3ap	2.21	-1.22	0.50	1.13	0.05	2.21	-1.22
h15	derm	tree	2.24	-1.26	0.55	1.13	0.04	2.24	-1.26
h15	derm	C3pp	0.53	0.69	0.00	1.26	0.90	0.00	1.26
h15	derm	C3ap	2.06	-1.07	0.57	1.13	0.04	2.06	-1.07
h15	ferr	tree	2.06	-1.07	0.47	1.12	0.06	2.06	-1.07
h15	ferr	C3pp	4.45	-3.43	0.27	1.30	0.12	0.00	1.30
h15	ferr	C3ap	2.45	-1.47	0.48	1.14	0.06	2.45	-1.47
h15	kand	tree	1.06	-0.01	0.18	1.12	0.18	0.00	1.12
h15	kand	C3pp	3.23	-2.16	0.21	1.27	0.16	0.00	1.27
h15	kand	C3ap	1.98	-0.99	0.52	1.13	0.05	1.98	-0.99
h15	sodo	tree	2.58	-1.65	0.60	1.10	0.04	2.58	-1.65
h15	sodo	C3pp	3.04	-1.98	0.18	1.26	0.19	0.00	1.26
h15	sodo	C3ap	2.86	-1.90	0.55	1.15	0.04	2.86	-1.90
h15	teno	tree	1.69	-0.67	0.34	1.13	0.09	1.69	-0.67
h15	teno	C3pp	3.80	-2.74	0.17	1.31	0.20	0.00	1.31
h15	teno	C3ap	2.34	-1.36	0.51	1.14	0.05	2.34	-1.36
h15	vert	tree	0.27	0.78	0.01	1.07	0.75	0.00	1.07
h15	vert	C3pp	2.81	-1.79	0.15	1.20	0.22	0.00	1.20
h15	vert	C3ap	3.03	-2.07	0.56	1.16	0.04	3.03	-2.07
l01	calc	tree	0.82	0.24	0.19	1.07	0.18	0.00	1.07
l01	calc	C3pp	1.51	-0.45	0.22	1.09	0.15	0.00	1.09
l01	calc	C3ap	1.30	-0.27	0.82	1.05	0.01	1.30	-0.27
l01	derm	tree	0.33	0.73	0.05	1.07	0.43	0.00	1.07
l01	derm	C3pp	-0.19	1.30	0.00	1.10	0.93	0.00	1.10
l01	derm	C3ap	1.29	-0.28	0.89	1.04	0.01	1.29	-0.28
l01	ferr	tree	0.61	0.45	0.03	1.07	0.52	0.00	1.07

Scenario	Soil type	Vegetation type	Calculated slope	Calculated intercept	r^2	Average RSF	p	Adopted slope	Adopted intercept
I01	ferr	C3pp	1.63	-0.55	0.21	1.11	0.16	0.00	1.11
I01	ferr	C3ap	1.31	-0.28	0.76	1.05	0.02	1.31	-0.28
I01	kand	tree	0.23	0.83	0.01	1.06	0.68	0.00	1.06
I01	kand	C3pp	1.18	-0.12	0.20	1.08	0.17	0.00	1.08
I01	kand	C3ap	1.21	-0.19	0.85	1.04	0.01	1.21	-0.19
I01	sodo	tree	0.93	0.13	0.12	1.08	0.26	0.00	1.08
I01	sodo	C3pp	1.46	-0.37	0.17	1.12	0.19	0.00	1.12
I01	sodo	C3ap	1.73	-0.70	0.69	1.07	0.02	1.73	-0.70
I01	teno	tree	0.12	0.95	0.00	1.06	0.87	0.00	1.06
I01	teno	C3pp	1.28	-0.21	0.20	1.09	0.17	0.00	1.09
I01	teno	C3ap	1.15	-0.12	0.75	1.05	0.02	1.15	-0.12
I01	vert	tree	1.66	-0.62	0.16	1.07	0.21	0.00	1.07
I01	vert	C3pp	1.64	-0.52	0.14	1.15	0.22	0.00	1.15
I01	vert	C3ap	2.18	-1.13	0.55	1.09	0.04	2.18	-1.13
I02	calc	tree	0.72	0.31	0.03	1.04	0.51	0.00	1.04
I02	calc	C3pp	5.65	-4.66	0.20	1.08	0.17	0.00	1.08
I02	calc	C3ap	1.95	-0.94	0.39	1.04	0.08	1.95	-0.94
I02	derm	tree	0.72	0.32	0.02	1.05	0.58	0.00	1.05
I02	derm	C3pp	6.37	-5.40	0.08	1.06	0.49	0.00	1.06
I02	derm	C3ap	1.89	-0.88	0.51	1.04	0.05	1.89	-0.88
I02	ferr	tree	-1.35	2.41	0.06	1.05	0.40	0.00	1.05
I02	ferr	C3pp	6.33	-5.35	0.21	1.09	0.16	0.00	1.09
I02	ferr	C3ap	2.13	-1.12	0.34	1.05	0.09	2.13	-1.12
I02	kand	tree	-1.72	2.79	0.09	1.04	0.31	0.00	1.04
I02	kand	C3pp	4.68	-3.68	0.16	1.07	0.20	0.00	1.07
I02	kand	C3ap	1.79	-0.78	0.40	1.04	0.08	1.79	-0.78
I02	sodo	tree	-1.31	2.37	0.04	1.04	0.48	0.00	1.04
I02	sodo	C3pp	3.69	-2.67	0.16	1.08	0.21	0.00	1.08
I02	sodo	C3ap	2.46	-1.44	0.47	1.06	0.06	2.46	-1.44
I02	teno	tree	-0.66	1.71	0.02	1.03	0.63	0.00	1.03
I02	teno	C3pp	5.47	-4.48	0.16	1.08	0.20	0.00	1.08
I02	teno	C3ap	2.07	-1.06	0.36	1.04	0.09	2.07	-1.06
I02	vert	tree	-4.48	5.59	0.26	1.04	0.13	0.00	1.04
I02	vert	C3pp	2.09	-1.05	0.16	1.08	0.21	0.00	1.08
I02	vert	C3ap	2.12	-1.08	0.20	1.07	0.16	0.00	1.07
I03	calc	tree	2.82	-1.81	0.37	0.92	0.08	2.82	-1.81
I03	calc	C3pp	0.32	0.62	0.00	0.93	0.83	0.00	0.93
I03	calc	C3ap	1.43	-0.41	0.51	0.97	0.05	1.43	-0.41
I03	derm	tree	2.40	-1.39	0.32	0.92	0.10	2.40	-1.39
I03	derm	C3pp	1.89	-0.93	0.09	0.91	0.46	0.00	0.91
I03	derm	C3ap	1.45	-0.43	0.59	0.97	0.04	1.45	-0.43
I03	ferr	tree	2.59	-1.59	0.35	0.92	0.09	2.59	-1.59
I03	ferr	C3pp	0.12	0.81	0.00	0.93	0.94	0.00	0.93
I03	ferr	C3ap	1.53	-0.50	0.48	0.97	0.05	1.53	-0.50
I03	kand	tree	2.18	-1.18	0.34	0.92	0.09	2.18	-1.18
I03	kand	C3pp	0.70	0.25	0.02	0.93	0.61	0.00	0.93
I03	kand	C3ap	1.36	-0.34	0.50	0.97	0.05	1.36	-0.34
I03	sodo	tree	2.81	-1.81	0.23	0.90	0.15	0.00	0.90
I03	sodo	C3pp	0.77	0.18	0.01	0.93	0.71	0.00	0.93
I03	sodo	C3ap	2.42	-1.36	0.71	0.98	0.02	2.42	-1.36
I03	teno	tree	2.86	-1.84	0.39	0.92	0.08	2.86	-1.84
I03	teno	C3pp	0.65	0.30	0.02	0.93	0.63	0.00	0.93
I03	teno	C3ap	1.27	-0.26	0.40	0.97	0.08	1.27	-0.26
I03	vert	tree	3.70	-2.66	0.24	0.91	0.14	0.00	0.91
I03	vert	C3pp	3.24	-2.21	0.15	0.92	0.21	0.00	0.92

Scenario	Soil type	Vegetation type	Calculated slope	Calculated intercept	r^2	Average RSF	p	Adopted slope	Adopted intercept
I03	vert	C3ap	3.46	-2.37	0.53	0.97	0.05	3.46	-2.37
I04	calc	tree	3.19	-2.16	0.54	0.96	0.04	3.19	-2.16
I04	calc	C3pp	3.11	-2.05	0.39	0.98	0.08	3.11	-2.05
I04	calc	C3ap	1.75	-0.73	0.84	0.98	0.01	1.75	-0.73
I04	derm	tree	2.69	-1.67	0.70	0.96	0.02	2.69	-1.67
I04	derm	C3pp	2.54	-1.50	0.50	0.99	0.11	0.00	0.99
I04	derm	C3ap	1.83	-0.81	0.87	0.98	0.01	1.83	-0.81
I04	ferr	tree	2.75	-1.74	0.50	0.95	0.05	2.75	-1.74
I04	ferr	C3pp	3.00	-1.94	0.36	0.99	0.09	3.00	-1.94
I04	ferr	C3ap	1.83	-0.81	0.82	0.98	0.01	1.83	-0.81
I04	kand	tree	2.53	-1.51	0.55	0.96	0.04	2.53	-1.51
I04	kand	C3pp	2.77	-1.72	0.41	0.98	0.07	2.77	-1.72
I04	kand	C3ap	1.61	-0.59	0.84	0.98	0.01	1.61	-0.59
I04	sodo	tree	2.43	-1.44	0.39	0.93	0.08	2.43	-1.44
I04	sodo	C3pp	2.52	-1.47	0.26	0.99	0.13	0.00	0.99
I04	sodo	C3ap	2.45	-1.41	0.82	0.98	0.01	2.45	-1.41
I04	teno	tree	2.74	-1.72	0.56	0.95	0.04	2.74	-1.72
I04	teno	C3pp	2.70	-1.64	0.34	0.99	0.09	2.70	-1.64
I04	teno	C3ap	1.89	-0.86	0.82	0.98	0.01	1.89	-0.86
I04	vert	tree	3.08	-2.09	0.41	0.92	0.07	3.08	-2.09
I04	vert	C3pp	1.98	-0.96	0.14	0.97	0.23	0.00	0.97
I04	vert	C3ap	3.32	-2.28	0.75	0.97	0.02	3.32	-2.28
I05	calc	tree	1.05	-0.04	0.28	0.98	0.12	0.00	0.98
I05	calc	C3pp	2.58	-1.54	0.15	0.99	0.21	0.00	0.99
I05	calc	C3ap	2.29	-1.25	0.80	1.00	0.01	2.29	-1.25
I05	derm	tree	1.07	-0.06	0.31	0.99	0.10	0.00	0.99
I05	derm	C3pp	-2.82	3.77	0.13	0.99	0.40	0.00	0.99
I05	derm	C3ap	2.23	-1.19	0.82	0.99	0.01	2.23	-1.19
I05	ferr	tree	1.91	-0.89	0.45	0.98	0.06	1.91	-0.89
I05	ferr	C3pp	2.86	-1.79	0.15	1.00	0.21	0.00	1.00
I05	ferr	C3ap	2.42	-1.37	0.77	1.00	0.02	2.42	-1.37
I05	kand	tree	1.20	-0.19	0.34	0.99	0.09	1.20	-0.19
I05	kand	C3pp	2.31	-1.27	0.14	0.99	0.22	0.00	0.99
I05	kand	C3ap	2.07	-1.04	0.78	0.99	0.02	2.07	-1.04
I05	sodo	tree	1.26	-0.27	0.23	0.97	0.14	0.00	0.97
I05	sodo	C3pp	3.15	-2.07	0.20	1.01	0.17	0.00	1.01
I05	sodo	C3ap	3.15	-2.08	0.86	1.01	0.01	3.15	-2.08
I05	teno	tree	1.81	-0.79	0.52	0.98	0.05	1.81	-0.79
I05	teno	C3pp	2.58	-1.53	0.13	1.00	0.24	0.00	1.00
I05	teno	C3ap	2.20	-1.16	0.70	1.00	0.02	2.20	-1.16
I05	vert	tree	1.62	-0.65	0.22	0.94	0.15	0.00	0.94
I05	vert	C3pp	3.48	-2.39	0.27	1.03	0.12	0.00	1.03
I05	vert	C3ap	4.07	-2.97	0.90	1.01	0.01	4.07	-2.97
I06	calc	tree	2.71	-1.66	0.79	0.93	0.01	2.71	-1.66
I06	calc	C3pp	4.39	-3.30	0.60	0.90	0.04	4.39	-3.30
I06	calc	C3ap	2.76	-1.71	0.95	0.93	0.00	2.76	-1.71
I06	derm	tree	2.49	-1.44	0.85	0.94	0.01	2.49	-1.44
I06	derm	C3pp	-3.54	4.37	0.20	0.94	0.35	0.00	0.94
I06	derm	C3ap	2.52	-1.48	0.95	0.94	0.00	2.52	-1.48
I06	ferr	tree	3.87	-2.78	0.80	0.92	0.01	3.87	-2.78
I06	ferr	C3pp	4.99	-3.87	0.59	0.89	0.04	4.99	-3.87
I06	ferr	C3ap	3.06	-1.99	0.94	0.93	0.00	3.06	-1.99
I06	kand	tree	2.85	-1.78	0.69	0.94	0.02	2.85	-1.78
I06	kand	C3pp	4.00	-2.92	0.61	0.91	0.03	4.00	-2.92
I06	kand	C3ap	2.49	-1.44	0.94	0.94	0.00	2.49	-1.44

Scenario	Soil type	Vegetation type	Calculated slope	Calculated intercept	r^2	Average RSF	p	Adopted slope	Adopted intercept
I06	sodo	tree	3.54	-2.47	0.74	0.92	0.02	3.54	-2.47
I06	sodo	C3pp	4.36	-3.26	0.47	0.92	0.06	4.36	-3.26
I06	sodo	C3ap	3.63	-2.55	0.93	0.93	0.00	3.63	-2.55
I06	teno	tree	3.48	-2.41	0.74	0.92	0.02	3.48	-2.41
I06	teno	C3pp	5.34	-4.21	0.66	0.89	0.03	5.34	-4.21
I06	teno	C3ap	2.78	-1.72	0.92	0.94	0.00	2.78	-1.72
I06	vert	tree	5.01	-3.87	0.79	0.92	0.01	5.01	-3.87
I06	vert	C3pp	4.56	-3.44	0.53	0.92	0.05	4.56	-3.44
I06	vert	C3ap	4.40	-3.29	0.92	0.92	0.00	4.40	-3.29
I07	calc	tree	1.48	-0.49	0.04	0.97	0.46	0.00	0.97
I07	calc	C3pp	5.04	-4.03	0.08	0.96	0.33	0.00	0.96
I07	calc	C3ap	1.50	-0.50	0.33	0.99	0.10	1.50	-0.50
I07	derm	tree	1.79	-0.79	0.04	0.98	0.47	0.00	0.98
I07	derm	C3pp	10.10	-9.05	0.31	0.95	0.18	0.00	0.95
I07	derm	C3ap	1.50	-0.50	0.44	0.99	0.06	1.50	-0.50
I07	ferr	tree	6.13	-5.11	0.26	0.97	0.13	0.00	0.97
I07	ferr	C3pp	4.35	-3.36	0.05	0.95	0.44	0.00	0.95
I07	ferr	C3ap	1.46	-0.45	0.22	0.99	0.15	0.00	0.99
I07	kand	tree	3.31	-2.30	0.16	0.98	0.21	0.00	0.98
I07	kand	C3pp	4.11	-3.10	0.06	0.97	0.42	0.00	0.97
I07	kand	C3ap	1.41	-0.41	0.34	0.99	0.09	1.41	-0.41
I07	sodo	tree	0.76	0.20	0.01	0.95	0.78	0.00	0.95
I07	sodo	C3pp	2.07	-1.10	0.01	0.95	0.69	0.00	0.95
I07	sodo	C3ap	1.03	-0.03	0.05	0.99	0.45	0.00	0.99
I07	teno	tree	4.81	-3.79	0.22	0.97	0.15	0.00	0.97
I07	teno	C3pp	4.88	-3.86	0.07	0.97	0.36	0.00	0.97
I07	teno	C3ap	1.76	-0.75	0.32	0.99	0.10	0.00	0.99
I07	vert	tree	5.83	-4.83	0.13	0.95	0.24	0.00	0.95
I07	vert	C3pp	-0.57	1.51	0.00	0.95	0.89	0.00	0.95
I07	vert	C3ap	0.86	0.14	0.02	0.99	0.63	0.00	0.99
I08	calc	tree	3.40	-2.38	0.78	0.96	0.02	3.40	-2.38
I08	calc	C3pp	5.42	-4.36	0.50	0.97	0.05	5.42	-4.36
I08	calc	C3ap	1.92	-0.90	0.83	0.99	0.01	1.92	-0.90
I08	derm	tree	1.71	-0.71	0.57	0.97	0.04	1.71	-0.71
I08	derm	C3pp	5.00	-3.98	0.36	0.93	0.17	0.00	0.93
I08	derm	C3ap	1.88	-0.86	0.89	0.99	0.01	1.88	-0.86
I08	ferr	tree	2.34	-1.35	0.65	0.96	0.03	2.34	-1.35
I08	ferr	C3pp	5.82	-4.75	0.48	0.98	0.06	5.82	-4.75
I08	ferr	C3ap	2.06	-1.03	0.80	1.00	0.01	2.06	-1.03
I08	kand	tree	2.19	-1.20	0.61	0.97	0.03	2.19	-1.20
I08	kand	C3pp	4.71	-3.66	0.50	0.98	0.05	4.71	-3.66
I08	kand	C3ap	1.80	-0.78	0.80	0.99	0.01	1.80	-0.78
I08	sodo	tree	2.36	-1.38	0.56	0.94	0.04	2.36	-1.38
I08	sodo	C3pp	6.34	-5.27	0.45	0.97	0.06	6.34	-5.27
I08	sodo	C3ap	2.25	-1.22	0.83	1.00	0.01	2.25	-1.22
I08	teno	tree	2.36	-1.36	0.86	0.96	0.01	2.36	-1.36
I08	teno	C3pp	4.86	-3.80	0.45	0.98	0.06	4.86	-3.80
I08	teno	C3ap	2.08	-1.06	0.80	0.99	0.01	2.08	-1.06
I08	vert	tree	1.74	-0.78	0.24	0.94	0.14	0.00	0.94
I08	vert	C3pp	6.18	-5.11	0.47	0.98	0.06	6.18	-5.11
I08	vert	C3ap	2.80	-1.76	0.72	1.00	0.02	2.80	-1.76
I09	calc	tree	1.05	-0.09	0.71	0.93	0.02	1.05	-0.09
I09	calc	C3pp	0.86	0.03	0.12	0.85	0.26	0.00	0.85
I09	calc	C3ap	2.39	-1.36	0.91	0.94	0.01	2.39	-1.36
I09	derm	tree	0.83	0.14	0.63	0.94	0.03	0.83	0.14

Scenario	Soil type	Vegetation type	Calculated slope	Calculated intercept	r^2	Average RSF	p	Adopted slope	Adopted intercept
I09	derm	C3pp	-0.61	1.46	0.06	0.87	0.56	0.00	0.87
I09	derm	C3ap	2.17	-1.14	0.91	0.94	0.01	2.17	-1.14
I09	ferr	tree	1.51	-0.53	0.69	0.92	0.02	1.51	-0.53
I09	ferr	C3pp	1.13	-0.24	0.15	0.85	0.21	0.00	0.85
I09	ferr	C3ap	2.62	-1.58	0.90	0.94	0.01	2.62	-1.58
I09	kand	tree	1.05	-0.08	0.63	0.93	0.03	1.05	-0.08
I09	kand	C3pp	0.74	0.16	0.10	0.87	0.29	0.00	0.87
I09	kand	C3ap	2.14	-1.11	0.91	0.94	0.01	2.14	-1.11
I09	sodo	tree	2.01	-1.02	0.62	0.92	0.03	2.01	-1.02
I09	sodo	C3pp	1.20	-0.28	0.21	0.87	0.16	0.00	0.87
I09	sodo	C3ap	3.57	-2.49	0.92	0.94	0.00	3.57	-2.49
I09	teno	tree	1.52	-0.55	0.67	0.91	0.03	1.52	-0.55
I09	teno	C3pp	1.31	-0.41	0.17	0.85	0.20	0.00	0.85
I09	teno	C3ap	2.21	-1.18	0.89	0.94	0.01	2.21	-1.18
I09	vert	tree	3.03	-2.00	0.73	0.92	0.02	3.03	-2.00
I09	vert	C3pp	2.53	-1.54	0.53	0.89	0.05	2.53	-1.54
I09	vert	C3ap	4.78	-3.66	0.92	0.94	0.01	4.78	-3.66
I10	calc	tree	2.57	-1.57	0.66	1.07	0.03	2.57	-1.57
I10	calc	C3pp	2.22	-1.16	0.64	1.12	0.03	2.22	-1.16
I10	calc	C3ap	1.26	-0.22	0.59	1.07	0.04	1.26	-0.22
I10	derm	tree	1.95	-0.93	0.56	1.06	0.04	1.95	-0.93
I10	derm	C3pp	2.32	-1.28	0.75	1.10	0.04	2.32	-1.28
I10	derm	C3ap	1.37	-0.35	0.75	1.06	0.02	1.37	-0.35
I10	ferr	tree	2.79	-1.78	0.68	1.08	0.03	2.79	-1.78
I10	ferr	C3pp	2.74	-1.67	0.64	1.14	0.03	2.74	-1.67
I10	ferr	C3ap	1.30	-0.26	0.52	1.07	0.05	1.30	-0.26
I10	kand	tree	1.87	-0.86	0.45	1.06	0.06	1.87	-0.86
I10	kand	C3pp	1.99	-0.93	0.67	1.10	0.03	1.99	-0.93
I10	kand	C3ap	1.19	-0.16	0.63	1.06	0.03	1.19	-0.16
I10	sodo	tree	3.03	-2.03	0.44	1.08	0.06	3.03	-2.03
I10	sodo	C3pp	3.50	-2.45	0.83	1.14	0.01	3.50	-2.45
I10	sodo	C3ap	2.37	-1.34	0.78	1.09	0.02	2.37	-1.34
I10	teno	tree	2.29	-1.28	0.50	1.06	0.05	2.29	-1.28
I10	teno	C3pp	2.00	-0.93	0.45	1.12	0.06	2.00	-0.93
I10	teno	C3ap	1.30	-0.27	0.59	1.07	0.04	1.30	-0.27
I10	vert	tree	3.85	-2.88	0.41	1.07	0.07	3.85	-2.88
I10	vert	C3pp	5.19	-4.16	0.87	1.16	0.01	5.19	-4.16
I10	vert	C3ap	3.18	-2.14	0.76	1.12	0.02	3.18	-2.14
I11	calc	tree	1.44	-0.44	0.69	1.02	0.02	1.44	-0.44
I11	calc	C3pp	3.14	-2.09	0.60	1.11	0.03	3.14	-2.09
I11	calc	C3ap	1.68	-0.65	0.72	1.06	0.02	1.68	-0.65
I11	derm	tree	1.38	-0.38	0.86	1.03	0.01	1.38	-0.38
I11	derm	C3pp	2.61	-1.57	0.34	1.09	0.18	0.00	1.09
I11	derm	C3ap	1.66	-0.64	0.82	1.05	0.01	1.66	-0.64
I11	ferr	tree	1.62	-0.61	0.62	1.04	0.03	1.62	-0.61
I11	ferr	C3pp	3.55	-2.49	0.58	1.12	0.04	3.55	-2.49
I11	ferr	C3ap	1.78	-0.75	0.68	1.06	0.03	1.78	-0.75
I11	kand	tree	1.34	-0.33	0.47	1.03	0.06	1.34	-0.33
I11	kand	C3pp	2.86	-1.82	0.66	1.10	0.03	2.86	-1.82
I11	kand	C3ap	1.53	-0.51	0.74	1.05	0.02	1.53	-0.51
I11	sodo	tree	1.46	-0.47	0.48	1.02	0.06	1.46	-0.47
I11	sodo	C3pp	2.96	-1.92	0.63	1.09	0.03	2.96	-1.92
I11	sodo	C3ap	2.21	-1.18	0.77	1.08	0.02	2.21	-1.18
I11	teno	tree	1.61	-0.61	0.67	1.03	0.03	1.61	-0.61
I11	teno	C3pp	3.00	-1.94	0.50	1.12	0.05	3.00	-1.94

Scenario	Soil type	Vegetation type	Calculated slope	Calculated intercept	r^2	Average RSF	p	Adopted slope	Adopted intercept
I11	teno	C3ap	1.69	-0.66	0.72	1.06	0.02	1.69	-0.66
I11	vert	tree	0.67	0.32	0.10	1.00	0.29	0.00	1.00
I11	vert	C3pp	2.32	-1.29	0.54	1.07	0.04	2.32	-1.29
I11	vert	C3ap	2.59	-1.56	0.75	1.08	0.02	2.59	-1.56
I12	calc	tree	1.57	-0.57	0.14	0.98	0.23	0.00	0.98
I12	calc	C3pp	12.31	-11.10	0.51	1.01	0.05	12.31	-11.10
I12	calc	C3ap	3.20	-2.15	0.67	1.00	0.03	3.20	-2.15
I12	derm	tree	2.32	-1.30	0.21	0.98	0.16	0.00	0.98
I12	derm	C3pp	9.72	-8.55	0.48	0.99	0.10	0.00	0.99
I12	derm	C3ap	2.77	-1.73	0.69	0.99	0.02	2.77	-1.73
I12	ferr	tree	1.31	-0.32	0.04	0.97	0.48	0.00	0.97
I12	ferr	C3pp	13.18	-11.95	0.50	1.01	0.05	13.18	-11.95
I12	ferr	C3ap	3.59	-2.54	0.62	1.00	0.03	3.59	-2.54
I12	kand	tree	0.56	0.43	0.01	0.98	0.72	0.00	0.98
I12	kand	C3pp	10.76	-9.58	0.49	1.01	0.05	10.76	-9.58
I12	kand	C3ap	3.09	-2.05	0.67	1.00	0.03	3.09	-2.05
I12	sodo	tree	0.98	0.00	0.03	0.96	0.52	0.00	0.96
I12	sodo	C3pp	10.59	-9.40	0.51	1.02	0.05	10.59	-9.40
I12	sodo	C3ap	2.69	-1.65	0.44	1.00	0.06	2.69	-1.65
I12	teno	tree	0.80	0.18	0.01	0.97	0.68	0.00	0.97
I12	teno	C3pp	12.08	-10.87	0.48	1.02	0.06	12.08	-10.87
I12	teno	C3ap	3.91	-2.85	0.67	1.00	0.03	3.91	-2.85
I12	vert	tree	-3.09	3.98	0.10	0.94	0.28	0.00	0.94
I12	vert	C3pp	3.73	-2.67	0.20	1.00	0.17	0.00	1.00
I12	vert	C3ap	1.14	-0.13	0.06	1.00	0.40	0.00	1.00
I13	calc	tree	1.49	-0.51	0.17	0.96	0.20	0.00	0.96
I13	calc	C3pp	2.76	-1.71	0.13	1.00	0.24	0.00	1.00
I13	calc	C3ap	1.49	-0.47	0.65	1.00	0.03	1.49	-0.47
I13	derm	tree	1.90	-0.90	0.34	0.98	0.09	1.90	-0.90
I13	derm	C3pp	4.08	-3.03	0.43	0.99	0.13	0.00	0.99
I13	derm	C3ap	1.47	-0.45	0.73	0.99	0.02	1.47	-0.45
I13	ferr	tree	1.52	-0.54	0.27	0.95	0.12	0.00	0.95
I13	ferr	C3pp	2.58	-1.54	0.11	1.00	0.27	0.00	1.00
I13	ferr	C3ap	1.55	-0.53	0.60	1.00	0.03	1.55	-0.53
I13	kand	tree	2.21	-1.20	0.57	0.97	0.04	2.21	-1.20
I13	kand	C3pp	2.52	-1.48	0.15	1.01	0.22	0.00	1.01
I13	kand	C3ap	1.38	-0.36	0.62	1.00	0.03	1.38	-0.36
I13	sodo	tree	1.70	-0.74	0.20	0.93	0.17	0.00	0.93
I13	sodo	C3pp	1.99	-0.97	0.08	0.99	0.33	0.00	0.99
I13	sodo	C3ap	1.71	-0.69	0.64	1.00	0.03	1.71	-0.69
I13	teno	tree	1.94	-0.95	0.42	0.96	0.07	1.94	-0.95
I13	teno	C3pp	2.65	-1.60	0.14	1.01	0.23	0.00	1.01
I13	teno	C3ap	1.59	-0.57	0.59	1.00	0.04	1.59	-0.57
I13	vert	tree	1.92	-0.99	0.18	0.91	0.18	0.00	0.91
I13	vert	C3pp	0.79	0.18	0.02	0.95	0.62	0.00	0.95
I13	vert	C3ap	2.05	-1.04	0.54	0.99	0.04	2.05	-1.04
I14	calc	tree	0.16	0.83	0.00	0.99	0.88	0.00	0.99
I14	calc	C3pp	1.96	-0.93	0.09	1.04	0.31	0.00	1.04
I14	calc	C3ap	1.64	-0.63	0.63	1.02	0.03	1.64	-0.63
I14	derm	tree	-0.09	1.09	0.00	1.00	0.87	0.00	1.00
I14	derm	C3pp	2.67	-1.67	0.07	1.01	0.50	0.00	1.01
I14	derm	C3ap	1.67	-0.66	0.72	1.02	0.02	1.67	-0.66
I14	ferr	tree	-1.23	2.22	0.14	0.98	0.22	0.00	0.98
I14	ferr	C3pp	1.76	-0.74	0.07	1.04	0.36	0.00	1.04
I14	ferr	C3ap	1.72	-0.71	0.57	1.02	0.04	1.72	-0.71

Scenario	Soil type	Vegetation type	Calculated slope	Calculated intercept	r^2	Average RSF	p	Adopted slope	Adopted intercept
l14	kand	tree	0.34	0.66	0.02	1.00	0.62	0.00	1.00
l14	kand	C3pp	1.92	-0.90	0.11	1.04	0.28	0.00	1.04
l14	kand	C3ap	1.44	-0.43	0.59	1.02	0.04	1.44	-0.43
l14	sodo	tree	-2.22	3.20	0.21	0.96	0.16	0.00	0.96
l14	sodo	C3pp	1.00	0.01	0.03	1.02	0.55	0.00	1.02
l14	sodo	C3ap	2.10	-1.08	0.56	1.03	0.04	2.10	-1.08
l14	teno	tree	0.62	0.36	0.05	0.99	0.41	0.00	0.99
l14	teno	C3pp	1.78	-0.75	0.06	1.04	0.38	0.00	1.04
l14	teno	C3ap	1.63	-0.62	0.53	1.02	0.05	1.63	-0.62
l14	vert	tree	-1.45	2.40	0.05	0.94	0.44	0.00	0.94
l14	vert	C3pp	-1.10	2.09	0.05	0.98	0.45	0.00	0.98
l14	vert	C3ap	2.60	-1.59	0.39	1.02	0.08	2.60	-1.59
l15	calc	tree	-0.16	1.20	0.00	1.03	0.85	0.00	1.03
l15	calc	C3pp	3.65	-2.66	0.30	1.06	0.11	0.00	1.06
l15	calc	C3ap	2.25	-1.25	0.50	1.04	0.05	2.25	-1.25
l15	derm	tree	1.39	-0.38	0.13	1.04	0.25	0.00	1.04
l15	derm	C3pp	1.18	-0.15	0.02	1.04	0.72	0.00	1.04
l15	derm	C3ap	2.18	-1.18	0.62	1.04	0.03	2.18	-1.18
l15	ferr	tree	-1.00	2.05	0.04	1.03	0.48	0.00	1.03
l15	ferr	C3pp	4.21	-3.22	0.34	1.06	0.09	4.21	-3.22
l15	ferr	C3ap	2.53	-1.53	0.47	1.04	0.06	2.53	-1.53
l15	kand	tree	-0.92	1.98	0.04	1.04	0.49	0.00	1.04
l15	kand	C3pp	3.56	-2.57	0.31	1.06	0.10	0.00	1.06
l15	kand	C3ap	2.07	-1.07	0.52	1.04	0.05	2.07	-1.07
l15	sodo	tree	2.63	-1.65	0.16	1.03	0.21	0.00	1.03
l15	sodo	C3pp	2.99	-1.99	0.17	1.06	0.20	0.00	1.06
l15	sodo	C3ap	2.99	-2.00	0.58	1.05	0.04	2.99	-2.00
l15	teno	tree	-3.36	4.45	0.31	1.03	0.10	0.00	1.03
l15	teno	C3pp	4.21	-3.22	0.29	1.07	0.11	0.00	1.07
l15	teno	C3ap	2.46	-1.46	0.54	1.04	0.04	2.46	-1.46
l15	vert	tree	-2.96	4.03	0.20	1.02	0.17	0.00	1.02
l15	vert	C3pp	3.48	-2.49	0.20	1.06	0.17	0.00	1.06
l15	vert	C3ap	2.70	-1.69	0.38	1.06	0.08	2.70	-1.69
m01	calc	tree	1.11	0.00	0.43	1.16	0.07	1.11	0.00
m01	calc	C3pp	1.65	-0.49	0.25	1.24	0.13	0.00	1.24
m01	calc	C3ap	1.36	-0.31	0.86	1.10	0.01	1.36	-0.31
m01	derm	tree	0.90	0.21	0.41	1.15	0.07	0.90	0.21
m01	derm	C3pp	0.07	1.20	0.00	1.28	0.98	0.00	1.28
m01	derm	C3ap	1.31	-0.27	0.90	1.10	0.01	1.31	-0.27
m01	ferr	tree	1.28	-0.16	0.32	1.18	0.10	0.00	1.18
m01	ferr	C3pp	1.84	-0.64	0.23	1.28	0.15	0.00	1.28
m01	ferr	C3ap	1.39	-0.34	0.80	1.11	0.01	1.39	-0.34
m01	kand	tree	0.76	0.35	0.28	1.14	0.13	0.00	1.14
m01	kand	C3pp	1.29	-0.13	0.23	1.21	0.15	0.00	1.21
m01	kand	C3ap	1.26	-0.22	0.88	1.10	0.01	1.26	-0.22
m01	sodo	tree	1.62	-0.50	0.41	1.19	0.07	1.62	-0.50
m01	sodo	C3pp	1.69	-0.46	0.16	1.31	0.20	0.00	1.31
m01	sodo	C3ap	1.73	-0.66	0.71	1.14	0.02	1.73	-0.66
m01	teno	tree	1.09	0.02	0.39	1.16	0.08	1.09	0.02
m01	teno	C3pp	1.39	-0.22	0.22	1.23	0.15	0.00	1.23
m01	teno	C3ap	1.20	-0.15	0.79	1.11	0.01	1.20	-0.15
m01	vert	tree	2.23	-1.13	0.49	1.19	0.05	2.23	-1.13
m01	vert	C3pp	1.81	-0.53	0.14	1.36	0.23	0.00	1.36
m01	vert	C3ap	2.25	-1.16	0.61	1.19	0.03	2.25	-1.16
m02	calc	tree	2.05	-1.03	0.30	1.09	0.11	0.00	1.09

Scenario	Soil type	Vegetation type	Calculated slope	Calculated intercept	r^2	Average RSF	p	Adopted slope	Adopted intercept
m02	calc	C3pp	4.60	-3.56	0.13	1.20	0.25	0.00	1.20
m02	calc	C3ap	1.68	-0.65	0.36	1.09	0.09	1.68	-0.65
m02	derm	tree	1.64	-0.60	0.18	1.10	0.19	0.00	1.10
m02	derm	C3pp	4.02	-2.98	0.03	1.17	0.63	0.00	1.17
m02	derm	C3ap	1.63	-0.60	0.45	1.08	0.06	1.63	-0.60
m02	ferr	tree	1.67	-0.62	0.16	1.10	0.21	0.00	1.10
m02	ferr	C3pp	5.35	-4.32	0.15	1.22	0.22	0.00	1.22
m02	ferr	C3ap	1.82	-0.79	0.32	1.10	0.10	1.82	-0.79
m02	kand	tree	1.32	-0.27	0.13	1.09	0.24	0.00	1.09
m02	kand	C3pp	3.86	-2.81	0.11	1.18	0.28	0.00	1.18
m02	kand	C3ap	1.53	-0.51	0.37	1.08	0.08	1.53	-0.51
m02	sodo	tree	0.30	0.78	0.01	1.09	0.77	0.00	1.09
m02	sodo	C3pp	3.27	-2.20	0.13	1.19	0.24	0.00	1.19
m02	sodo	C3ap	1.99	-0.95	0.40	1.11	0.07	1.99	-0.95
m02	teno	tree	0.69	0.37	0.03	1.09	0.56	0.00	1.09
m02	teno	C3pp	4.19	-3.13	0.09	1.21	0.30	0.00	1.21
m02	teno	C3ap	1.71	-0.67	0.30	1.09	0.11	0.00	1.09
m02	vert	tree	-0.86	1.97	0.03	1.08	0.55	0.00	1.08
m02	vert	C3pp	1.87	-0.77	0.15	1.17	0.22	0.00	1.17
m02	vert	C3ap	1.90	-0.84	0.23	1.13	0.15	0.00	1.13
m03	calc	tree	2.66	-1.62	0.24	0.84	0.14	0.00	0.84
m03	calc	C3pp	0.00	0.87	0.00	0.87	1.00	0.00	0.87
m03	calc	C3ap	1.32	-0.28	0.44	0.94	0.06	1.32	-0.28
m03	derm	tree	2.17	-1.17	0.28	0.84	0.12	0.00	0.84
m03	derm	C3pp	1.93	-0.99	0.09	0.80	0.56	0.00	0.80
m03	derm	C3ap	1.30	-0.27	0.50	0.93	0.05	1.30	-0.27
m03	ferr	tree	3.10	-2.02	0.37	0.84	0.08	3.10	-2.02
m03	ferr	C3pp	-0.19	1.05	0.00	0.88	0.91	0.00	0.88
m03	ferr	C3ap	1.39	-0.34	0.42	0.94	0.07	1.39	-0.34
m03	kand	tree	2.26	-1.25	0.31	0.84	0.10	0.00	0.84
m03	kand	C3pp	0.44	0.47	0.01	0.88	0.75	0.00	0.88
m03	kand	C3ap	1.24	-0.20	0.43	0.94	0.07	1.24	-0.20
m03	sodo	tree	2.56	-1.55	0.22	0.81	0.15	0.00	0.81
m03	sodo	C3pp	0.43	0.48	0.00	0.88	0.84	0.00	0.88
m03	sodo	C3ap	2.07	-0.97	0.68	0.94	0.02	2.07	-0.97
m03	teno	tree	2.98	-1.90	0.37	0.84	0.08	2.98	-1.90
m03	teno	C3pp	0.20	0.69	0.00	0.87	0.89	0.00	0.87
m03	teno	C3ap	1.13	-0.11	0.32	0.93	0.10	1.13	-0.11
m03	vert	tree	3.13	-2.07	0.25	0.81	0.14	0.00	0.81
m03	vert	C3pp	2.79	-1.71	0.11	0.86	0.28	0.00	0.86
m03	vert	C3ap	2.79	-1.65	0.51	0.92	0.05	2.79	-1.65
m04	calc	tree	3.26	-2.18	0.55	0.91	0.04	3.26	-2.18
m04	calc	C3pp	2.42	-1.30	0.29	0.99	0.11	0.00	0.99
m04	calc	C3ap	1.70	-0.66	0.84	0.95	0.01	1.70	-0.66
m04	derm	tree	2.79	-1.73	0.64	0.91	0.03	2.79	-1.73
m04	derm	C3pp	1.89	-0.80	0.39	1.01	0.17	0.00	1.01
m04	derm	C3ap	1.73	-0.69	0.87	0.95	0.01	1.73	-0.69
m04	ferr	tree	2.98	-1.92	0.43	0.90	0.07	2.98	-1.92
m04	ferr	C3pp	2.39	-1.27	0.26	0.99	0.13	0.00	0.99
m04	ferr	C3ap	1.83	-0.78	0.83	0.95	0.01	1.83	-0.78
m04	kand	tree	2.82	-1.75	0.62	0.91	0.03	2.82	-1.75
m04	kand	C3pp	2.22	-1.12	0.32	0.98	0.10	0.00	0.98
m04	kand	C3ap	1.58	-0.54	0.84	0.95	0.01	1.58	-0.54
m04	sodo	tree	2.57	-1.59	0.41	0.85	0.07	2.57	-1.59
m04	sodo	C3pp	1.94	-0.85	0.18	0.99	0.19	0.00	0.99

Scenario	Soil type	Vegetation type	Calculated slope	Calculated intercept	r^2	Average RSF	p	Adopted slope	Adopted intercept
m04	sodo	C3ap	2.35	-1.29	0.88	0.93	0.01	2.35	-1.29
m04	teno	tree	3.21	-2.13	0.47	0.91	0.06	3.21	-2.13
m04	teno	C3pp	2.13	-1.02	0.24	0.99	0.14	0.00	0.99
m04	teno	C3ap	1.79	-0.75	0.82	0.95	0.01	1.79	-0.75
m04	vert	tree	2.81	-1.84	0.28	0.82	0.12	0.00	0.82
m04	vert	C3pp	1.79	-0.76	0.13	0.94	0.24	0.00	0.94
m04	vert	C3ap	3.19	-2.11	0.79	0.91	0.01	3.19	-2.11
m05	calc	tree	1.12	-0.10	0.26	0.96	0.13	0.00	0.96
m05	calc	C3pp	2.17	-1.06	0.13	1.01	0.25	0.00	1.01
m05	calc	C3ap	2.23	-1.14	0.82	0.99	0.01	2.23	-1.14
m05	derm	tree	1.33	-0.30	0.33	0.97	0.10	1.33	-0.30
m05	derm	C3pp	-4.19	5.05	0.18	1.01	0.34	0.00	1.01
m05	derm	C3ap	2.13	-1.04	0.83	0.98	0.01	2.13	-1.04
m05	ferr	tree	1.71	-0.66	0.44	0.97	0.06	1.71	-0.66
m05	ferr	C3pp	2.36	-1.22	0.13	1.03	0.25	0.00	1.03
m05	ferr	C3ap	2.40	-1.29	0.80	0.99	0.01	2.40	-1.29
m05	kand	tree	1.38	-0.34	0.44	0.97	0.06	1.38	-0.34
m05	kand	C3pp	1.93	-0.83	0.12	1.00	0.26	0.00	1.00
m05	kand	C3ap	2.03	-0.95	0.80	0.99	0.01	2.03	-0.95
m05	sodo	tree	1.63	-0.62	0.41	0.93	0.07	1.63	-0.62
m05	sodo	C3pp	2.60	-1.42	0.17	1.05	0.20	0.00	1.05
m05	sodo	C3ap	3.01	-1.87	0.87	1.00	0.01	3.01	-1.87
m05	teno	tree	1.80	-0.76	0.53	0.96	0.05	1.80	-0.76
m05	teno	C3pp	2.18	-1.06	0.12	1.01	0.27	0.00	1.01
m05	teno	C3ap	2.13	-1.04	0.73	0.99	0.02	2.13	-1.04
m05	vert	tree	1.33	-0.37	0.30	0.89	0.11	0.00	0.89
m05	vert	C3pp	3.13	-1.91	0.27	1.07	0.12	0.00	1.07
m05	vert	C3ap	3.82	-2.64	0.89	1.00	0.01	3.82	-2.64
m06	calc	tree	2.89	-1.75	0.68	0.85	0.02	2.89	-1.75
m06	calc	C3pp	3.77	-2.57	0.52	0.81	0.05	3.77	-2.57
m06	calc	C3ap	2.65	-1.53	0.94	0.85	0.00	2.65	-1.53
m06	derm	tree	2.47	-1.36	0.74	0.86	0.02	2.47	-1.36
m06	derm	C3pp	-3.63	4.27	0.21	0.91	0.30	0.00	0.91
m06	derm	C3ap	2.40	-1.30	0.94	0.85	0.00	2.40	-1.30
m06	ferr	tree	3.13	-1.98	0.70	0.84	0.02	3.13	-1.98
m06	ferr	C3pp	4.27	-3.03	0.52	0.80	0.05	4.27	-3.03
m06	ferr	C3ap	2.93	-1.79	0.94	0.84	0.00	2.93	-1.79
m06	kand	tree	2.60	-1.48	0.72	0.86	0.02	2.60	-1.48
m06	kand	C3pp	3.56	-2.38	0.56	0.82	0.04	3.56	-2.38
m06	kand	C3ap	2.41	-1.30	0.93	0.86	0.00	2.41	-1.30
m06	sodo	tree	3.58	-2.40	0.80	0.82	0.01	3.58	-2.40
m06	sodo	C3pp	3.65	-2.44	0.38	0.84	0.08	3.65	-2.44
m06	sodo	C3ap	3.34	-2.18	0.95	0.82	0.00	3.34	-2.18
m06	teno	tree	3.05	-1.91	0.76	0.83	0.02	3.05	-1.91
m06	teno	C3pp	4.58	-3.32	0.60	0.79	0.03	4.58	-3.32
m06	teno	C3ap	2.67	-1.55	0.92	0.85	0.01	2.67	-1.55
m06	vert	tree	3.95	-2.74	0.72	0.80	0.02	3.95	-2.74
m06	vert	C3pp	3.79	-2.56	0.46	0.84	0.06	3.79	-2.56
m06	vert	C3ap	3.98	-2.78	0.92	0.80	0.00	3.98	-2.78
m07	calc	tree	0.56	0.38	0.02	0.93	0.63	0.00	0.93
m07	calc	C3pp	3.91	-2.89	0.06	0.93	0.41	0.00	0.93
m07	calc	C3ap	1.49	-0.49	0.37	0.97	0.08	1.49	-0.49
m07	derm	tree	1.46	-0.49	0.10	0.94	0.30	0.00	0.94
m07	derm	C3pp	7.71	-6.61	0.23	0.92	0.27	0.00	0.92
m07	derm	C3ap	1.50	-0.49	0.46	0.97	0.06	1.50	-0.49

Scenario	Soil type	Vegetation type	Calculated slope	Calculated intercept	r^2	Average RSF	p	Adopted slope	Adopted intercept
m07	ferr	tree	1.29	-0.34	0.05	0.92	0.44	0.00	0.92
m07	ferr	C3pp	3.92	-2.92	0.04	0.91	0.46	0.00	0.91
m07	ferr	C3ap	1.60	-0.59	0.30	0.97	0.11	0.00	0.97
m07	kand	tree	1.25	-0.28	0.10	0.94	0.30	0.00	0.94
m07	kand	C3pp	3.72	-2.69	0.06	0.94	0.38	0.00	0.94
m07	kand	C3ap	1.37	-0.36	0.38	0.97	0.08	1.37	-0.36
m07	sodo	tree	0.70	0.21	0.01	0.89	0.68	0.00	0.89
m07	sodo	C3pp	1.95	-1.01	0.01	0.90	0.69	0.00	0.90
m07	sodo	C3ap	1.81	-0.81	0.15	0.95	0.21	0.00	0.95
m07	teno	tree	1.95	-0.97	0.16	0.93	0.20	0.00	0.93
m07	teno	C3pp	4.37	-3.33	0.06	0.93	0.38	0.00	0.93
m07	teno	C3ap	1.73	-0.72	0.37	0.97	0.08	1.73	-0.72
m07	vert	tree	0.40	0.49	0.00	0.88	0.85	0.00	0.88
m07	vert	C3pp	-0.16	1.03	0.00	0.88	0.96	0.00	0.88
m07	vert	C3ap	1.35	-0.38	0.04	0.94	0.47	0.00	0.94
m08	calc	tree	3.14	-2.12	0.81	0.91	0.01	3.14	-2.12
m08	calc	C3pp	5.18	-4.03	0.47	0.96	0.06	5.18	-4.03
m08	calc	C3ap	1.89	-0.84	0.83	0.98	0.01	1.89	-0.84
m08	derm	tree	2.95	-1.92	0.80	0.92	0.01	2.95	-1.92
m08	derm	C3pp	4.93	-3.86	0.41	0.87	0.16	0.00	0.87
m08	derm	C3ap	1.82	-0.78	0.88	0.97	0.01	1.82	-0.78
m08	ferr	tree	3.26	-2.23	0.74	0.91	0.02	3.26	-2.23
m08	ferr	C3pp	5.60	-4.43	0.46	0.97	0.06	5.60	-4.43
m08	ferr	C3ap	2.02	-0.97	0.82	0.98	0.01	2.02	-0.97
m08	kand	tree	2.86	-1.83	0.88	0.92	0.01	2.86	-1.83
m08	kand	C3pp	4.44	-3.32	0.48	0.96	0.06	4.44	-3.32
m08	kand	C3ap	1.76	-0.72	0.82	0.98	0.01	1.76	-0.72
m08	sodo	tree	3.27	-2.28	0.69	0.87	0.02	3.27	-2.28
m08	sodo	C3pp	5.74	-4.58	0.41	0.96	0.07	5.74	-4.58
m08	sodo	C3ap	2.24	-1.18	0.86	0.98	0.01	2.24	-1.18
m08	teno	tree	3.17	-2.14	0.85	0.91	0.01	3.17	-2.14
m08	teno	C3pp	4.67	-3.53	0.42	0.97	0.07	4.67	-3.53
m08	teno	C3ap	1.98	-0.93	0.81	0.98	0.01	1.98	-0.93
m08	vert	tree	3.15	-2.18	0.56	0.86	0.04	3.15	-2.18
m08	vert	C3pp	5.67	-4.52	0.44	0.95	0.06	5.67	-4.52
m08	vert	C3ap	2.76	-1.69	0.77	0.97	0.02	2.76	-1.69
m09	calc	tree	1.21	-0.27	0.68	0.84	0.03	1.21	-0.27
m09	calc	C3pp	0.83	-0.05	0.15	0.71	0.21	0.00	0.71
m09	calc	C3ap	2.32	-1.25	0.92	0.86	0.00	2.32	-1.25
m09	derm	tree	1.11	-0.16	0.82	0.85	0.01	1.11	-0.16
m09	derm	C3pp	-0.63	1.35	0.06	0.75	0.57	0.00	0.75
m09	derm	C3ap	2.09	-1.04	0.92	0.87	0.00	2.09	-1.04
m09	ferr	tree	1.47	-0.51	0.74	0.83	0.02	1.47	-0.51
m09	ferr	C3pp	1.05	-0.26	0.19	0.70	0.18	0.00	0.70
m09	ferr	C3ap	2.54	-1.46	0.91	0.86	0.01	2.54	-1.46
m09	kand	tree	1.14	-0.19	0.68	0.84	0.03	1.14	-0.19
m09	kand	C3pp	0.78	0.02	0.15	0.73	0.22	0.00	0.73
m09	kand	C3ap	2.09	-1.03	0.92	0.87	0.01	2.09	-1.03
m09	sodo	tree	2.11	-1.11	0.75	0.81	0.02	2.11	-1.11
m09	sodo	C3pp	1.03	-0.21	0.23	0.73	0.15	0.00	0.73
m09	sodo	C3ap	3.36	-2.21	0.93	0.85	0.00	3.36	-2.21
m09	teno	tree	1.37	-0.42	0.77	0.82	0.02	1.37	-0.42
m09	teno	C3pp	1.21	-0.40	0.20	0.70	0.17	0.00	0.70
m09	teno	C3ap	2.16	-1.11	0.90	0.86	0.01	2.16	-1.11
m09	vert	tree	3.02	-1.94	0.72	0.82	0.02	3.02	-1.94

Scenario	Soil type	Vegetation type	Calculated slope	Calculated intercept	r^2	Average RSF	p	Adopted slope	Adopted intercept
m09	vert	C3pp	2.22	-1.24	0.56	0.78	0.04	2.22	-1.24
m09	vert	C3ap	4.48	-3.23	0.93	0.85	0.00	4.48	-3.23
m10	calc	tree	2.93	-1.94	0.79	1.16	0.01	2.93	-1.94
m10	calc	C3pp	2.49	-1.33	0.67	1.30	0.03	2.49	-1.33
m10	calc	C3ap	1.31	-0.24	0.64	1.15	0.03	1.31	-0.24
m10	derm	tree	2.35	-1.34	0.76	1.15	0.02	2.35	-1.34
m10	derm	C3pp	2.45	-1.34	0.72	1.28	0.04	2.45	-1.34
m10	derm	C3ap	1.38	-0.33	0.77	1.14	0.02	1.38	-0.33
m10	ferr	tree	3.36	-2.37	0.77	1.19	0.02	3.36	-2.37
m10	ferr	C3pp	2.96	-1.78	0.64	1.35	0.03	2.96	-1.78
m10	ferr	C3ap	1.36	-0.28	0.58	1.16	0.04	1.36	-0.28
m10	kand	tree	2.28	-1.27	0.75	1.14	0.02	2.28	-1.27
m10	kand	C3pp	2.11	-0.97	0.67	1.26	0.03	2.11	-0.97
m10	kand	C3ap	1.23	-0.17	0.68	1.14	0.03	1.23	-0.17
m10	sodo	tree	3.98	-3.01	0.67	1.20	0.03	3.98	-3.01
m10	sodo	C3pp	3.96	-2.84	0.84	1.36	0.01	3.96	-2.84
m10	sodo	C3ap	2.29	-1.22	0.78	1.20	0.01	2.29	-1.22
m10	teno	tree	2.80	-1.80	0.73	1.16	0.02	2.80	-1.80
m10	teno	C3pp	2.10	-0.92	0.45	1.31	0.06	2.10	-0.92
m10	teno	C3ap	1.32	-0.24	0.63	1.15	0.03	1.32	-0.24
m10	vert	tree	4.17	-3.23	0.52	1.18	0.05	4.17	-3.23
m10	vert	C3pp	5.84	-4.80	0.89	1.39	0.01	5.84	-4.80
m10	vert	C3ap	3.29	-2.23	0.82	1.25	0.01	3.29	-2.23
m11	calc	tree	2.06	-1.08	0.85	1.06	0.01	2.06	-1.08
m11	calc	C3pp	3.44	-2.30	0.60	1.29	0.04	3.44	-2.30
m11	calc	C3ap	1.74	-0.68	0.74	1.13	0.02	1.74	-0.68
m11	derm	tree	1.97	-0.98	0.93	1.07	0.00	1.97	-0.98
m11	derm	C3pp	2.61	-1.46	0.27	1.26	0.21	0.00	1.26
m11	derm	C3ap	1.69	-0.65	0.82	1.11	0.01	1.69	-0.65
m11	ferr	tree	2.35	-1.36	0.74	1.08	0.02	2.35	-1.36
m11	ferr	C3pp	3.82	-2.66	0.55	1.31	0.04	3.82	-2.66
m11	ferr	C3ap	1.87	-0.81	0.71	1.14	0.02	1.87	-0.81
m11	kand	tree	1.76	-0.78	0.85	1.06	0.01	1.76	-0.78
m11	kand	C3pp	3.04	-1.91	0.64	1.26	0.03	3.04	-1.91
m11	kand	C3ap	1.59	-0.54	0.76	1.11	0.02	1.59	-0.54
m11	sodo	tree	1.87	-0.91	0.72	1.04	0.02	1.87	-0.91
m11	sodo	C3pp	3.21	-2.11	0.66	1.24	0.03	3.21	-2.11
m11	sodo	C3ap	2.25	-1.19	0.79	1.15	0.01	2.25	-1.19
m11	teno	tree	2.07	-1.07	0.89	1.08	0.01	2.07	-1.07
m11	teno	C3pp	3.20	-2.04	0.47	1.30	0.06	3.20	-2.04
m11	teno	C3ap	1.74	-0.69	0.74	1.13	0.02	1.74	-0.69
m11	vert	tree	1.63	-0.69	0.64	1.01	0.03	1.63	-0.69
m11	vert	C3pp	2.29	-1.24	0.57	1.15	0.04	2.29	-1.24
m11	vert	C3ap	2.70	-1.65	0.81	1.16	0.01	2.70	-1.65
m12	calc	tree	0.60	0.37	0.02	0.94	0.60	0.00	0.94
m12	calc	C3pp	13.84	-12.25	0.53	1.05	0.05	13.84	-12.25
m12	calc	C3ap	3.34	-2.22	0.67	0.99	0.03	3.34	-2.22
m12	derm	tree	2.22	-1.17	0.35	0.96	0.09	2.22	-1.17
m12	derm	C3pp	10.18	-8.74	0.41	1.01	0.13	0.00	1.01
m12	derm	C3ap	3.05	-1.95	0.71	0.98	0.02	3.05	-1.95
m12	ferr	tree	1.02	-0.04	0.03	0.94	0.52	0.00	0.94
m12	ferr	C3pp	15.54	-13.88	0.52	1.06	0.05	15.54	-13.88
m12	ferr	C3ap	3.72	-2.59	0.63	0.99	0.03	3.72	-2.59
m12	kand	tree	1.29	-0.28	0.09	0.95	0.31	0.00	0.95
m12	kand	C3pp	11.93	-10.43	0.51	1.04	0.05	11.93	-10.43

Scenario	Soil type	Vegetation type	Calculated slope	Calculated intercept	r^2	Average RSF	p	Adopted slope	Adopted intercept
m12	kand	C3ap	3.25	-2.14	0.68	0.99	0.02	3.25	-2.14
m12	sodo	tree	-0.85	1.72	0.03	0.91	0.53	0.00	0.91
m12	sodo	C3pp	11.65	-10.14	0.51	1.06	0.05	11.65	-10.14
m12	sodo	C3ap	3.08	-1.98	0.54	0.98	0.04	3.08	-1.98
m12	teno	tree	1.03	-0.05	0.04	0.94	0.50	0.00	0.94
m12	teno	C3pp	13.63	-12.04	0.50	1.06	0.05	13.63	-12.04
m12	teno	C3ap	4.16	-3.00	0.68	0.99	0.03	4.16	-3.00
m12	vert	tree	-1.78	2.59	0.06	0.87	0.39	0.00	0.87
m12	vert	C3pp	4.53	-3.35	0.26	1.01	0.13	0.00	1.01
m12	vert	C3ap	1.54	-0.51	0.12	0.96	0.26	0.00	0.96
m13	calc	tree	1.27	-0.32	0.18	0.91	0.19	0.00	0.91
m13	calc	C3pp	2.43	-1.31	0.11	1.04	0.27	0.00	1.04
m13	calc	C3ap	1.47	-0.43	0.61	0.99	0.03	1.47	-0.43
m13	derm	tree	1.42	-0.44	0.29	0.94	0.11	0.00	0.94
m13	derm	C3pp	3.94	-2.78	0.52	1.01	0.10	0.00	1.01
m13	derm	C3ap	1.44	-0.41	0.67	0.98	0.03	1.44	-0.41
m13	ferr	tree	1.21	-0.26	0.13	0.91	0.25	0.00	0.91
m13	ferr	C3pp	2.30	-1.19	0.09	1.03	0.31	0.00	1.03
m13	ferr	C3ap	1.55	-0.50	0.58	0.99	0.04	1.55	-0.50
m13	kand	tree	1.50	-0.51	0.30	0.94	0.11	0.00	0.94
m13	kand	C3pp	2.14	-1.03	0.11	1.03	0.29	0.00	1.03
m13	kand	C3ap	1.38	-0.34	0.59	0.99	0.04	1.38	-0.34
m13	sodo	tree	1.18	-0.29	0.18	0.84	0.19	0.00	0.84
m13	sodo	C3pp	1.45	-0.40	0.05	1.00	0.45	0.00	1.00
m13	sodo	C3ap	1.71	-0.68	0.66	0.97	0.03	1.71	-0.68
m13	teno	tree	1.28	-0.31	0.17	0.92	0.19	0.00	0.92
m13	teno	C3pp	2.57	-1.43	0.13	1.05	0.24	0.00	1.05
m13	teno	C3ap	1.57	-0.53	0.56	0.99	0.04	1.57	-0.53
m13	vert	tree	0.98	-0.14	0.08	0.81	0.34	0.00	0.81
m13	vert	C3pp	0.53	0.39	0.01	0.90	0.73	0.00	0.90
m13	vert	C3ap	1.87	-0.87	0.51	0.94	0.05	1.87	-0.87
m14	calc	tree	0.82	0.13	0.07	0.97	0.35	0.00	0.97
m14	calc	C3pp	1.99	-0.91	0.08	1.11	0.35	0.00	1.11
m14	calc	C3ap	1.78	-0.76	0.67	1.04	0.03	1.78	-0.76
m14	derm	tree	0.59	0.40	0.12	0.99	0.25	0.00	0.99
m14	derm	C3pp	1.29	-0.26	0.02	1.05	0.73	0.00	1.05
m14	derm	C3ap	1.73	-0.72	0.72	1.04	0.02	1.73	-0.72
m14	ferr	tree	0.61	0.35	0.04	0.96	0.50	0.00	0.96
m14	ferr	C3pp	1.89	-0.81	0.07	1.11	0.38	0.00	1.11
m14	ferr	C3ap	1.93	-0.90	0.64	1.05	0.03	1.93	-0.90
m14	kand	tree	0.79	0.19	0.11	0.99	0.27	0.00	0.99
m14	kand	C3pp	1.82	-0.74	0.08	1.11	0.33	0.00	1.11
m14	kand	C3ap	1.57	-0.55	0.63	1.04	0.03	1.57	-0.55
m14	sodo	tree	-0.80	1.72	0.05	0.91	0.43	0.00	0.91
m14	sodo	C3pp	1.13	-0.09	0.03	1.05	0.51	0.00	1.05
m14	sodo	C3ap	2.28	-1.27	0.69	1.04	0.02	2.28	-1.27
m14	teno	tree	1.04	-0.08	0.12	0.97	0.25	0.00	0.97
m14	teno	C3pp	1.83	-0.74	0.05	1.11	0.42	0.00	1.11
m14	teno	C3ap	1.71	-0.69	0.57	1.04	0.04	1.71	-0.69
m14	vert	tree	-0.26	1.15	0.00	0.88	0.83	0.00	0.88
m14	vert	C3pp	-0.87	1.84	0.03	0.96	0.54	0.00	0.96
m14	vert	C3ap	2.67	-1.69	0.45	1.02	0.06	2.67	-1.69
m15	calc	tree	2.18	-1.19	0.49	1.08	0.05	2.18	-1.19
m15	calc	C3pp	3.47	-2.45	0.25	1.17	0.13	0.00	1.17
m15	calc	C3ap	2.14	-1.15	0.47	1.09	0.06	2.14	-1.15

Scenario	Soil type	Vegetation type	Calculated slope	Calculated intercept	r^2	Average RSF	p	Adopted slope	Adopted intercept
m15	derm	tree	1.73	-0.72	0.36	1.09	0.09	1.73	-0.72
m15	derm	C3pp	0.48	0.64	0.00	1.14	0.90	0.00	1.14
m15	derm	C3ap	2.03	-1.04	0.55	1.08	0.04	2.03	-1.04
m15	ferr	tree	2.00	-1.01	0.43	1.08	0.07	2.00	-1.01
m15	ferr	C3pp	4.26	-3.26	0.29	1.17	0.11	0.00	1.17
m15	ferr	C3ap	2.37	-1.37	0.44	1.09	0.06	2.37	-1.37
m15	kand	tree	1.08	-0.04	0.15	1.08	0.22	0.00	1.08
m15	kand	C3pp	3.21	-2.19	0.23	1.16	0.15	0.00	1.16
m15	kand	C3ap	1.94	-0.94	0.48	1.08	0.05	1.94	-0.94
m15	sodo	tree	2.02	-1.04	0.42	1.06	0.07	2.02	-1.04
m15	sodo	C3pp	2.84	-1.81	0.15	1.15	0.21	0.00	1.15
m15	sodo	C3ap	2.77	-1.78	0.52	1.10	0.05	2.77	-1.78
m15	teno	tree	1.08	-0.05	0.15	1.08	0.22	0.00	1.08
m15	teno	C3pp	3.67	-2.65	0.18	1.18	0.18	0.00	1.18
m15	teno	C3ap	2.28	-1.29	0.48	1.09	0.06	2.28	-1.29
m15	vert	tree	1.15	-0.15	0.08	1.05	0.34	0.00	1.05
m15	vert	C3pp	3.09	-2.10	0.16	1.12	0.20	0.00	1.12
m15	vert	C3ap	2.81	-1.81	0.48	1.11	0.06	2.81	-1.81

10 Appendix III – Recharge scaling factor maps under Scenario C

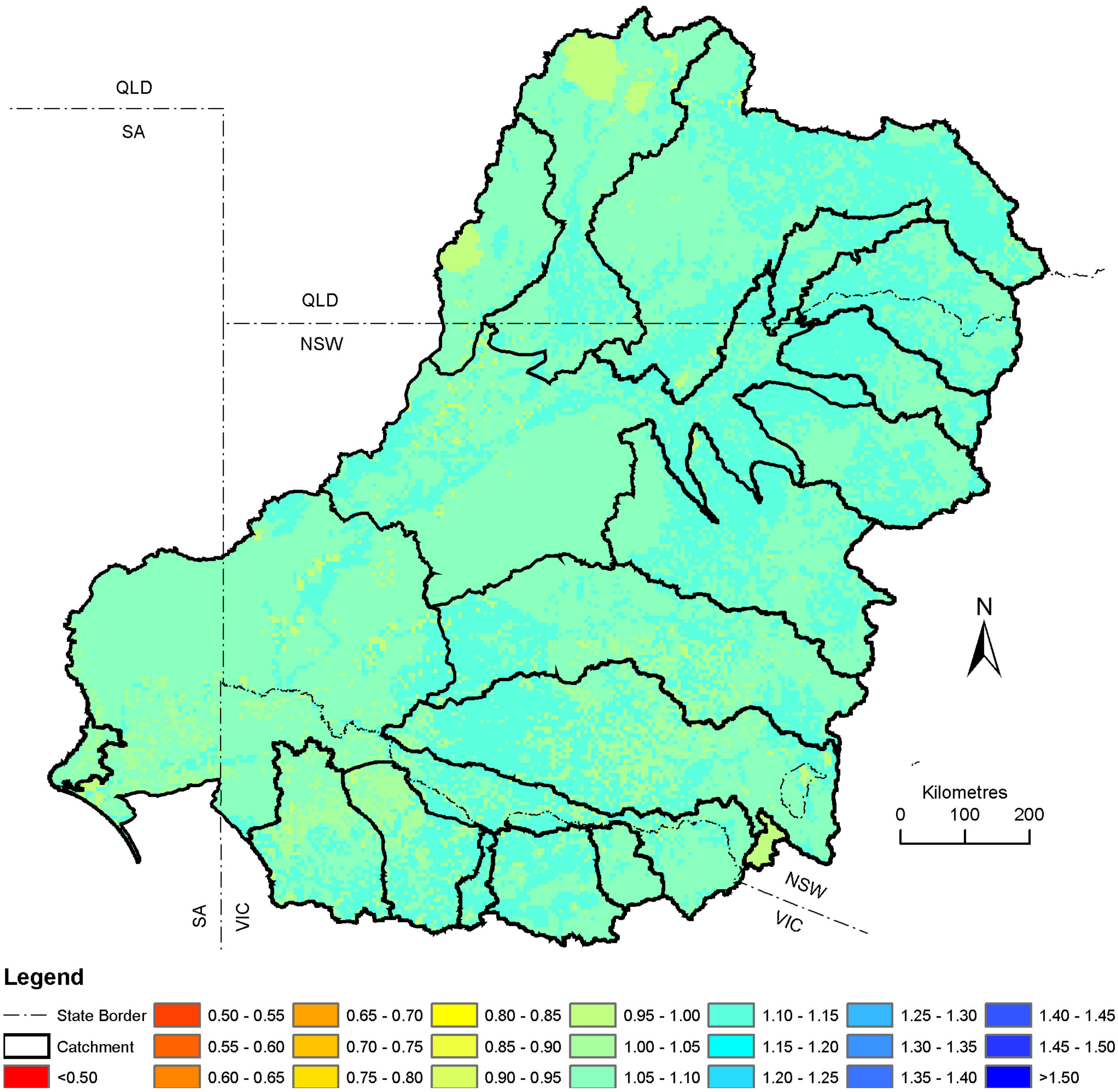

Figure 10-1. Recharge scaling factors for the cccma_t47 global climate model under the low global warming scenario

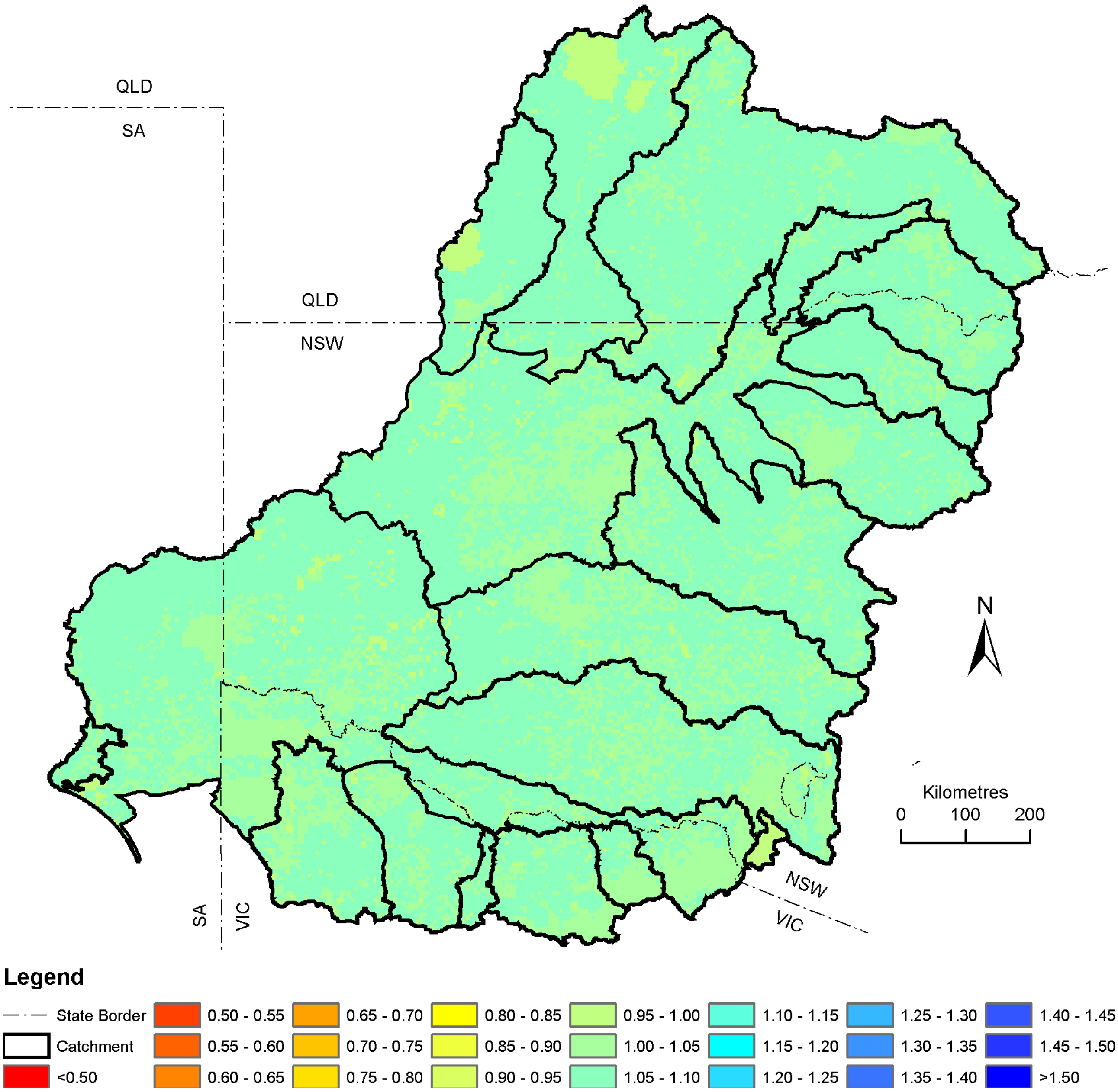

Figure 10-2. Recharge scaling factors for the cccma_t63 global climate model under the low global warming scenario

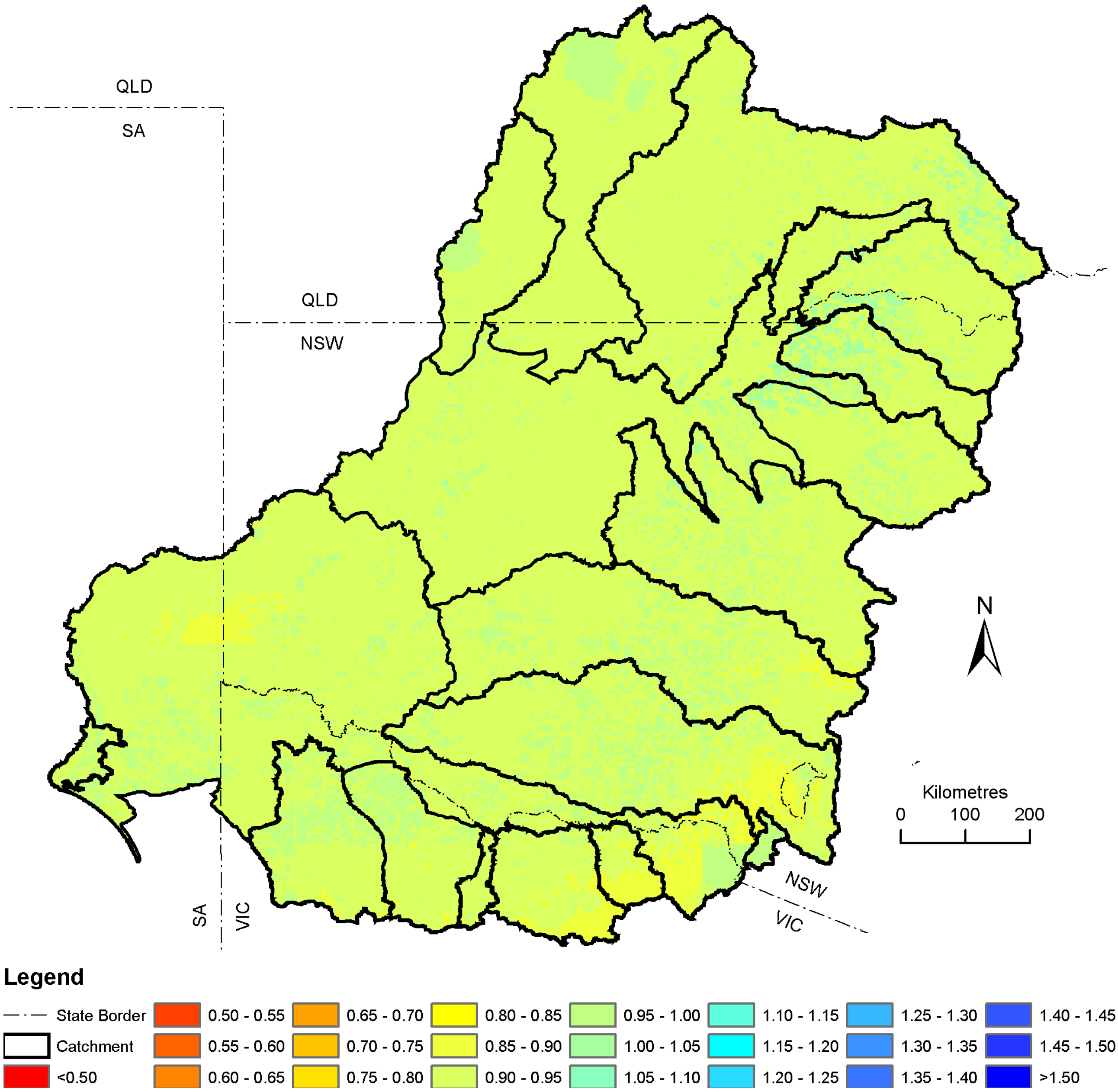

Figure 10-3. Recharge scaling factors for the cnrm global climate model under the low global warming scenario

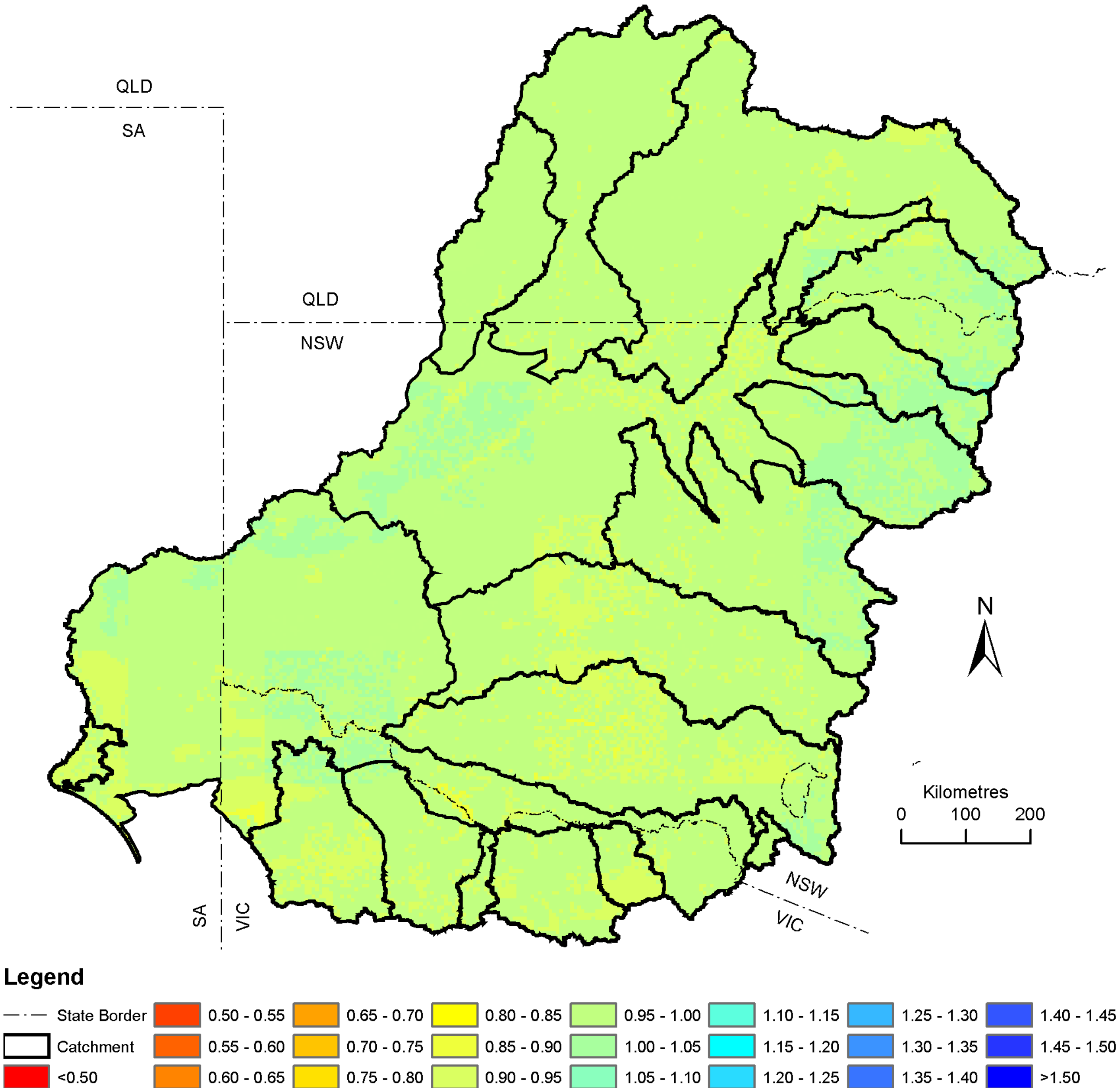

Figure 10-4. Recharge scaling factors for the csiro global climate model under the low global warming scenario

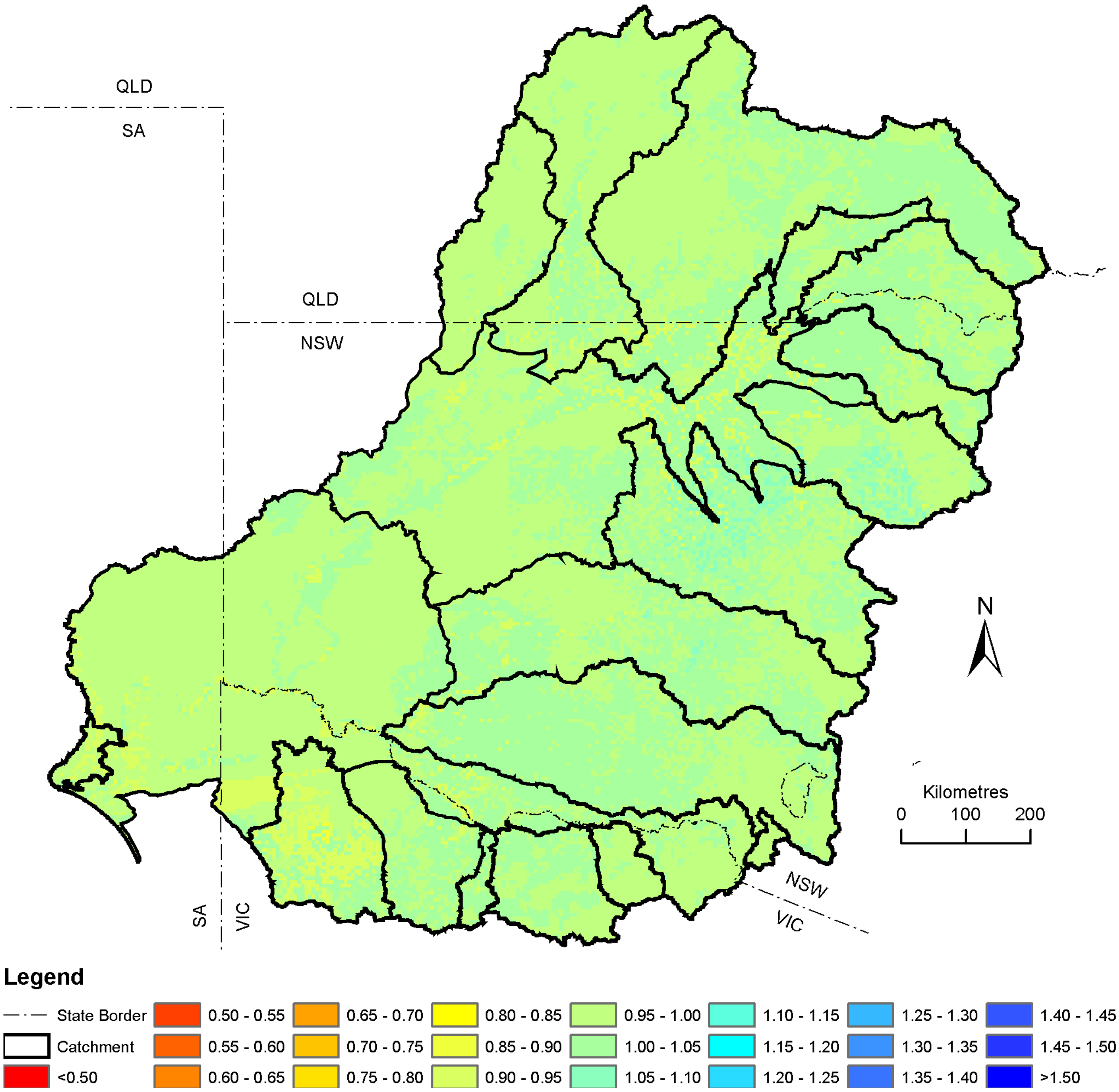

Figure 10-5. Recharge scaling factors for the gfdl global climate model under the low global warming scenario

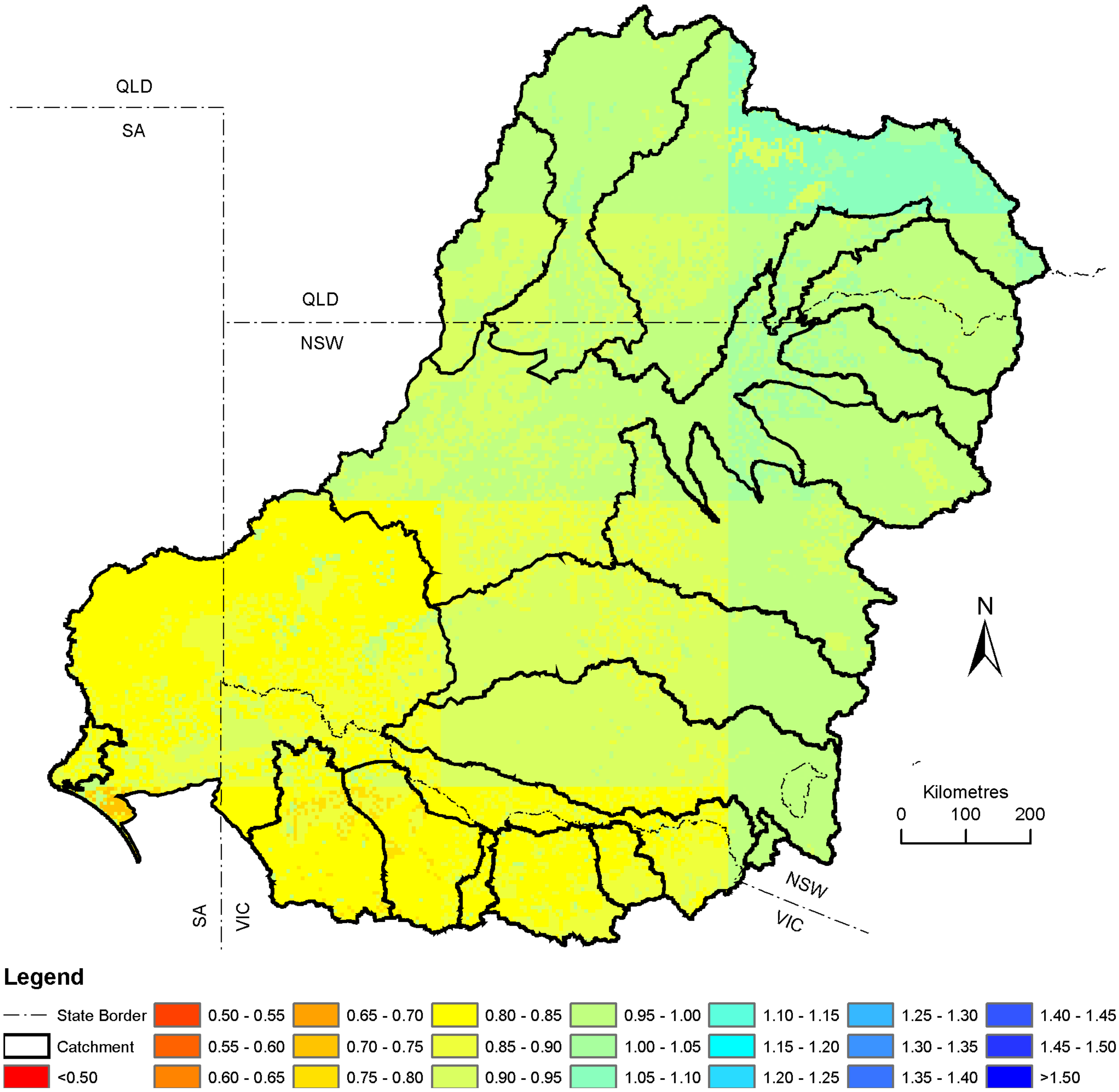

Figure 10-6. Recharge scaling factors for the giss_aom global climate model under the low global warming scenario

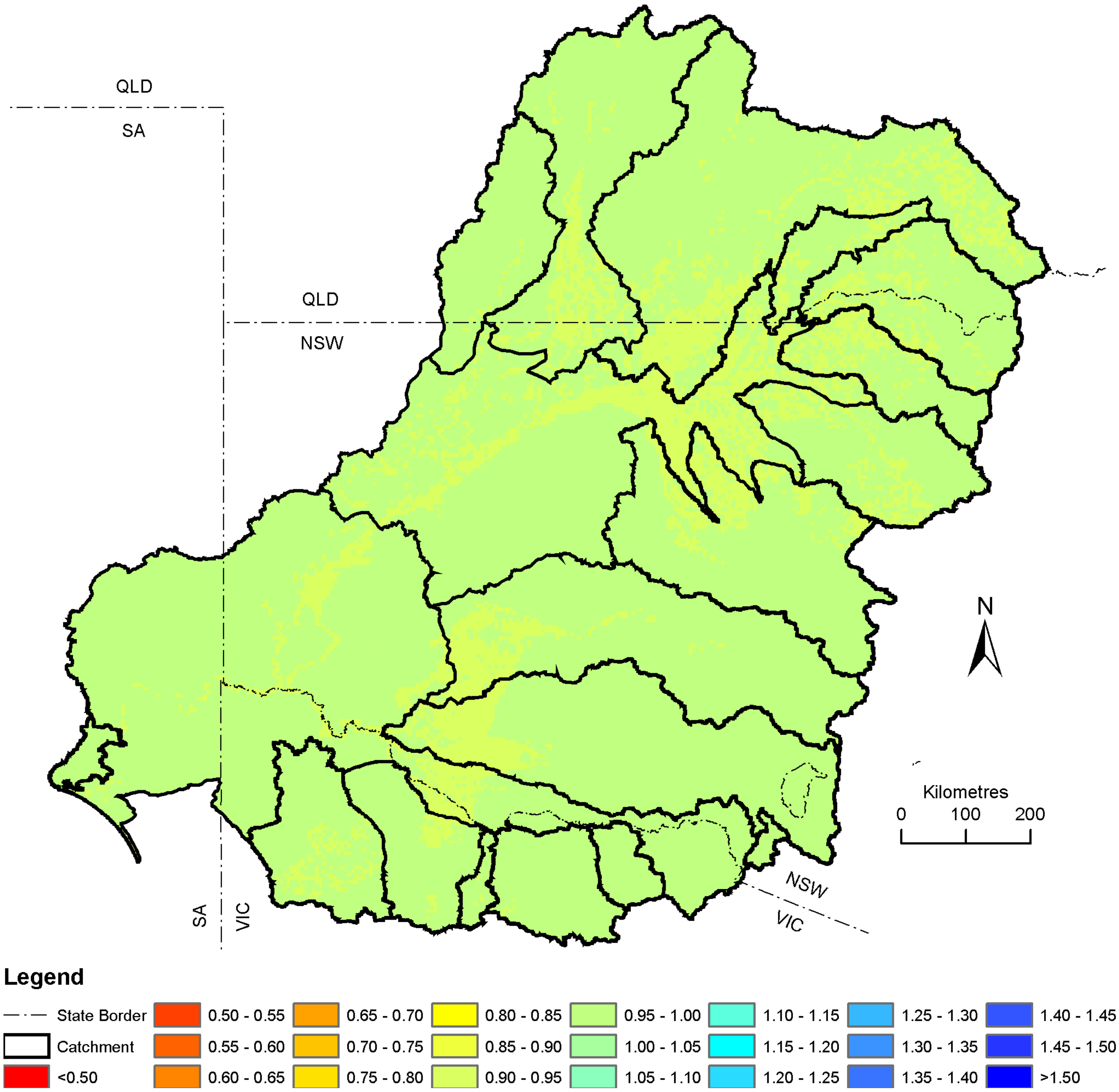

Figure 10-7. Recharge scaling factors for the iap global climate model under the low global warming scenario

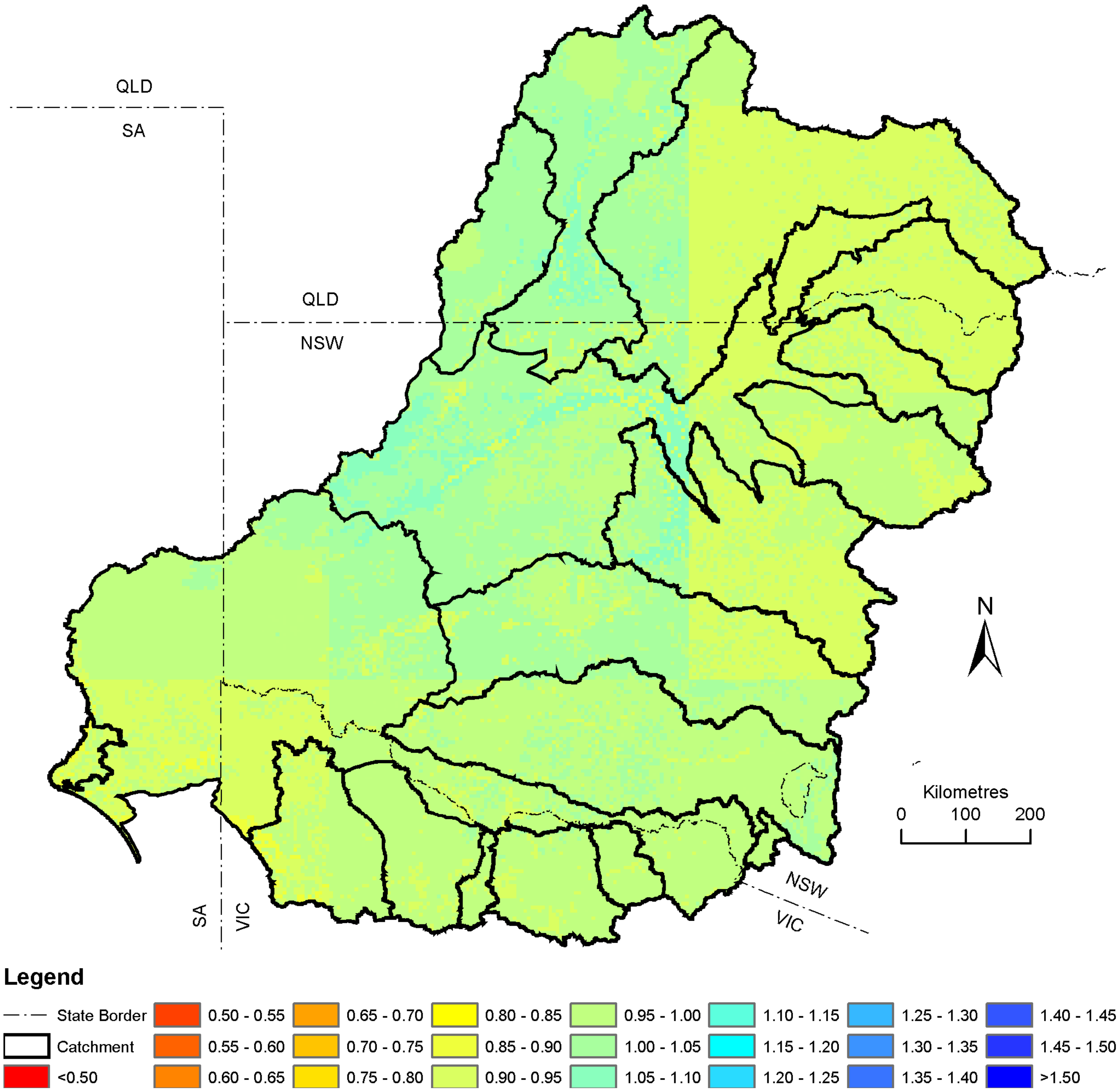

Figure 10-8. Recharge scaling factors for the inmcm global climate model under the low global warming scenario

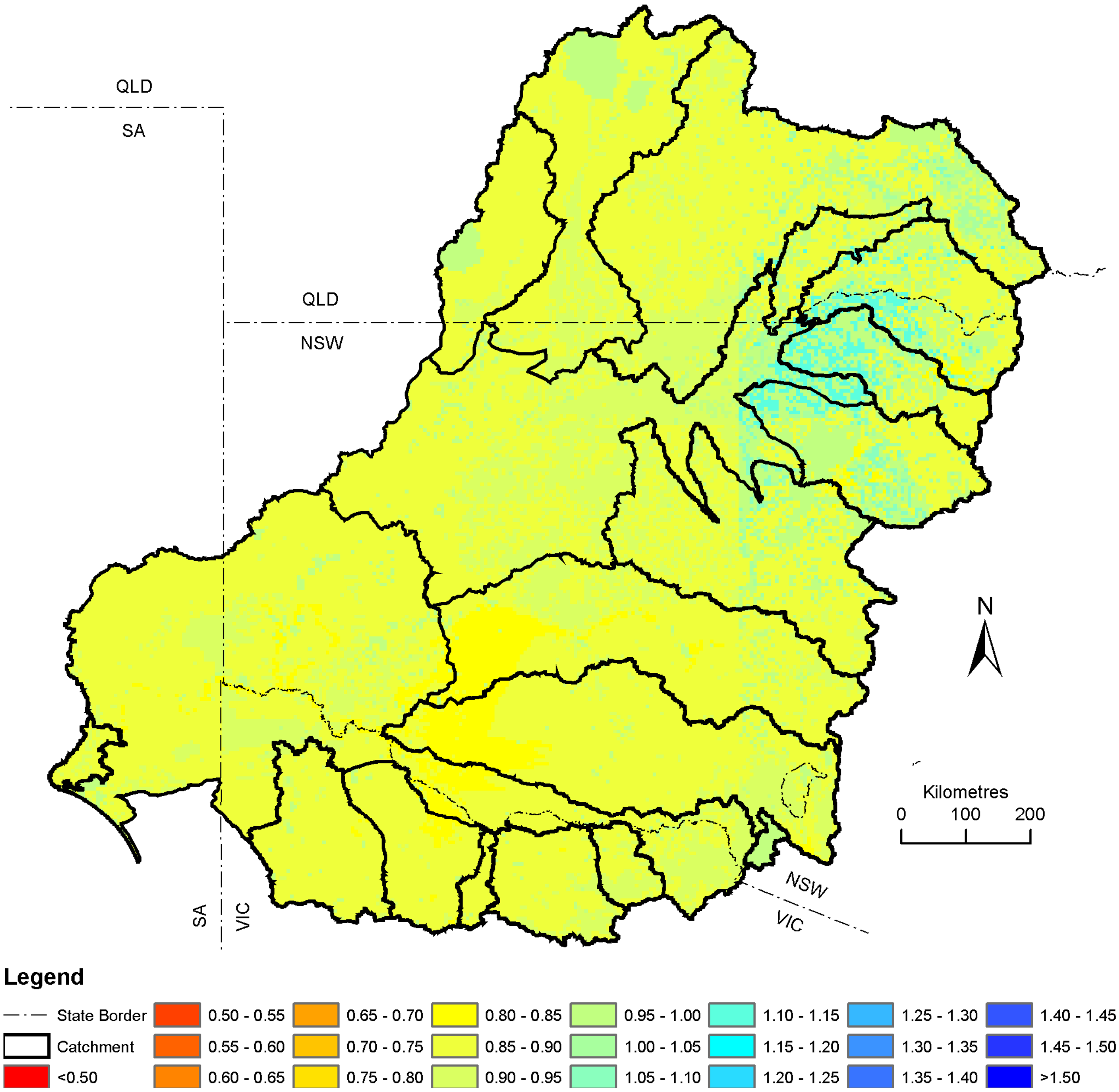

Figure 10-9. Recharge scaling factors for the ipsl global climate model under the low global warming scenario

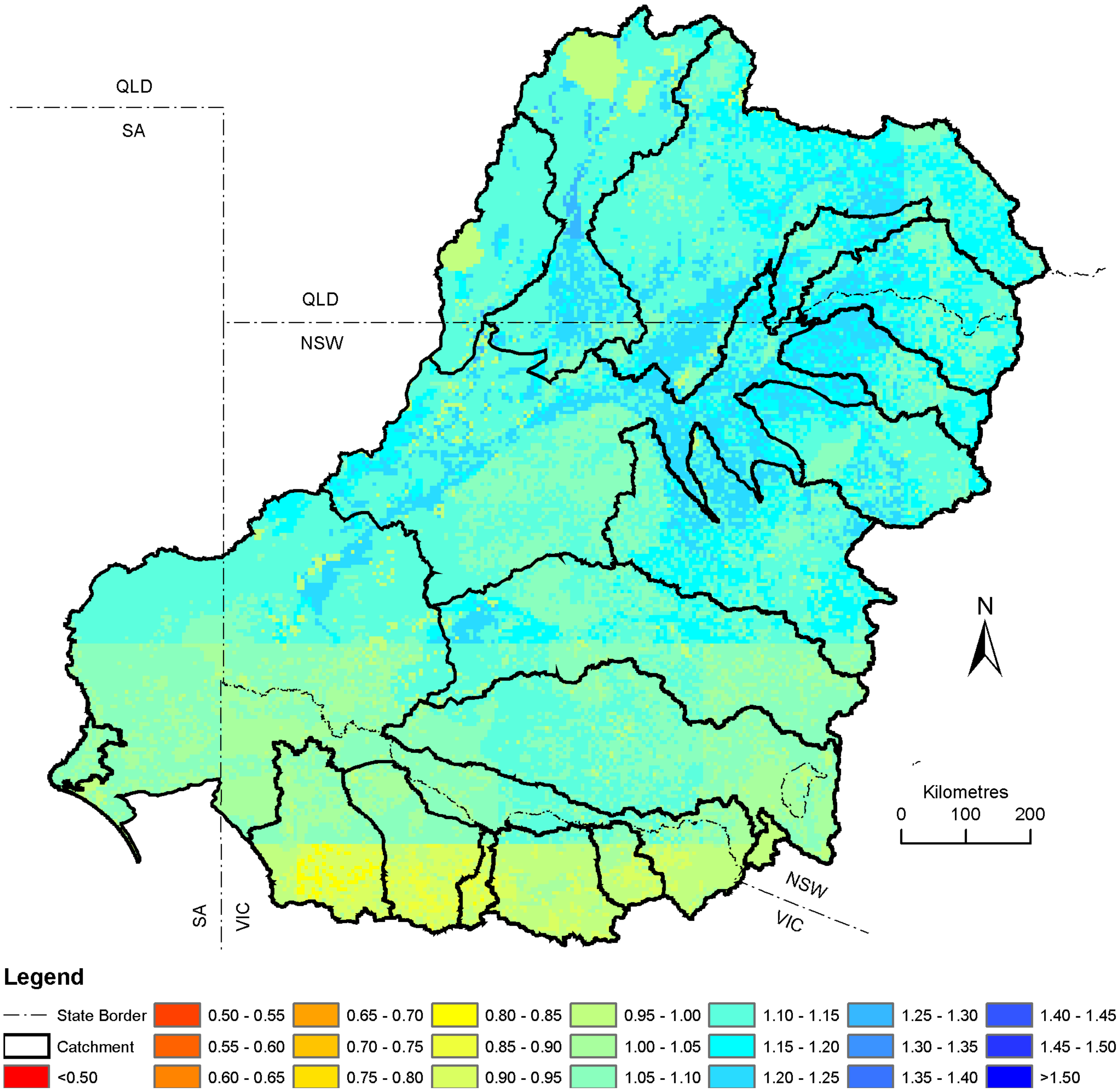

Figure 10-10. Recharge scaling factors for the miroc global climate model under the low global warming scenario

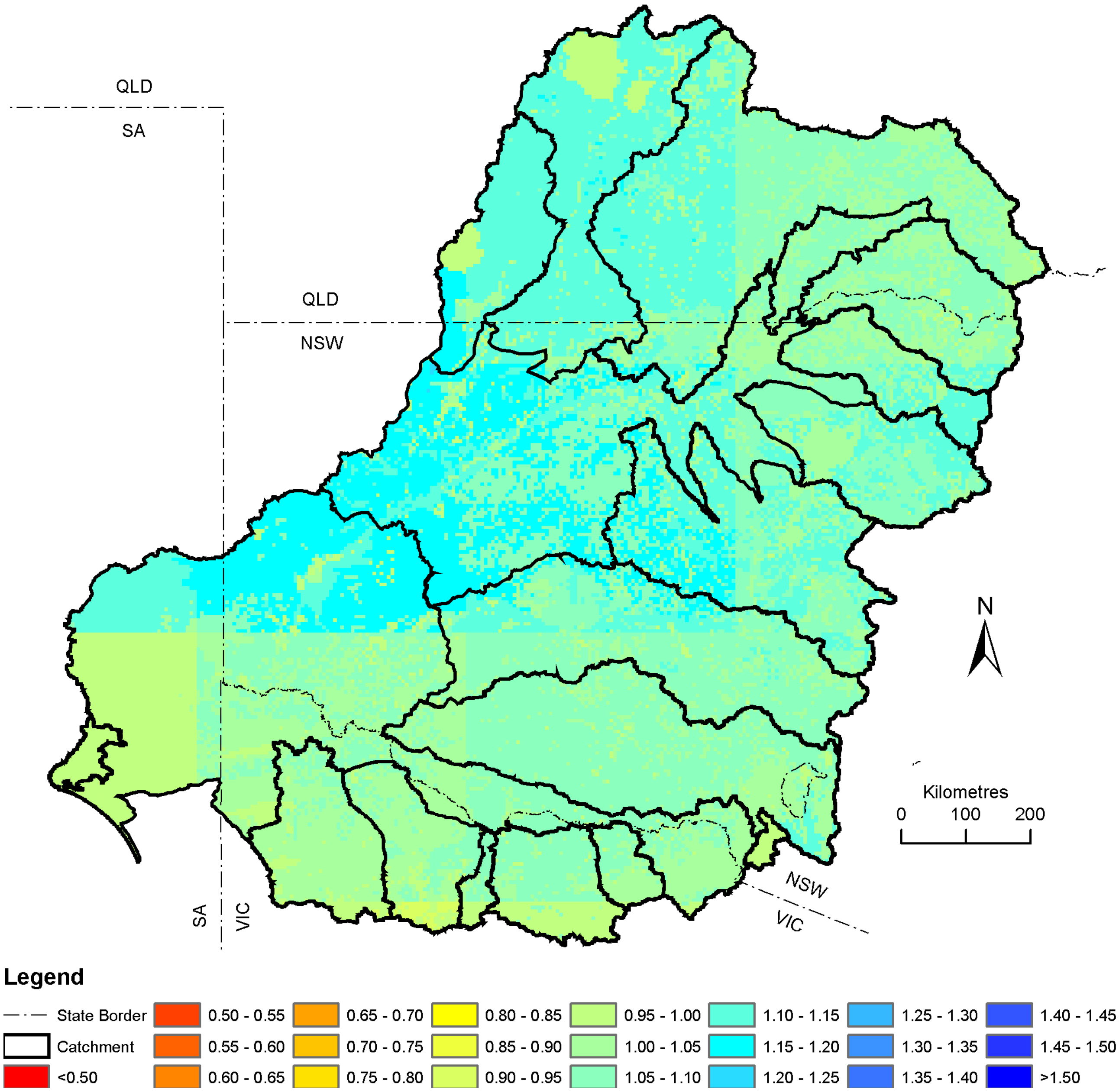

Figure 10-11. Recharge scaling factors for the miub global climate model under the low global warming scenario

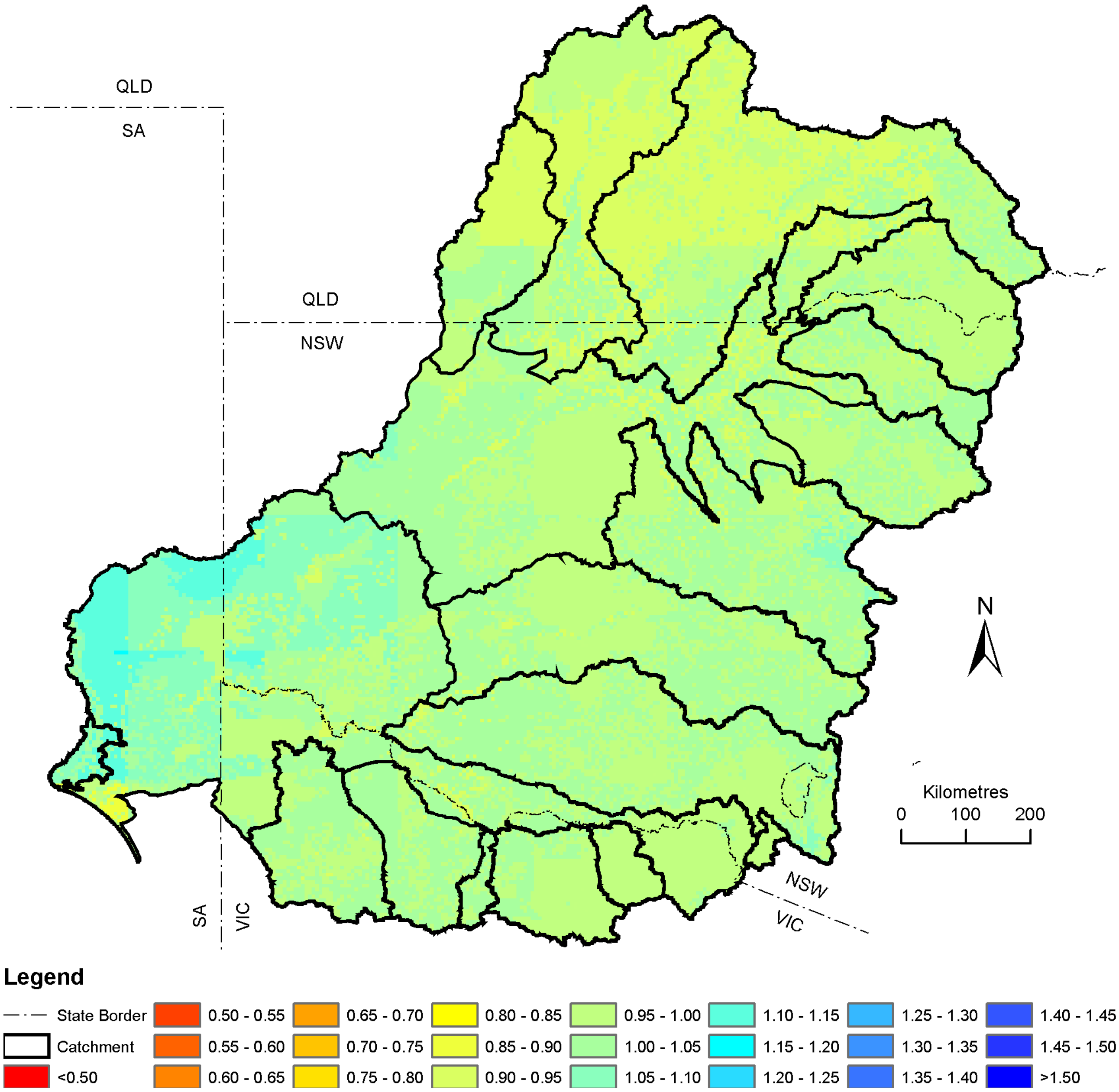

Figure 10-12. Recharge scaling factors for the mpi global climate model under the low global warming scenario

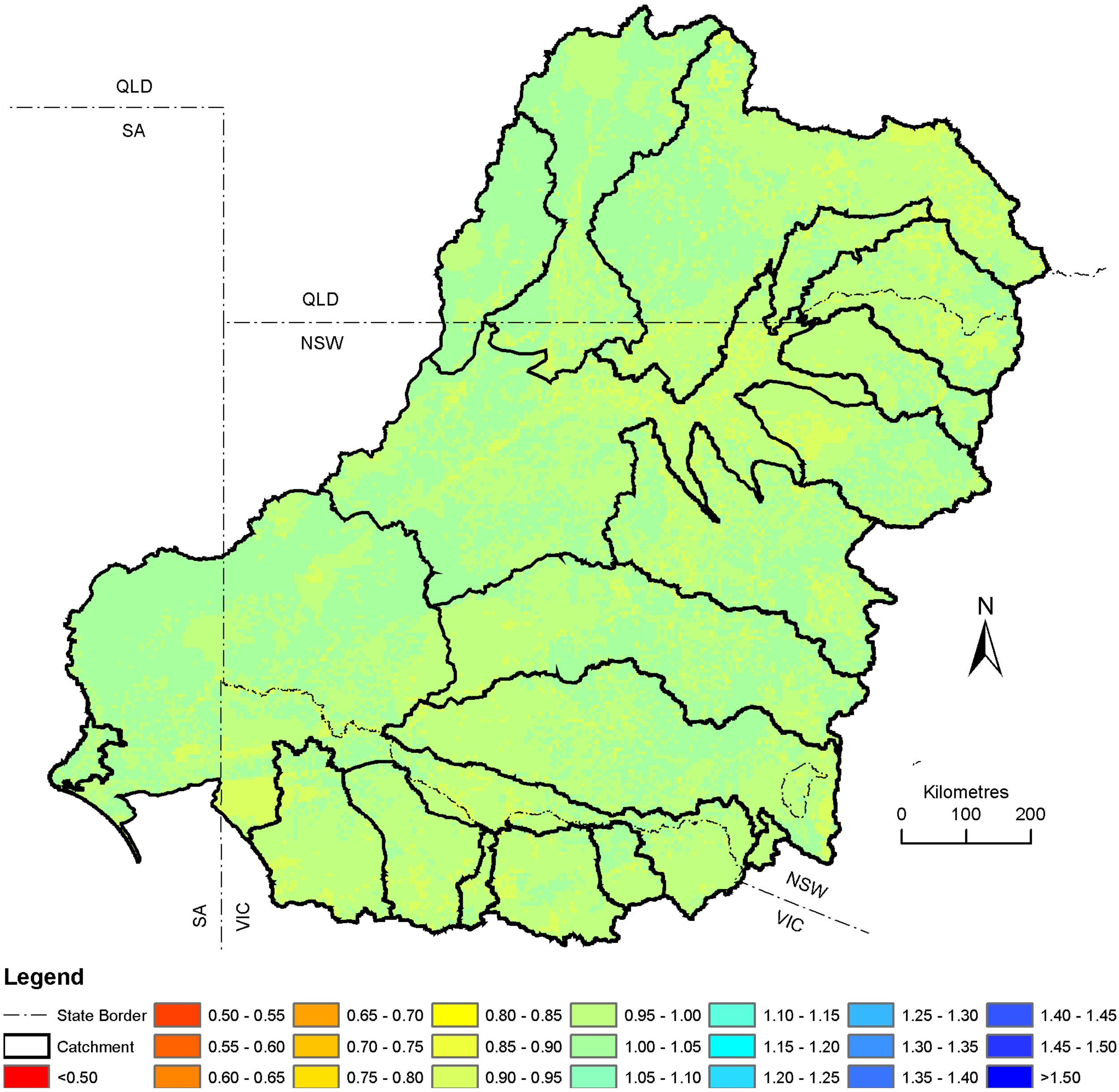

Figure 10-13. Recharge scaling factors for the mri global climate model under the low global warming scenario

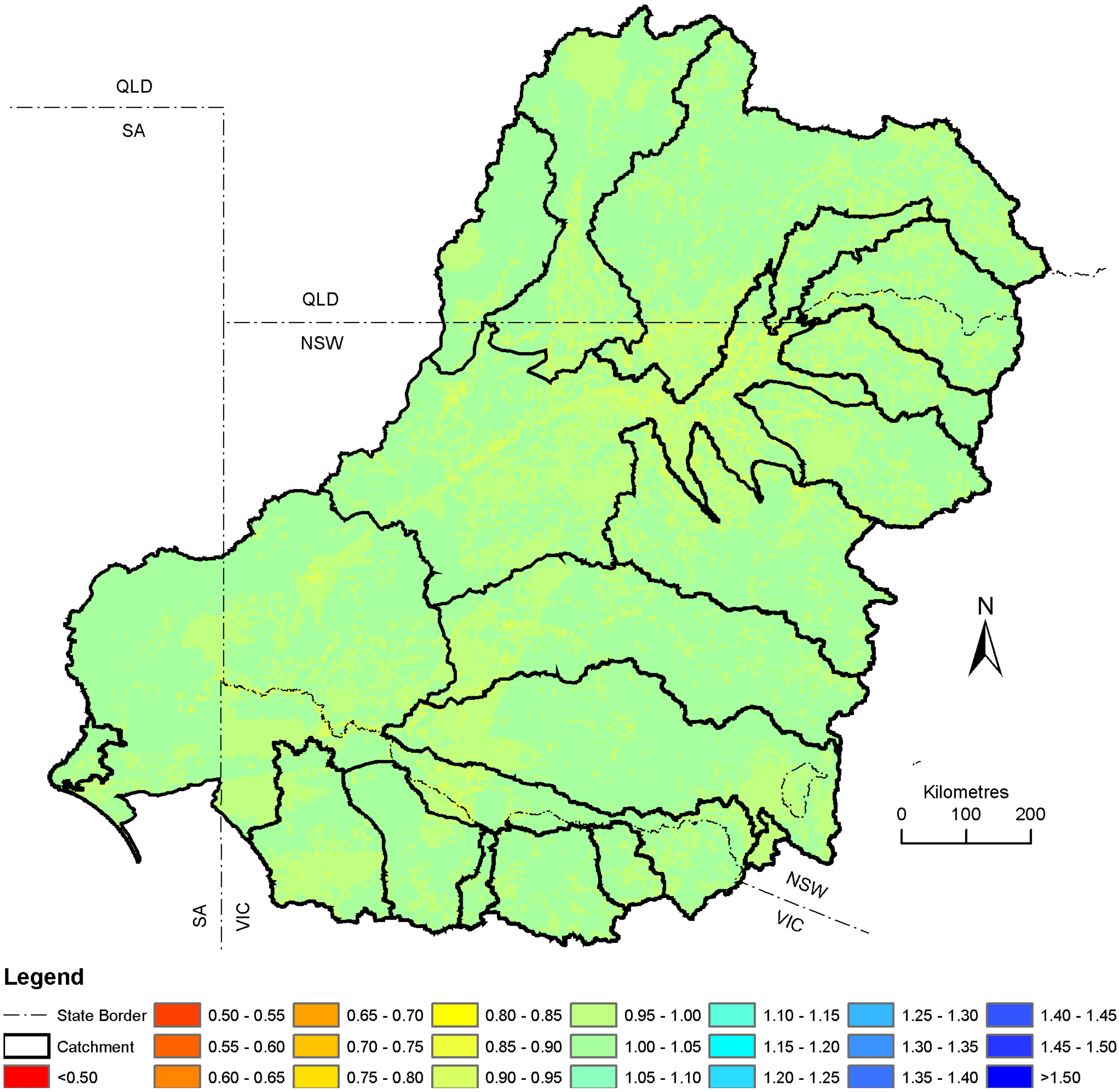

Figure 10-14. Recharge scaling factors for the ncar_ccsm global climate model under the low global warming scenario

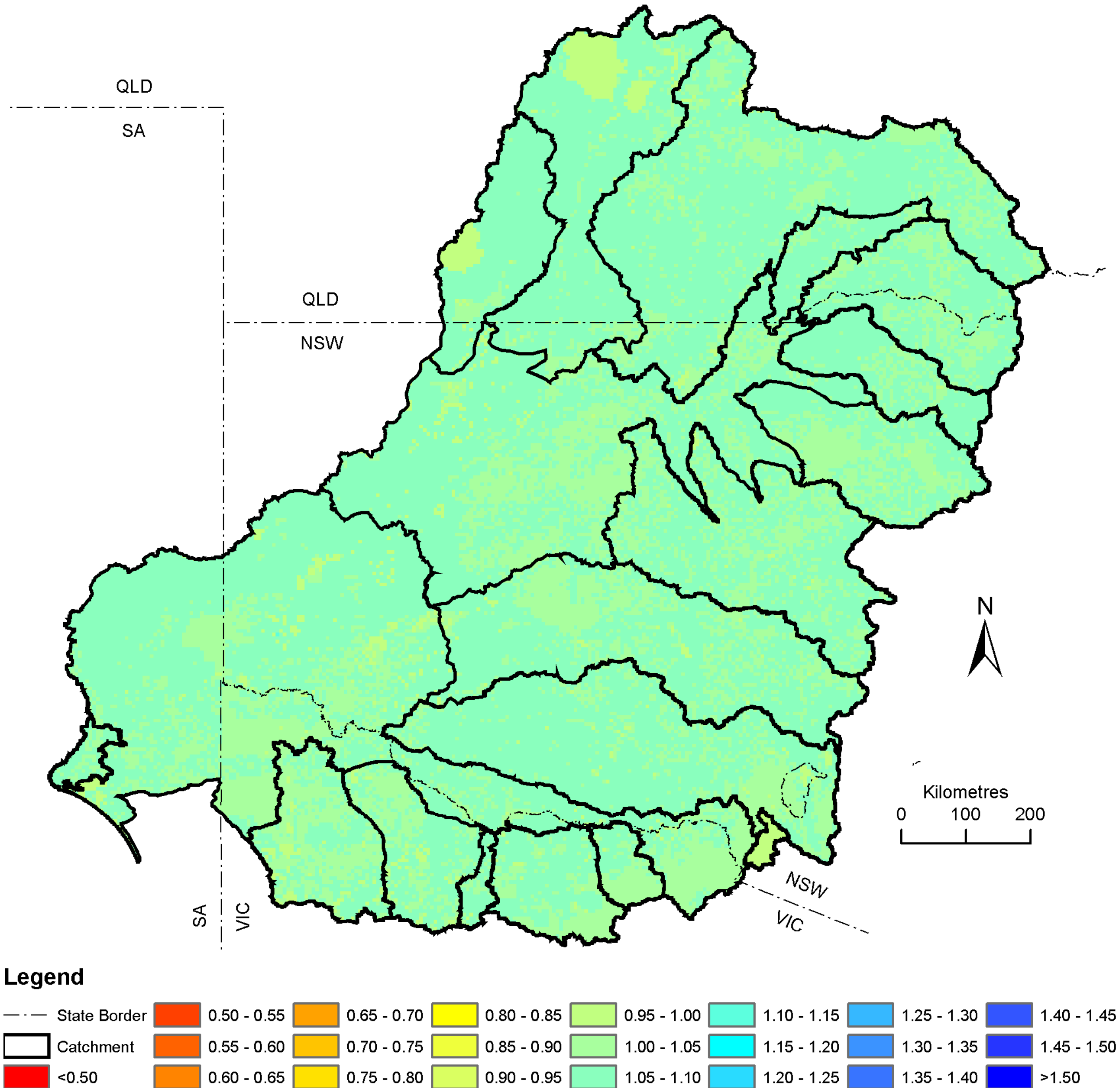

Figure 10-15. Recharge scaling factors for the ncar_pcm global climate model under the low global warming scenario

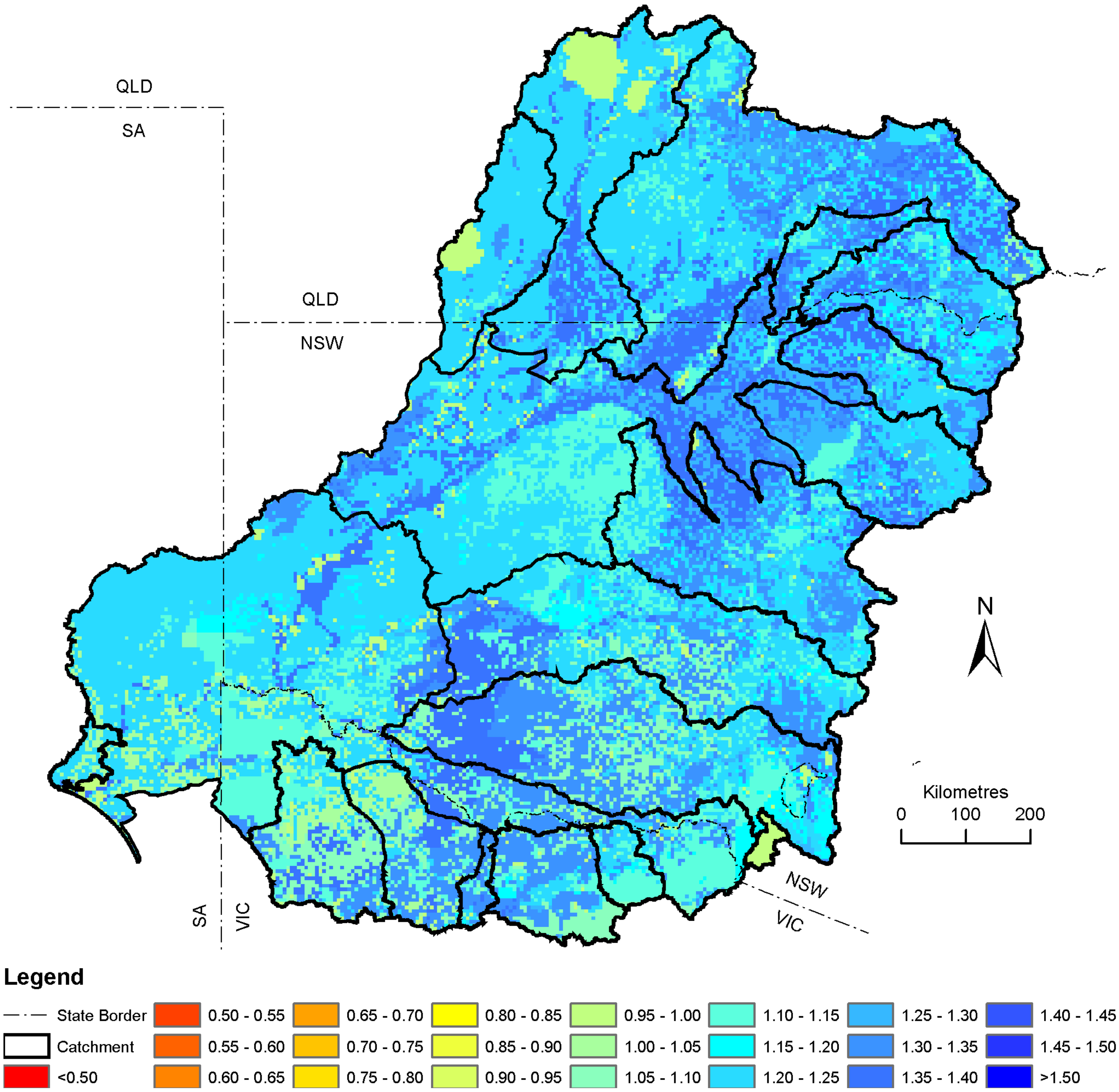

Figure 10-16. Recharge scaling factors for the cccma_t47 global climate model under the medium global warming scenario

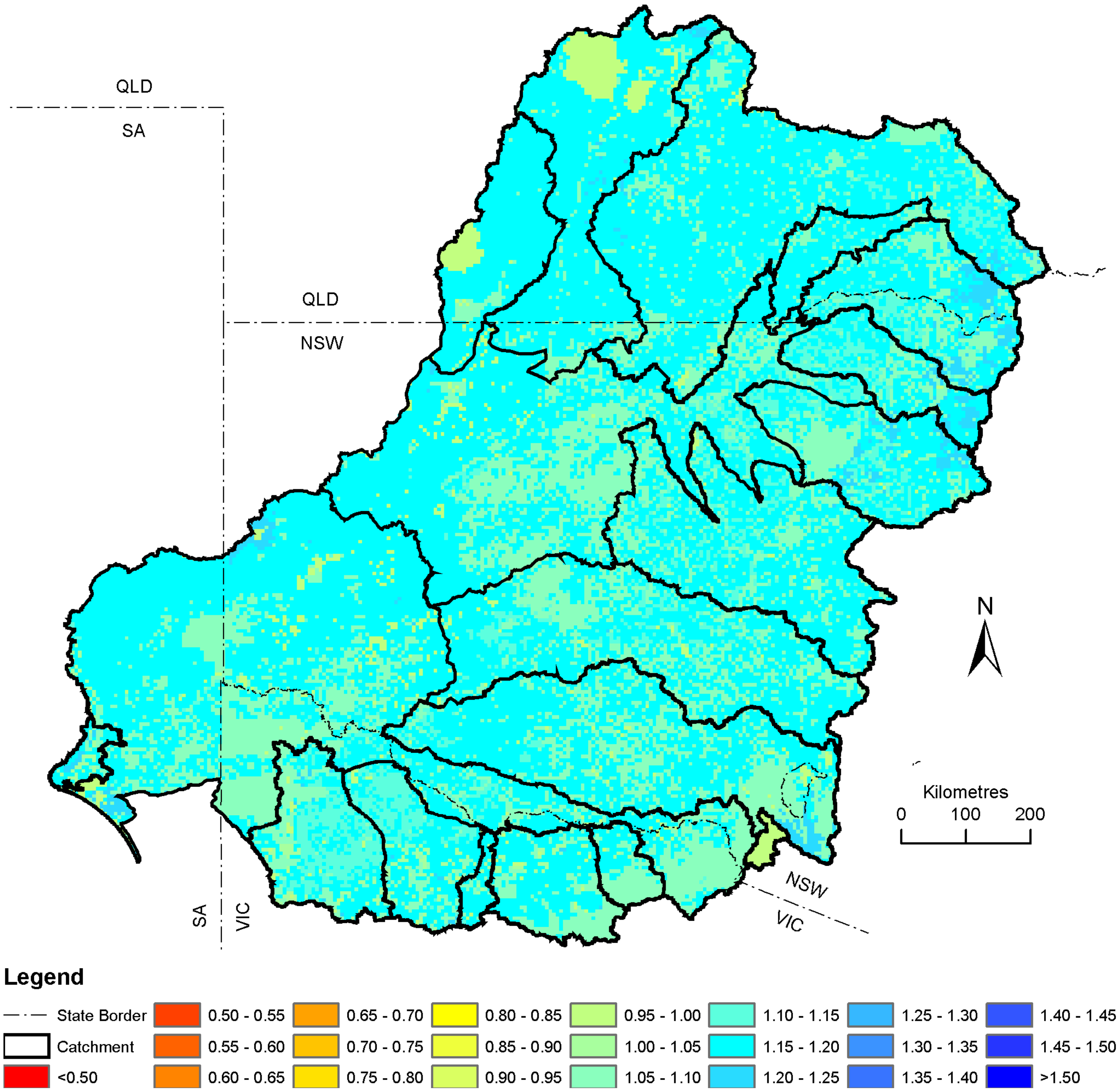

Figure 10-17. Recharge scaling factors for the cccma_t63 global climate model under the medium global warming scenario

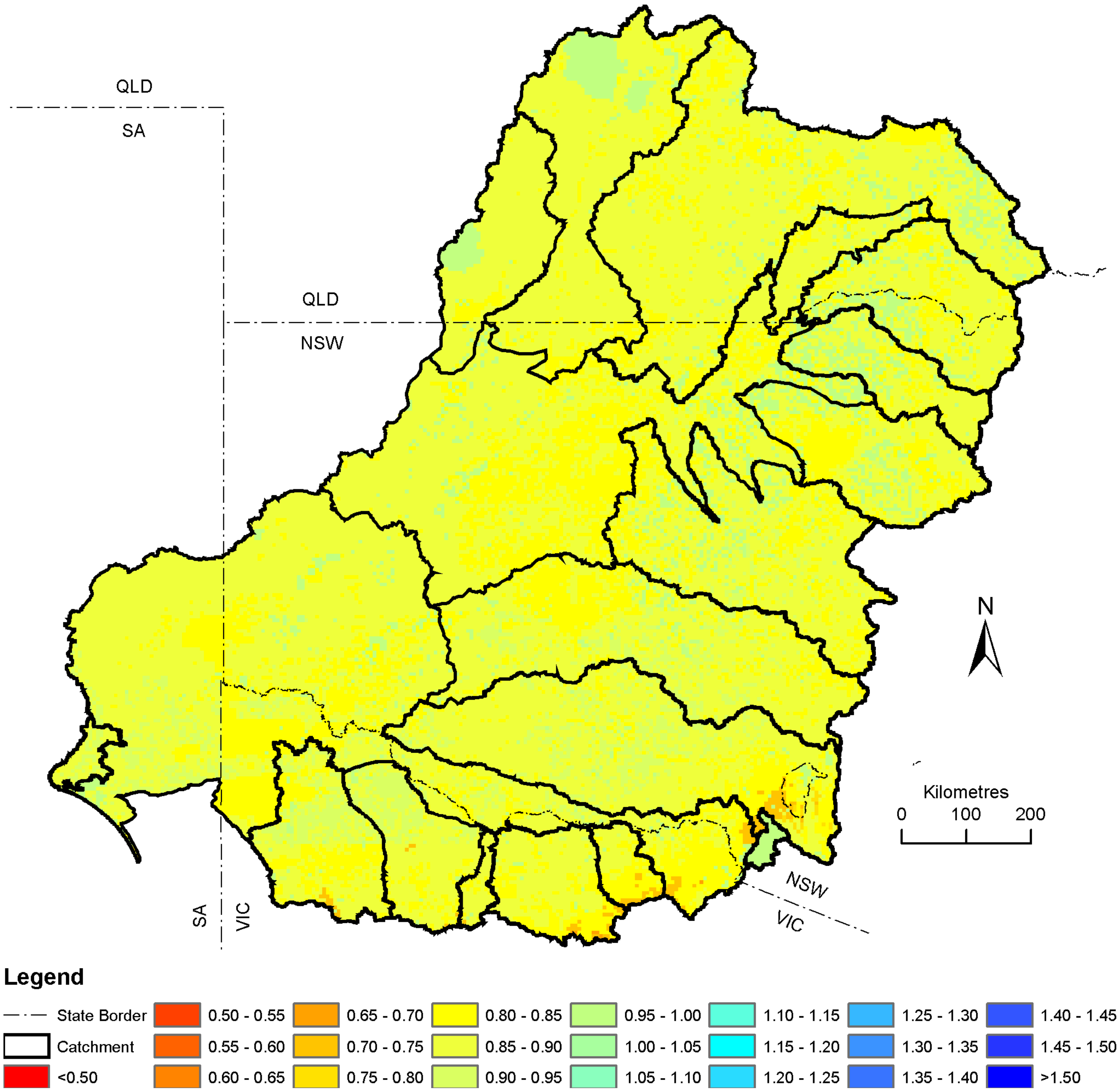

Figure 10-18. Recharge scaling factors for the cnrm global climate model under the medium global warming scenario

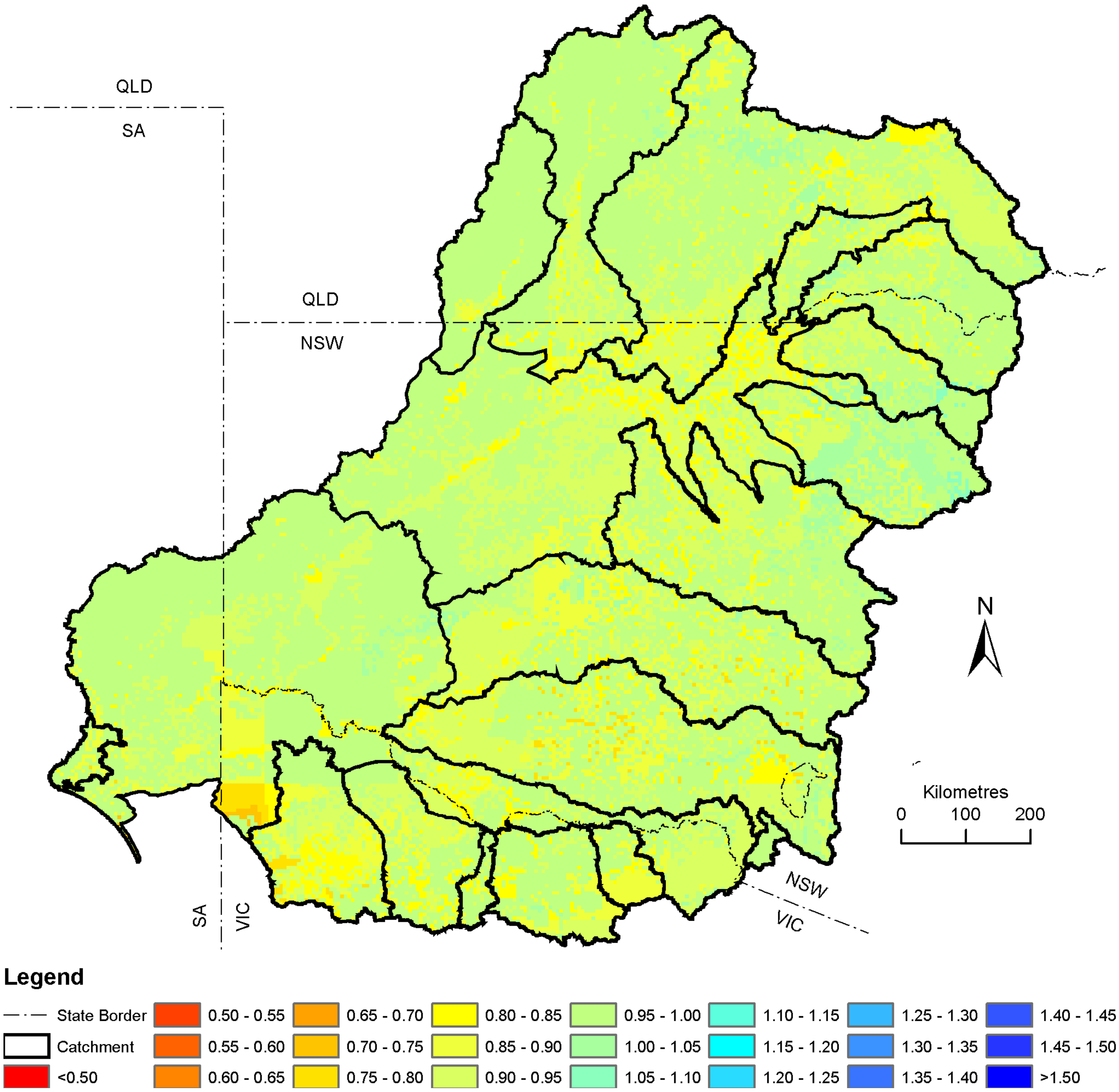

Figure 10-19. Recharge scaling factors for the csiro global climate model under the medium global warming scenario

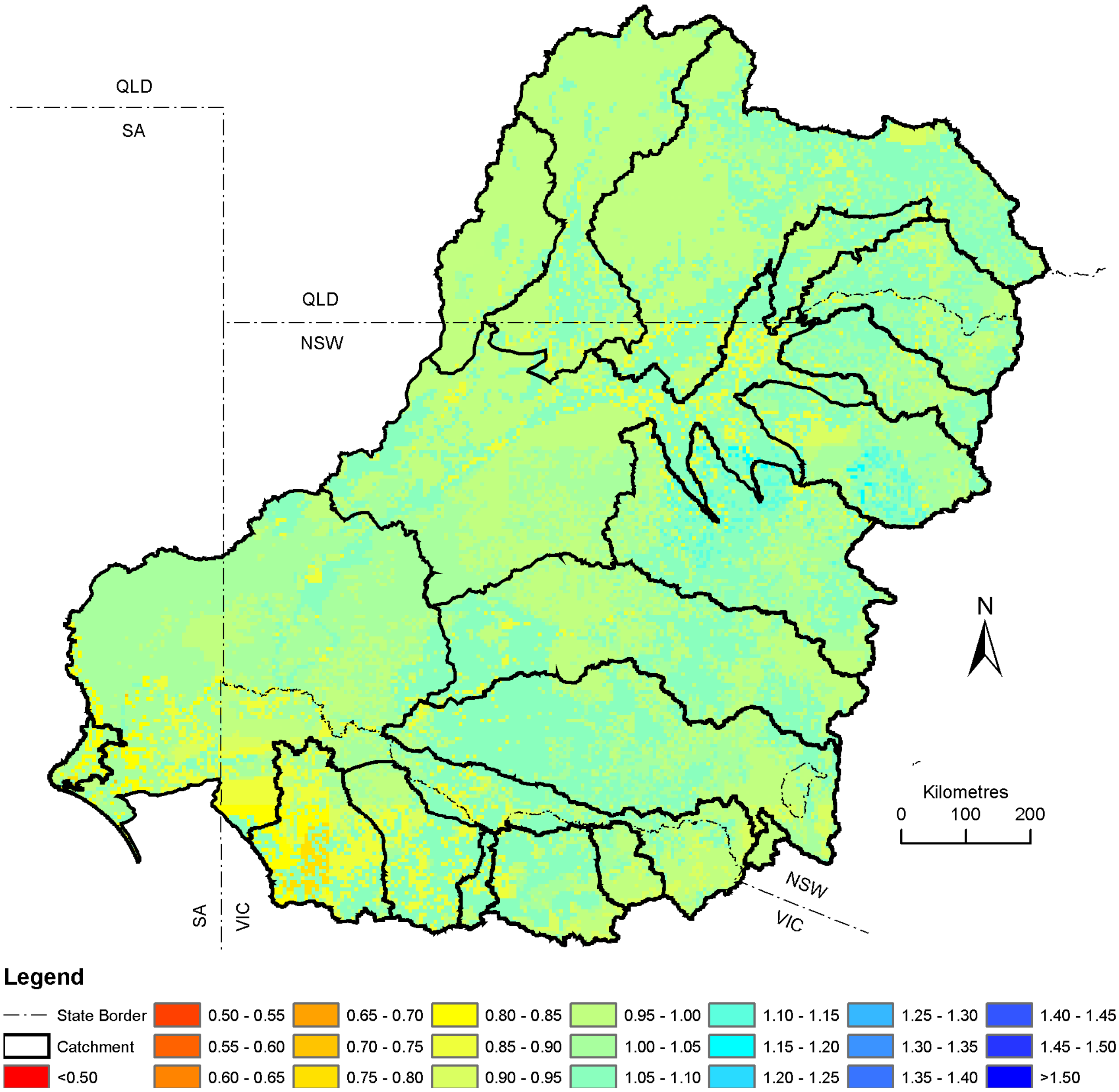

Figure 10-20. Recharge scaling factors for the gfdl global climate model under the medium global warming scenario

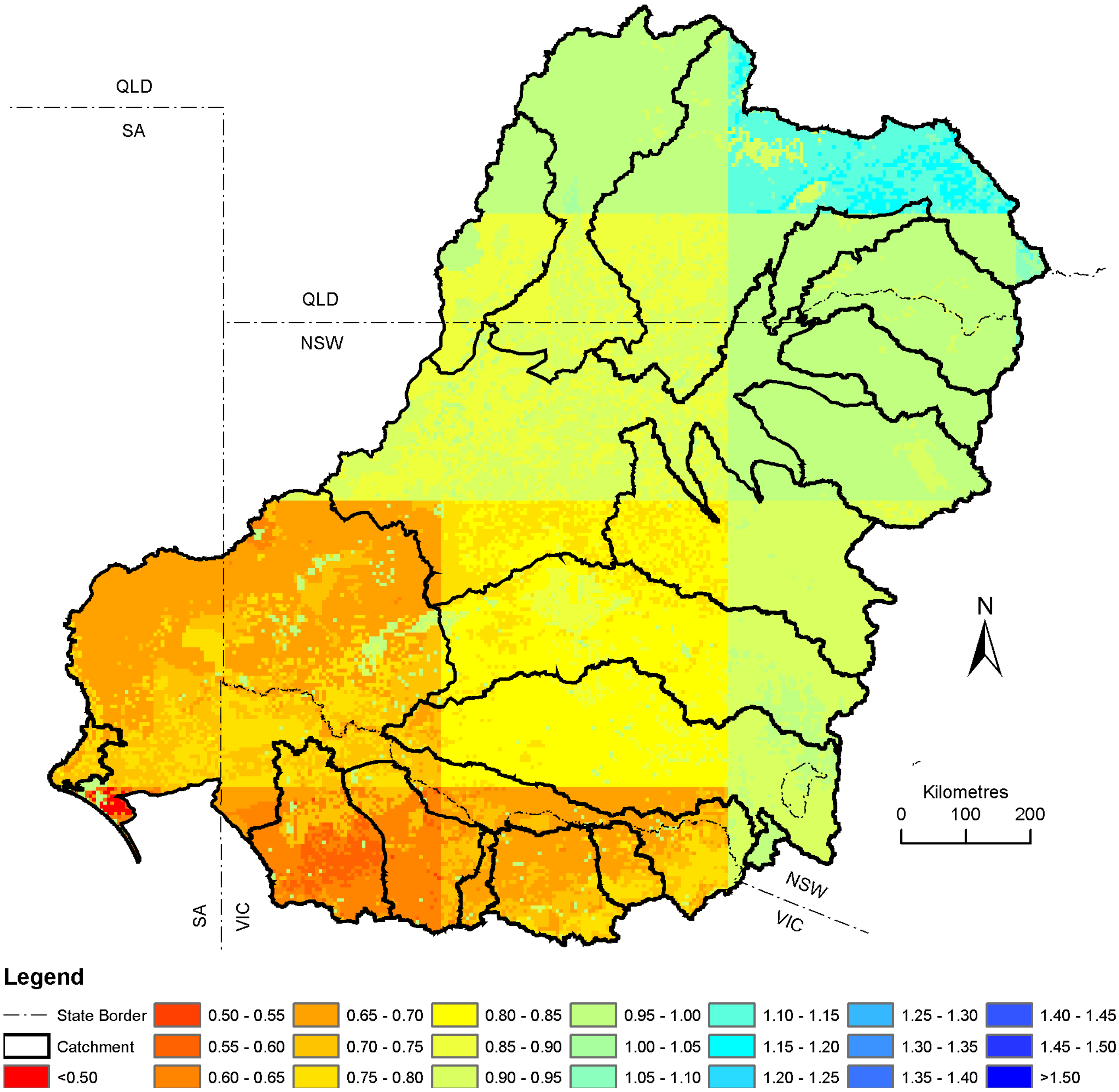

Figure 10-21. Recharge scaling factors for the giss_aom global climate model under the medium global warming scenario

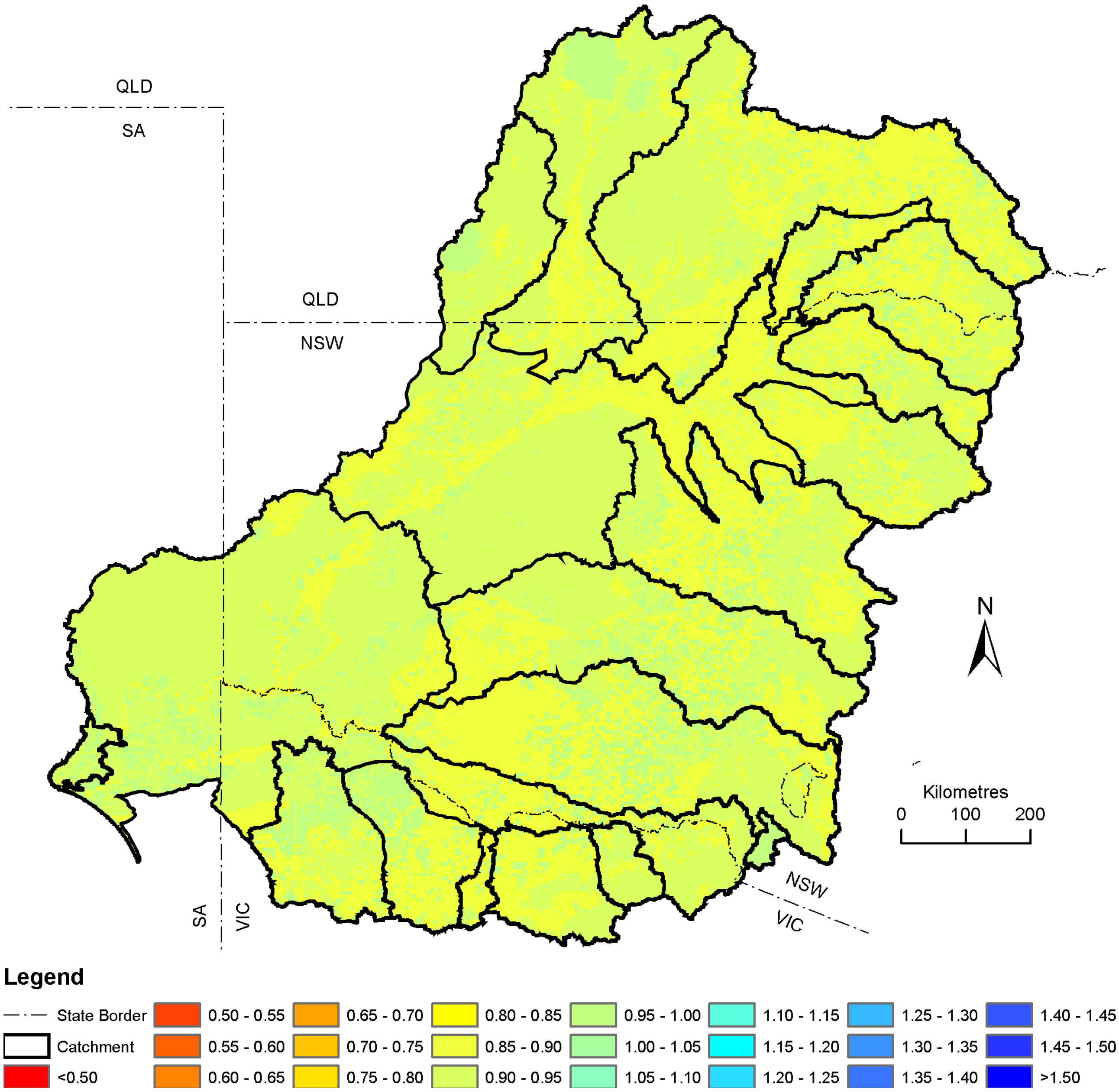

Figure 10-22. Recharge scaling factors for the iap global climate model under the medium global warming scenario

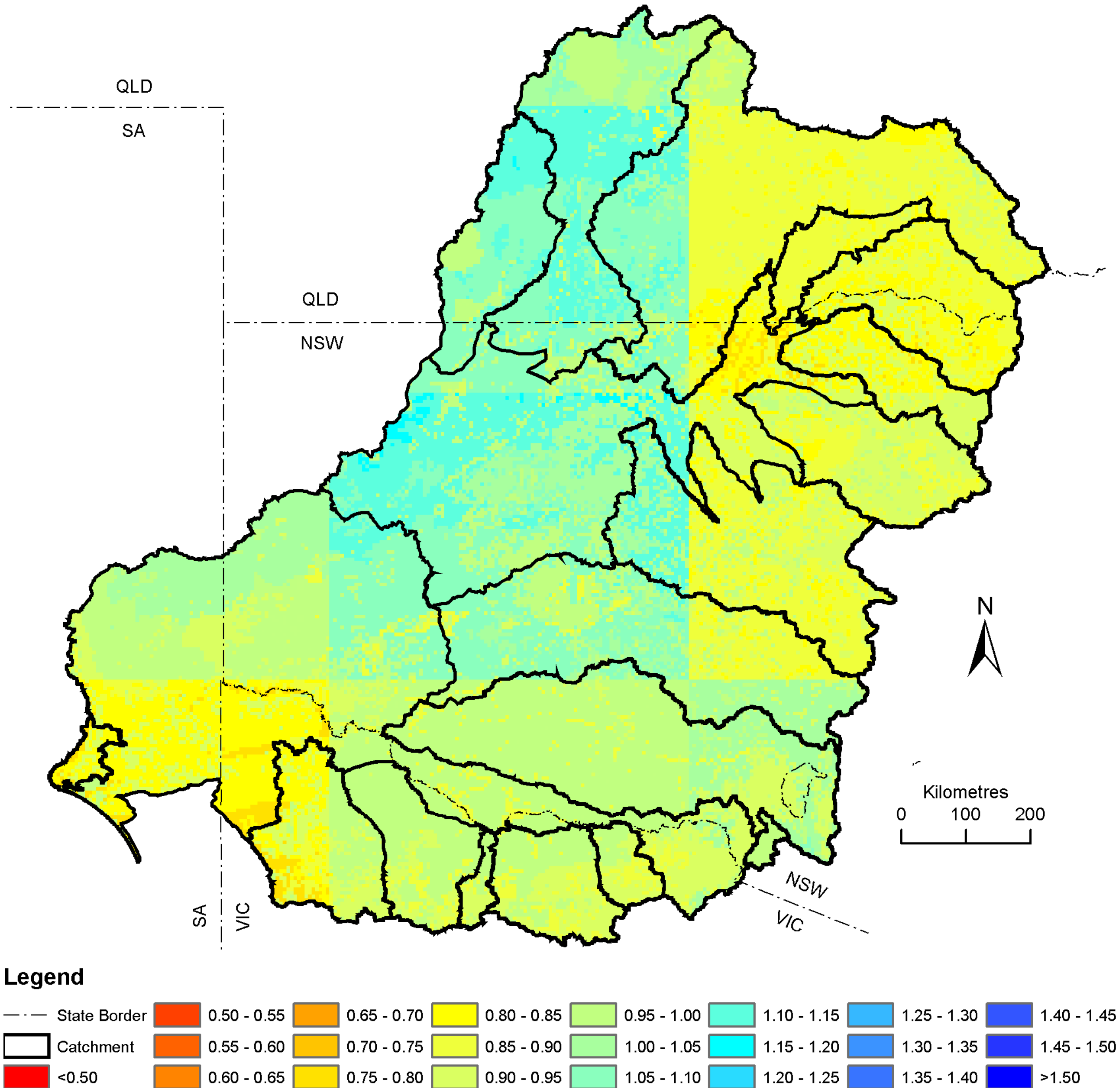

Figure 10-23. Recharge scaling factors for the inmcm global climate model under the medium global warming scenario

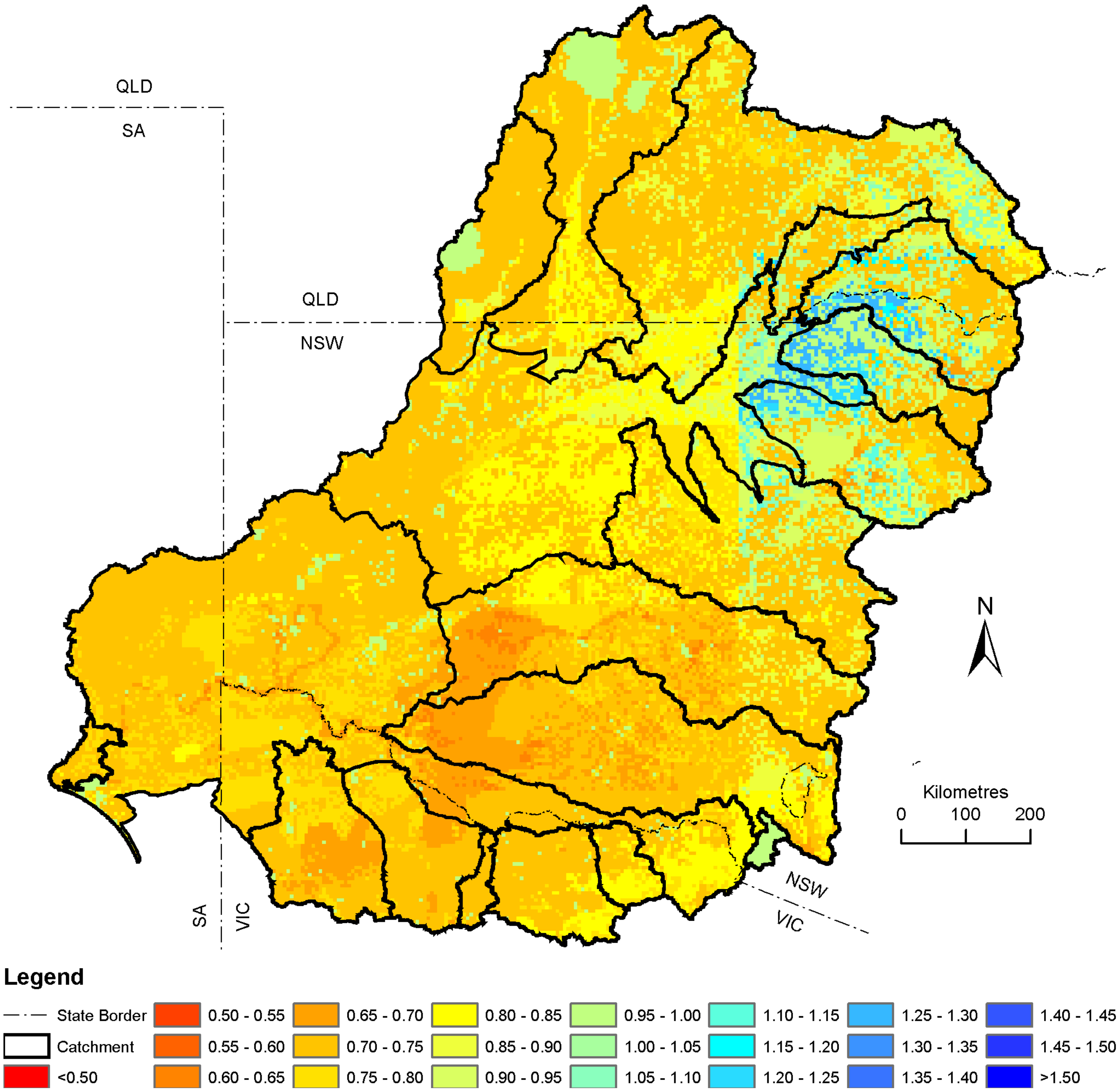

Figure 10-24. Recharge scaling factors for the ipsl global climate model under the medium global warming scenario

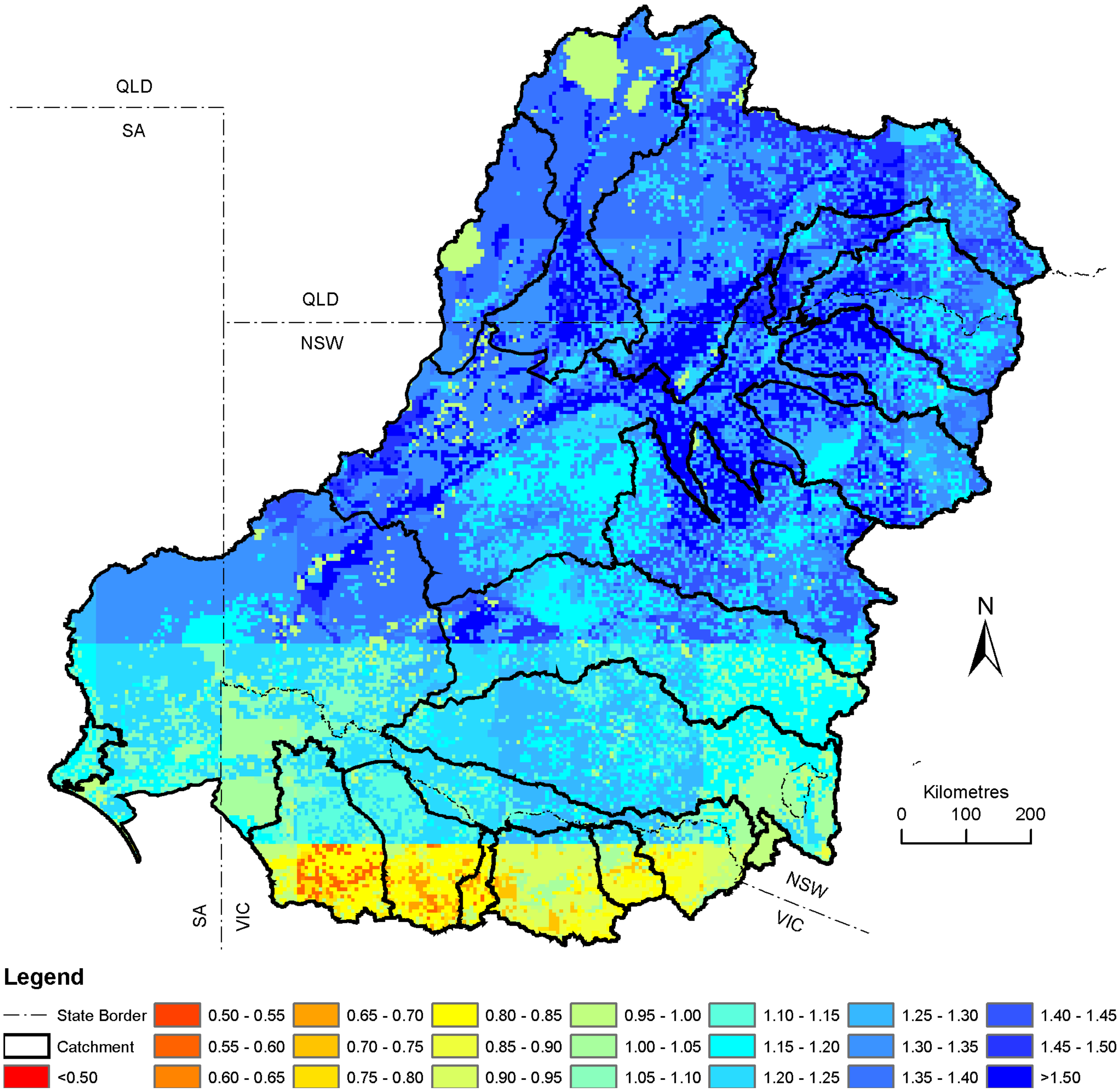

Figure 10-25. Recharge scaling factors for the miroc global climate model under the medium global warming scenario

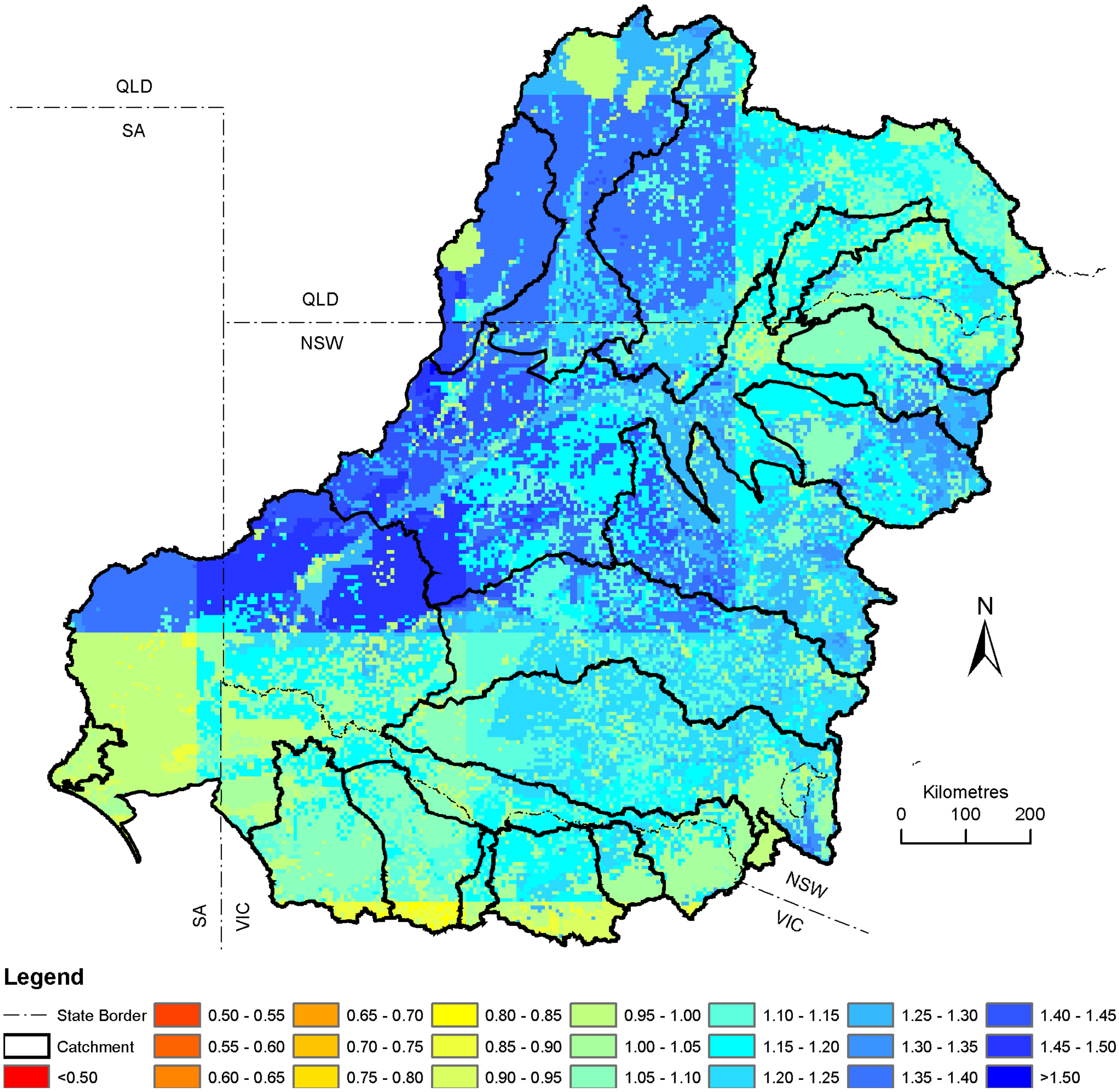

Figure 10-26. Recharge scaling factors for the miub global climate model under the medium global warming scenario

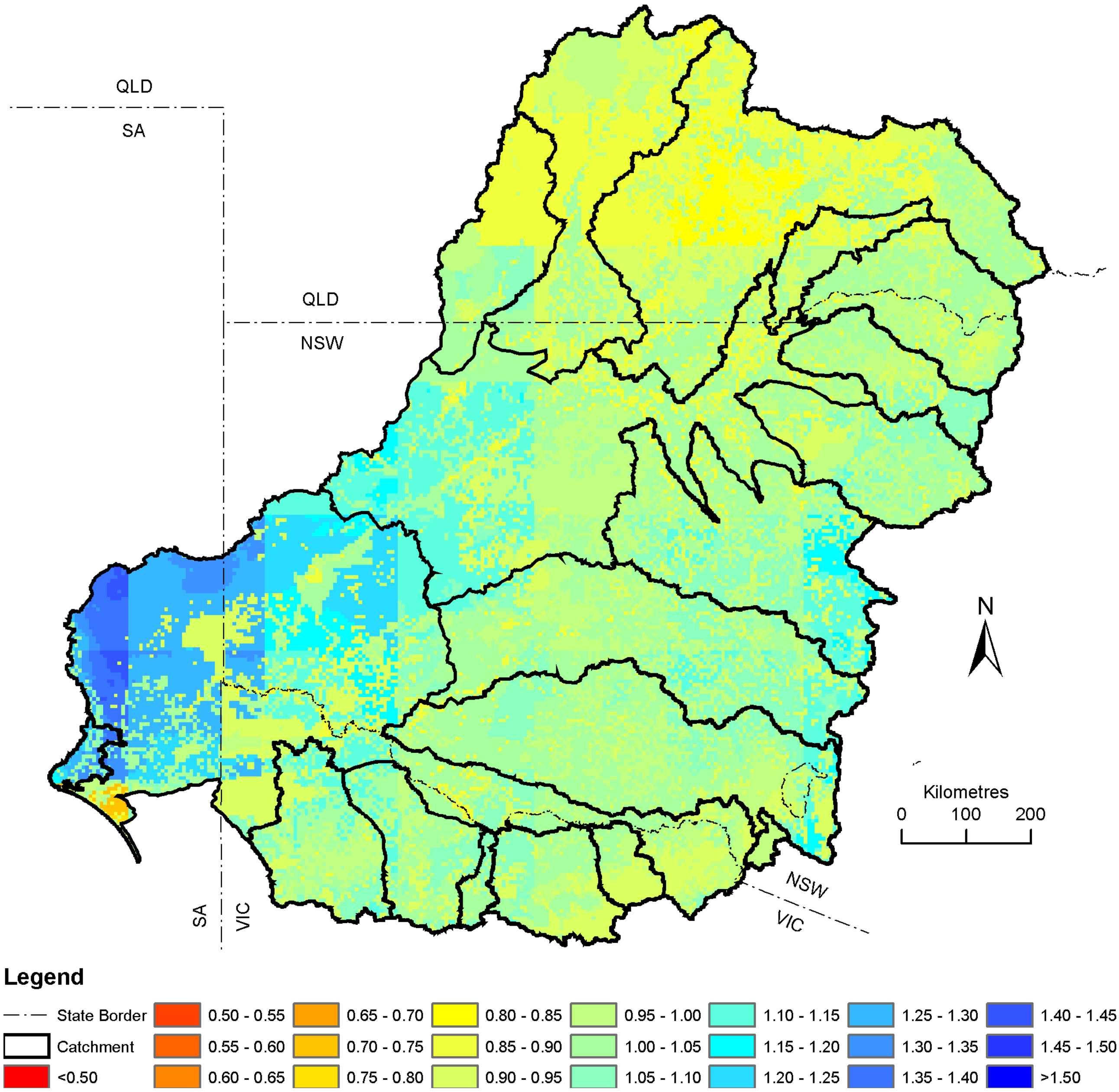

Figure 10-27. Recharge scaling factors for the mpi global climate model under the medium global warming scenario

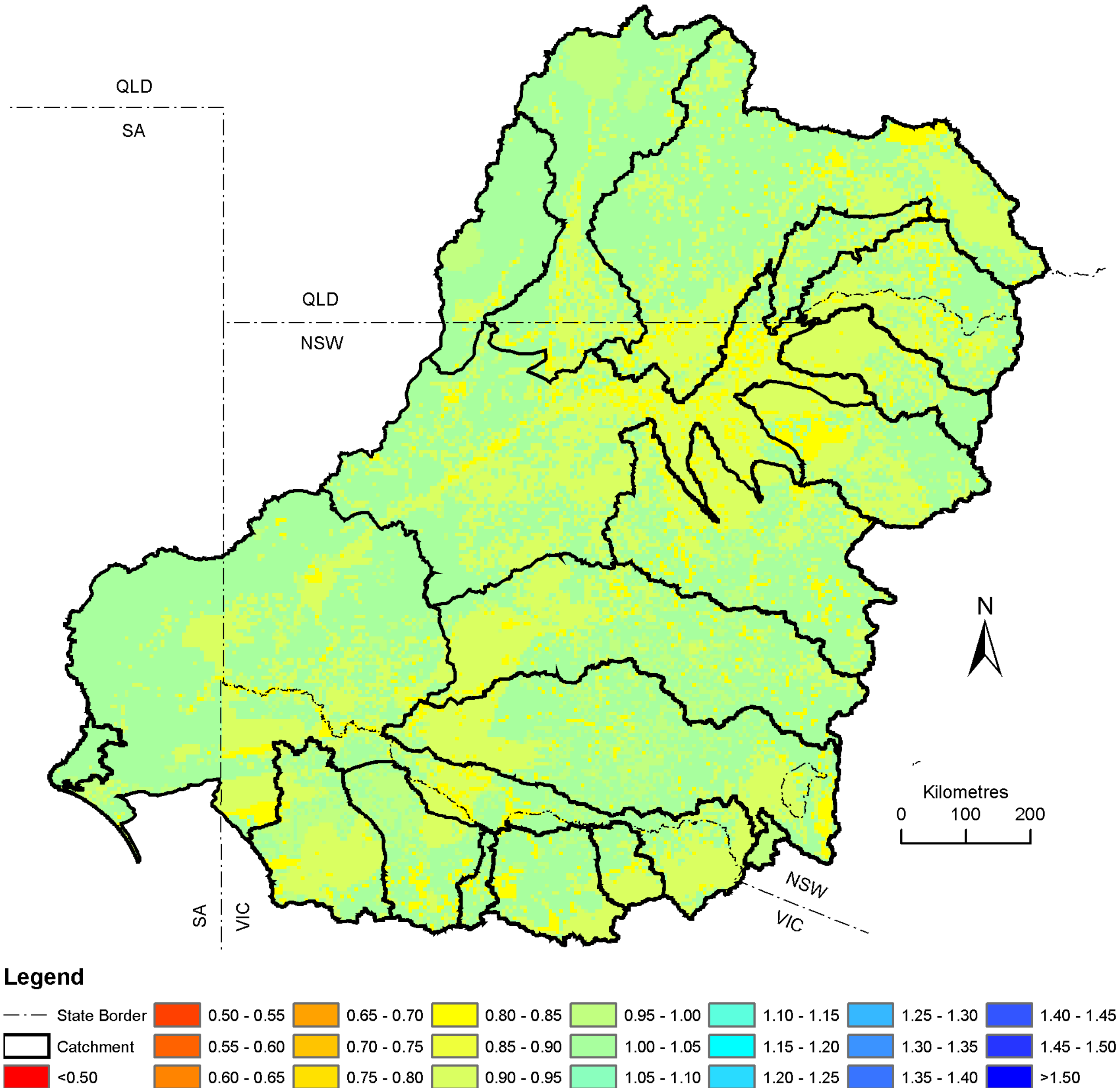

Figure 10-28. Recharge scaling factors for the mri global climate model under the medium global warming scenario

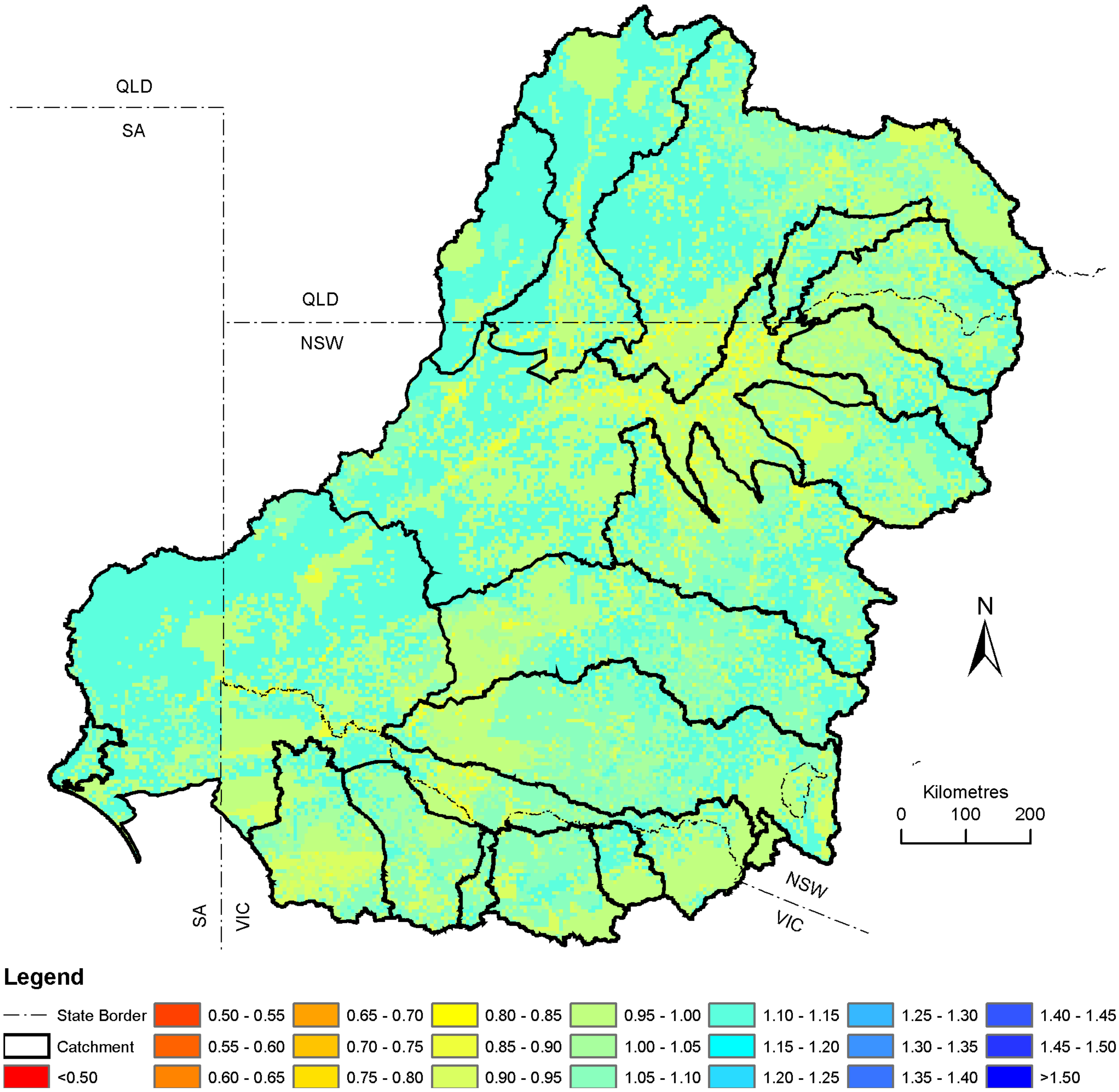

Figure 10-29. Recharge scaling factors for the ncar_cccm global climate model under the medium global warming scenario

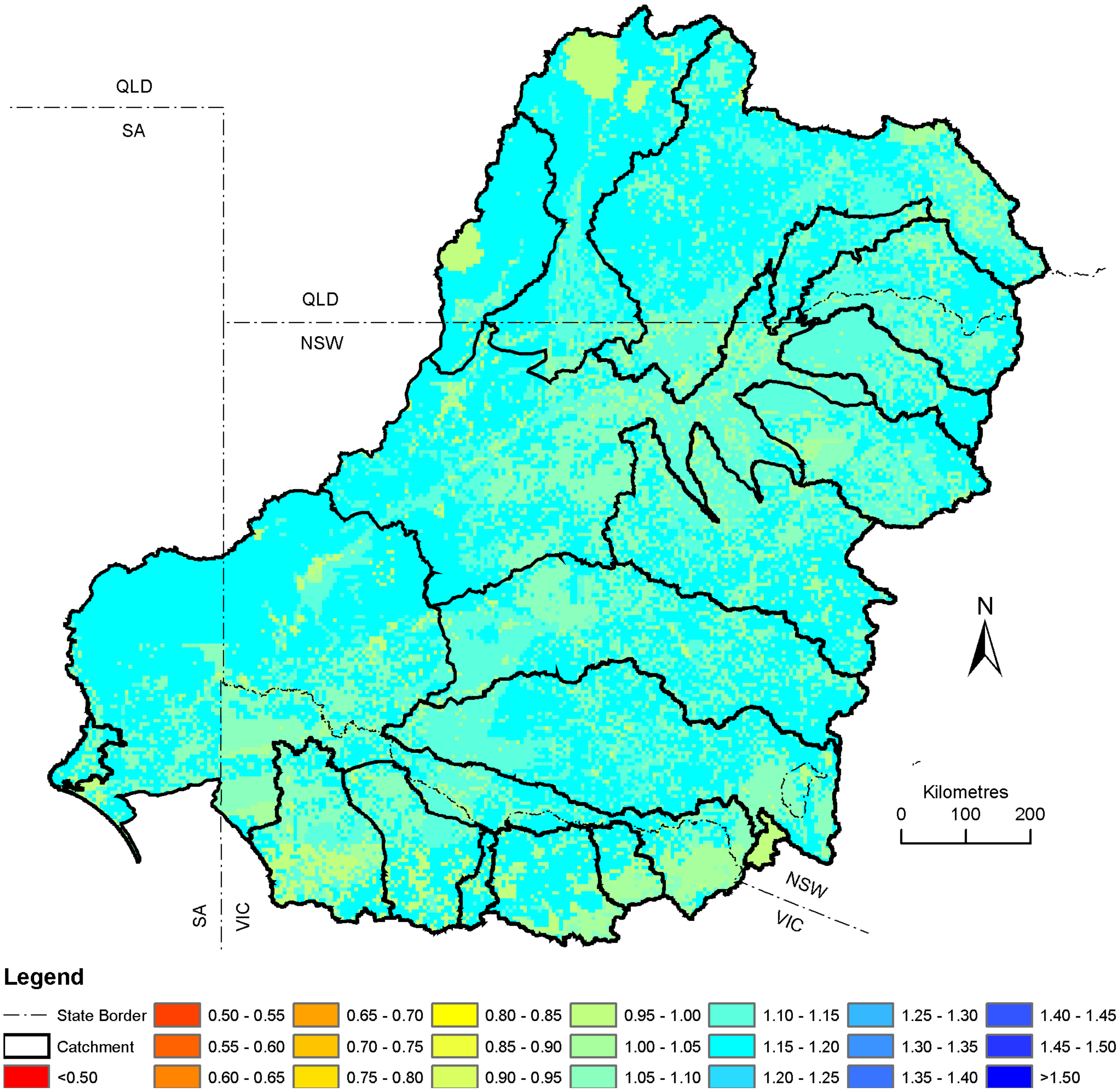

Figure 10-30. Recharge scaling factors for the ncar_pcm global climate model under the medium global warming scenario

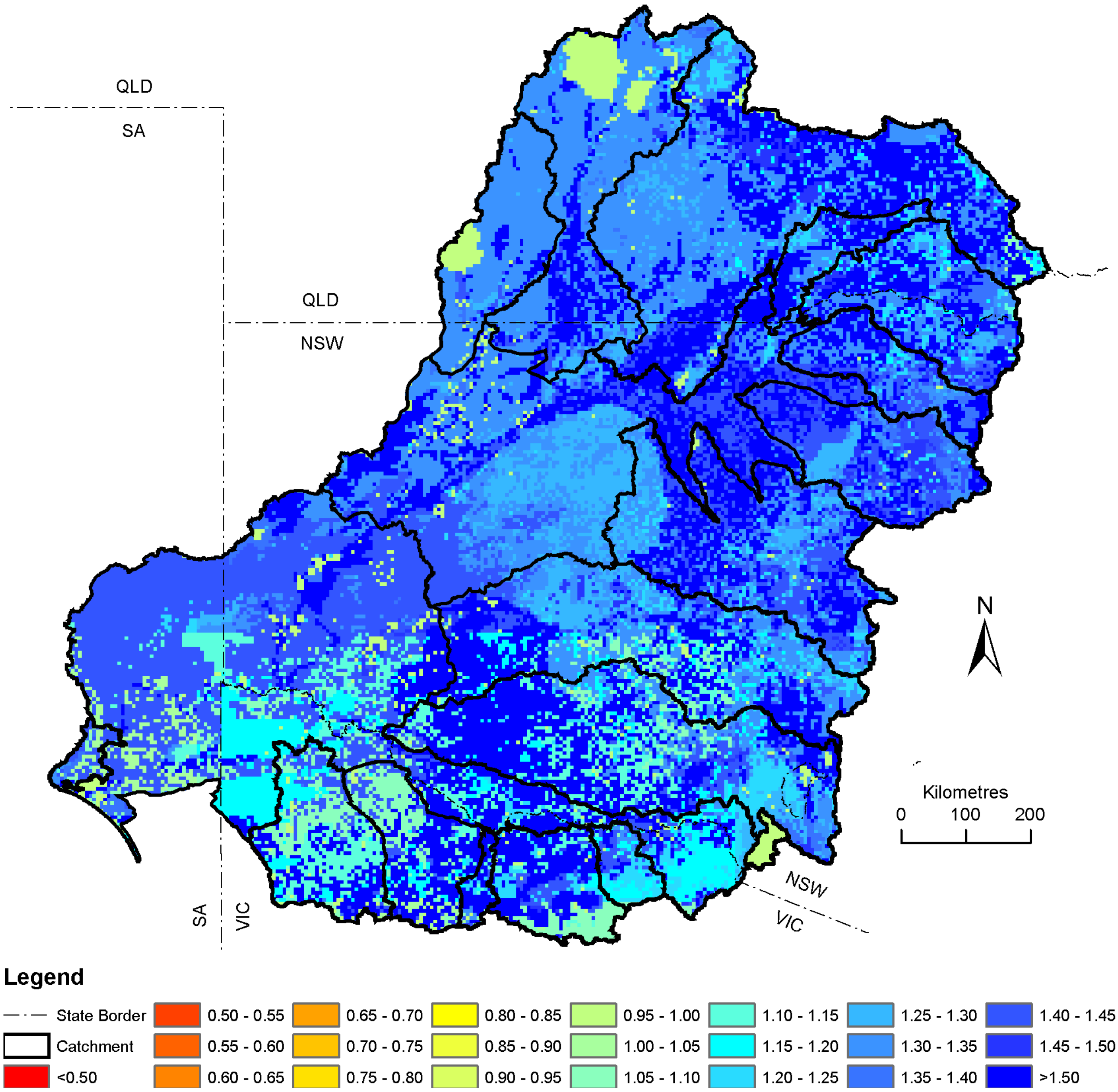

Figure 10-31. Recharge scaling factors for the cccma_t47 global climate model under the high global warming scenario

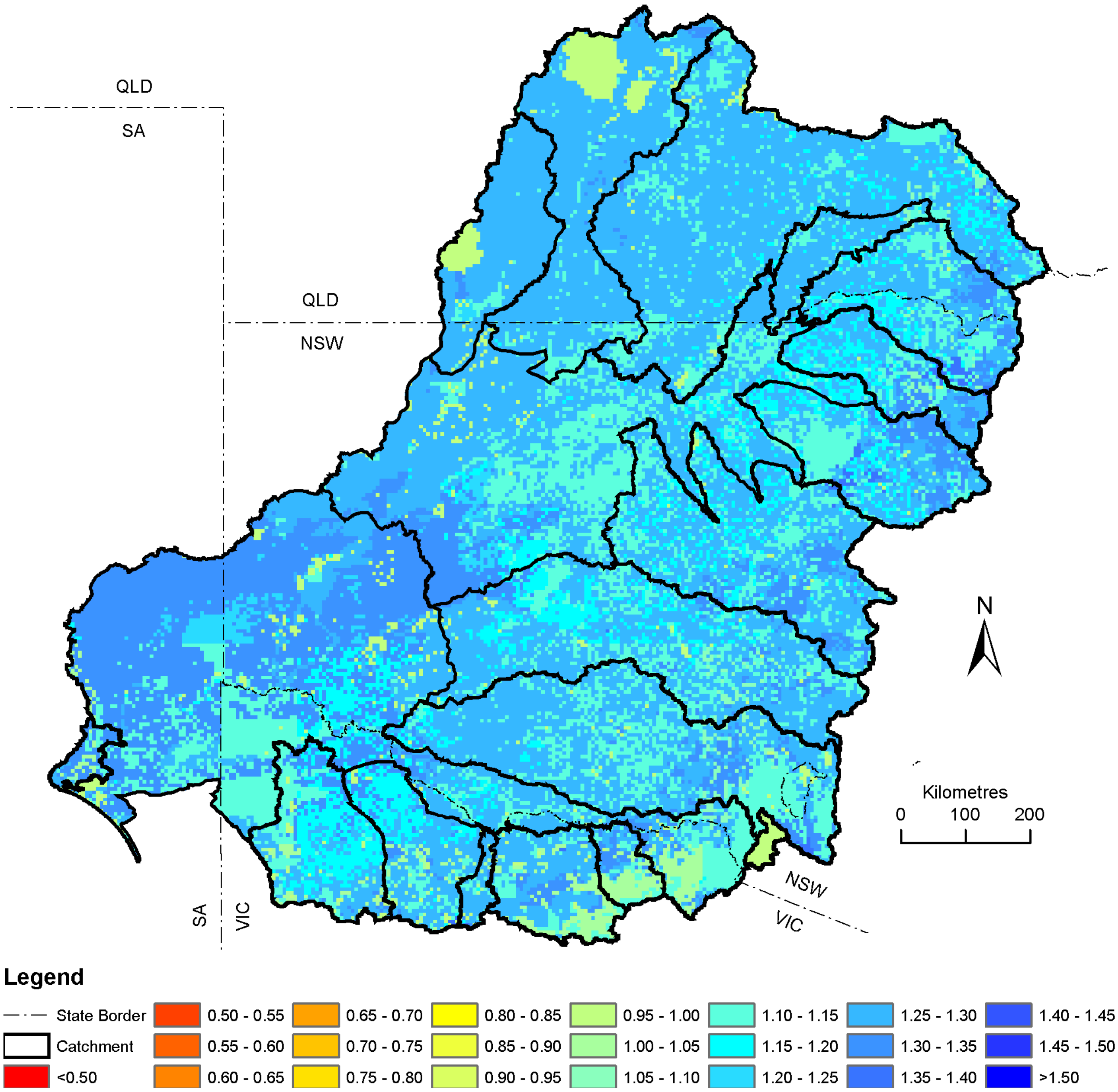

Figure 10-32. Recharge scaling factors for the cccma_t63 global climate model under the high global warming scenario

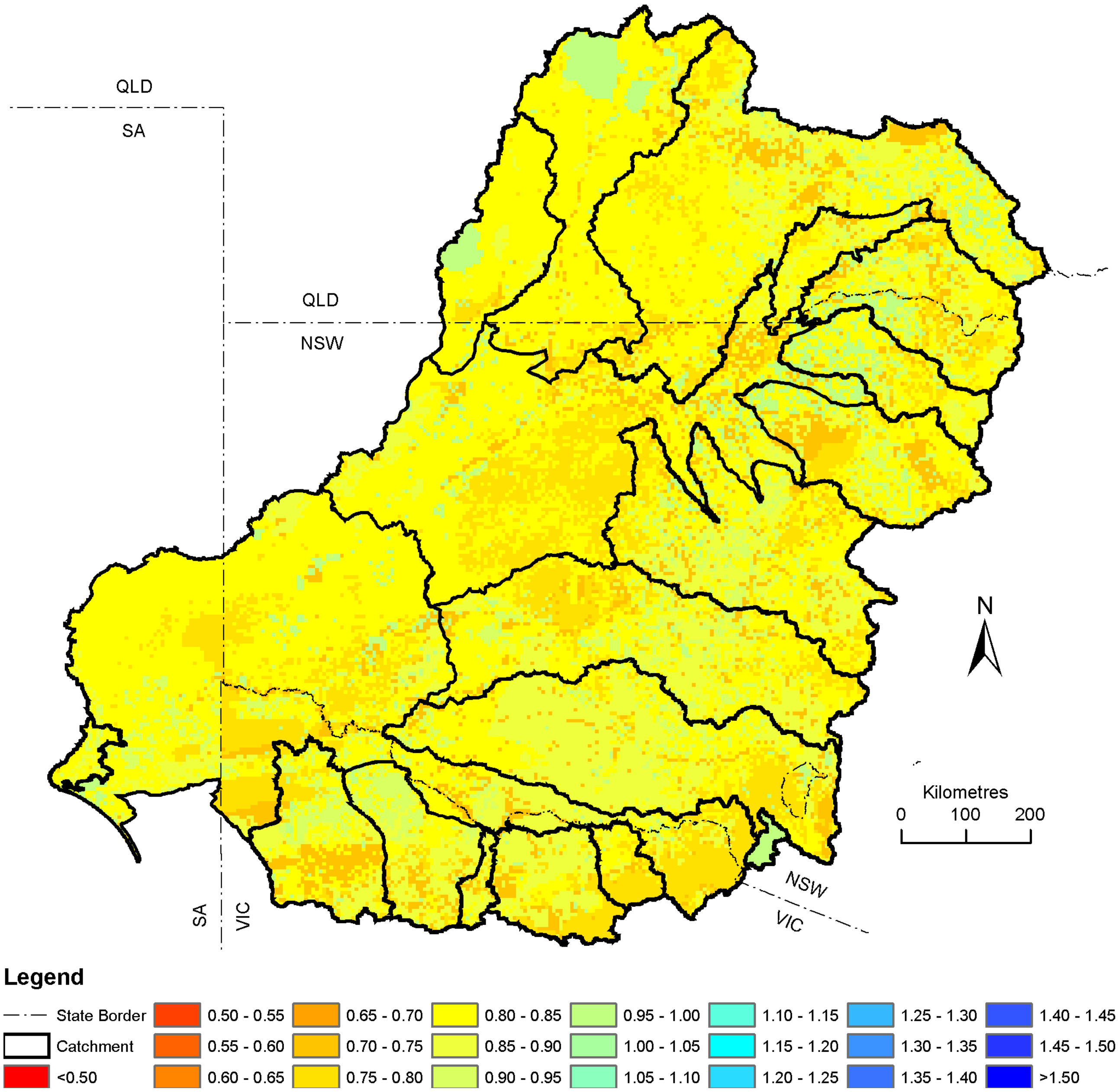

Figure 10-33. Recharge scaling factors for the cnrm global climate model under the high global warming scenario

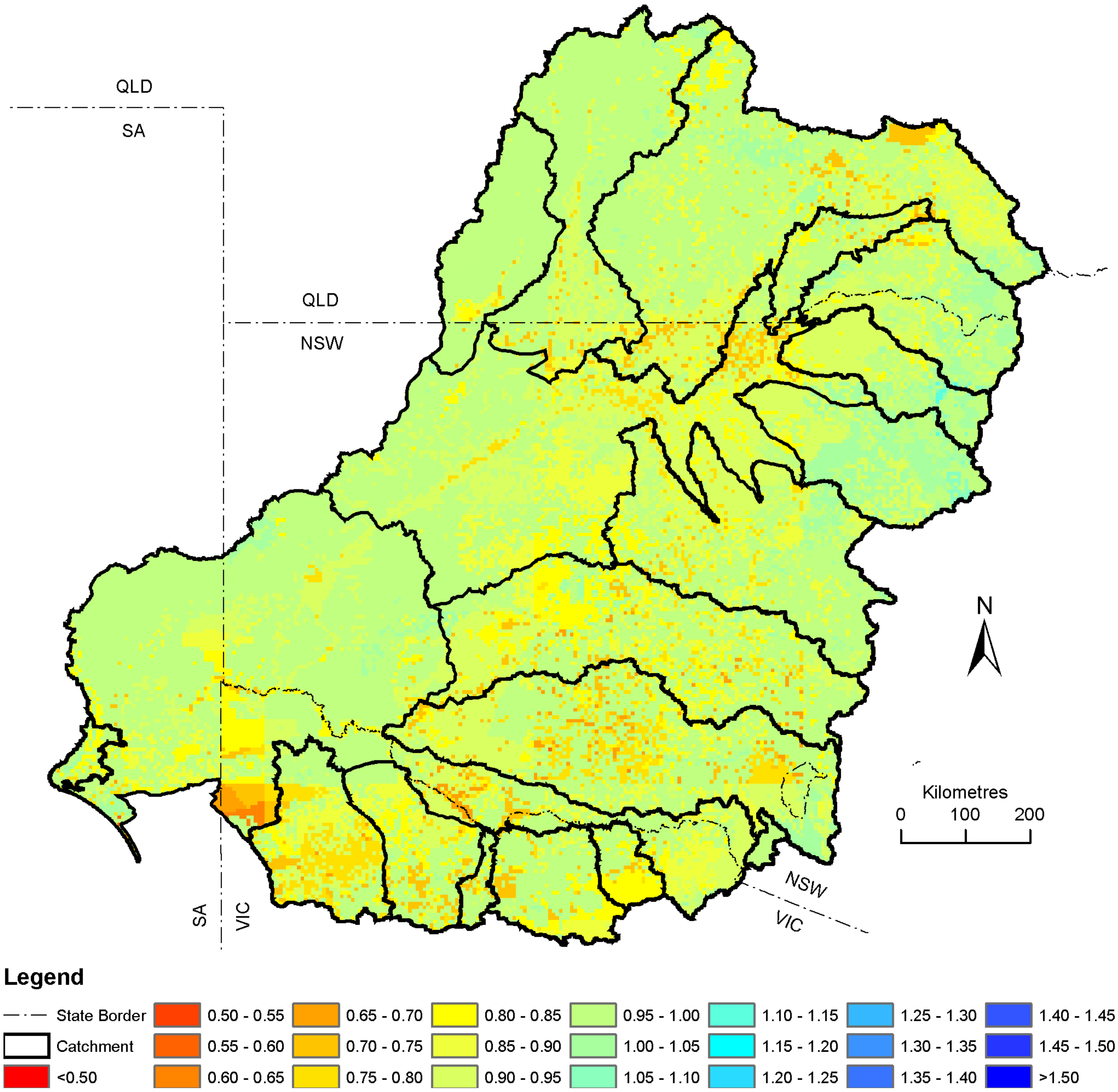

Figure 10-34. Recharge scaling factors for the csiro global climate model under the high global warming scenario

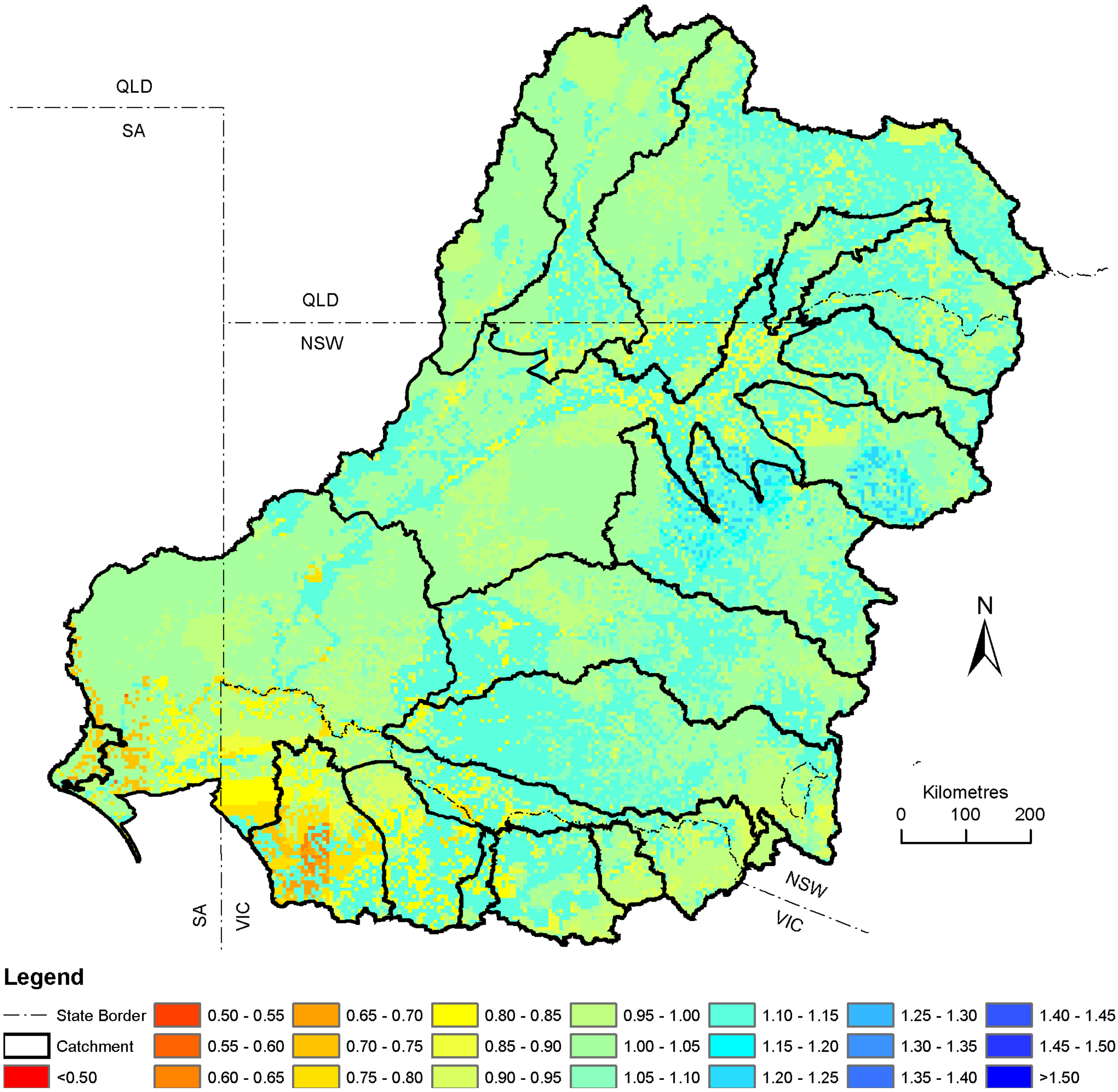

Figure 10-35. Recharge scaling factors for the gfdl global climate model under the high global warming scenario

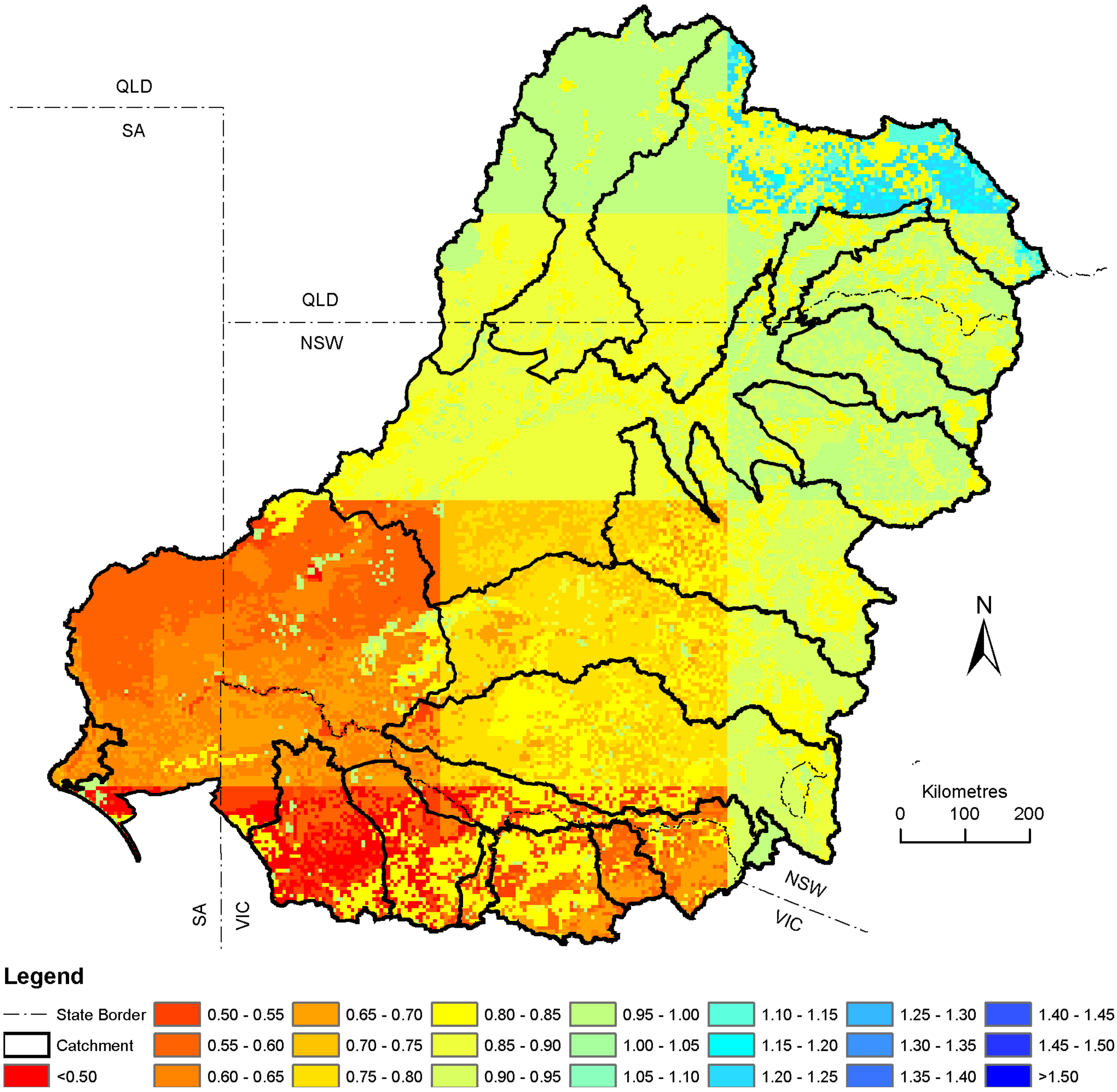

Figure 10-36. Recharge scaling factors for the giss_aom global climate model under the high global warming scenario

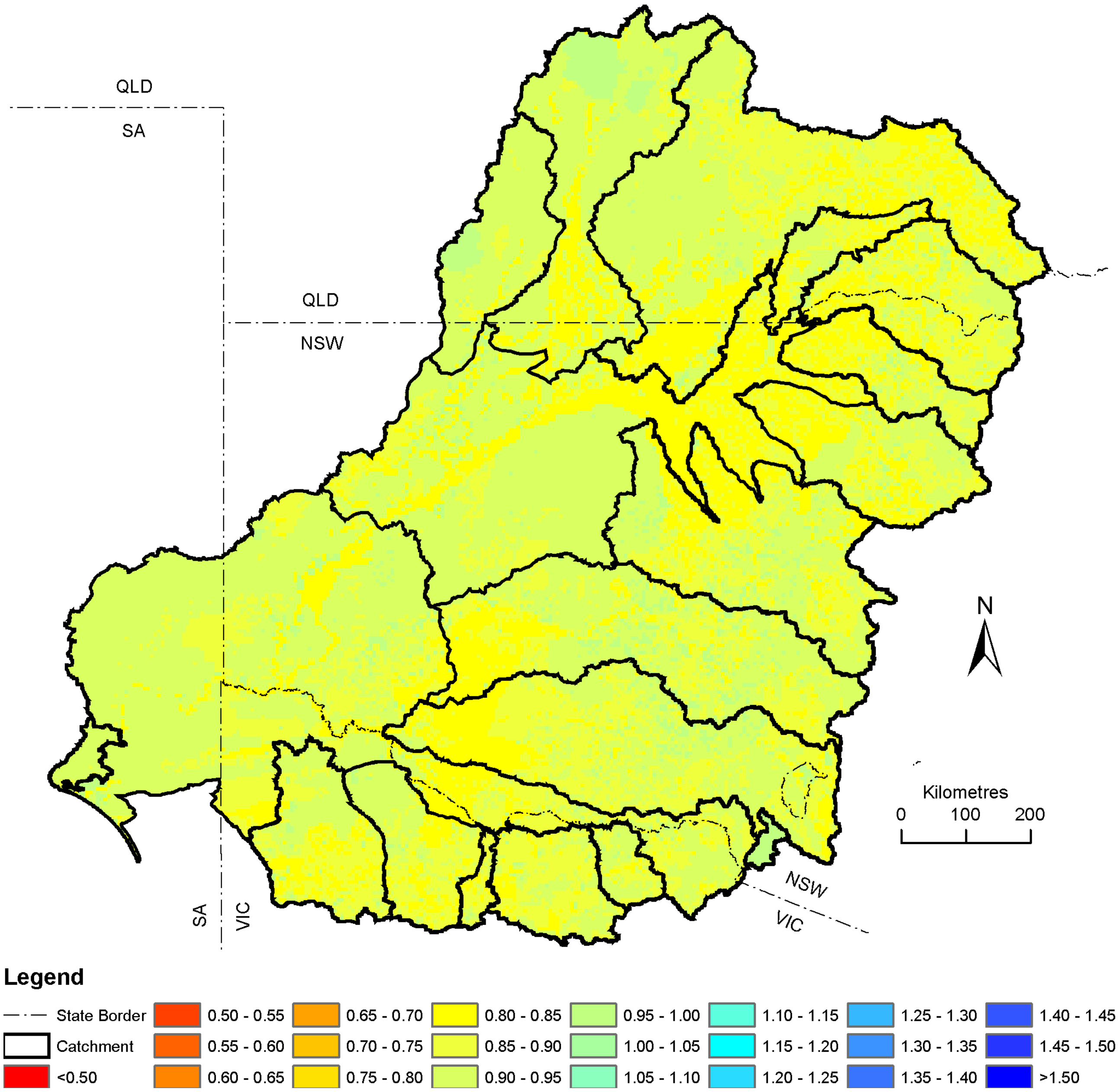

Figure 10-37. Recharge scaling factors for the iap global climate model under the high global warming scenario

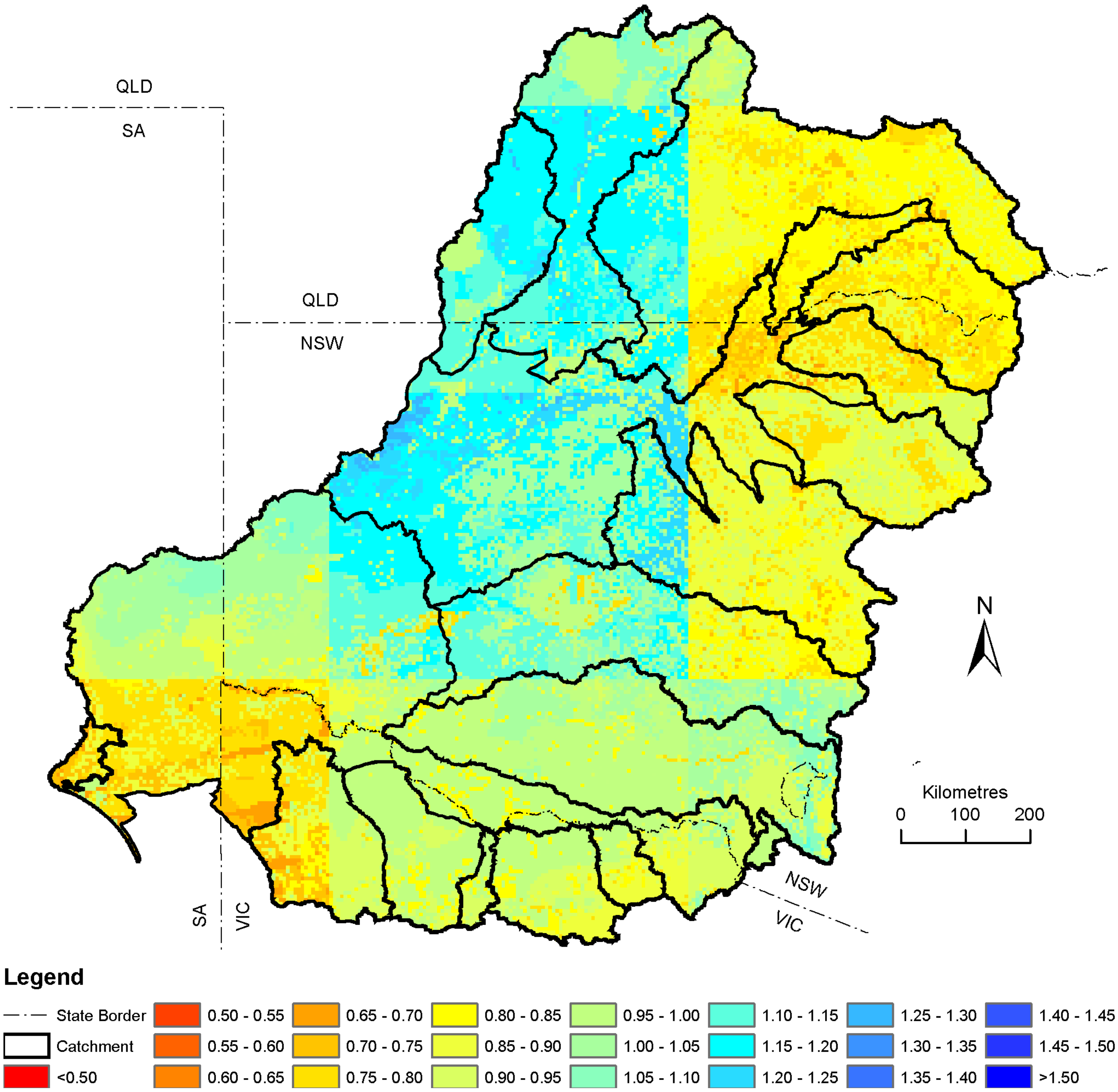

Figure 10-38. Recharge scaling factors for the inmcm global climate model under the high global warming scenario

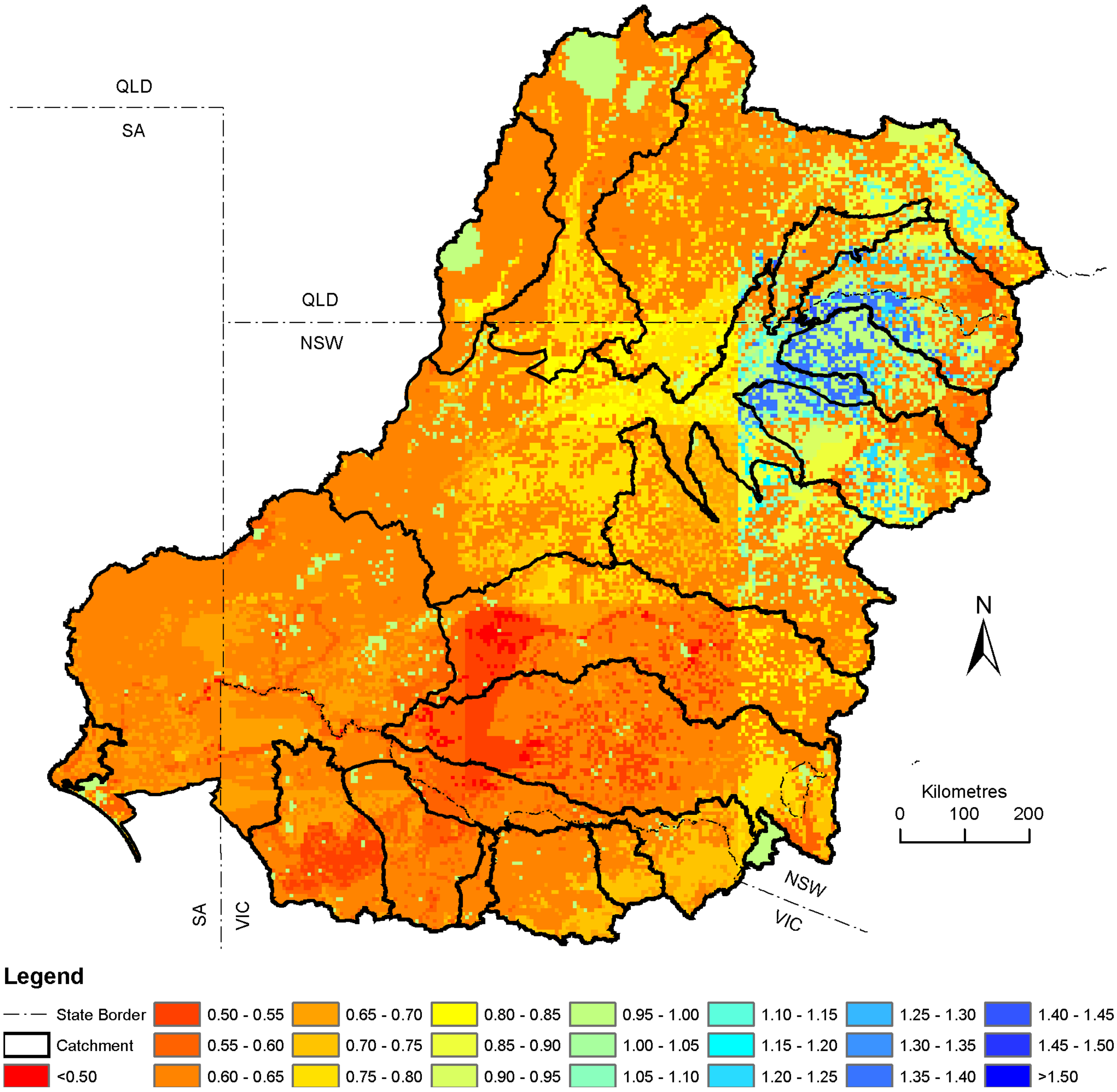

Figure 10-39. Recharge scaling factors for the ipsl global climate model under the high global warming scenario

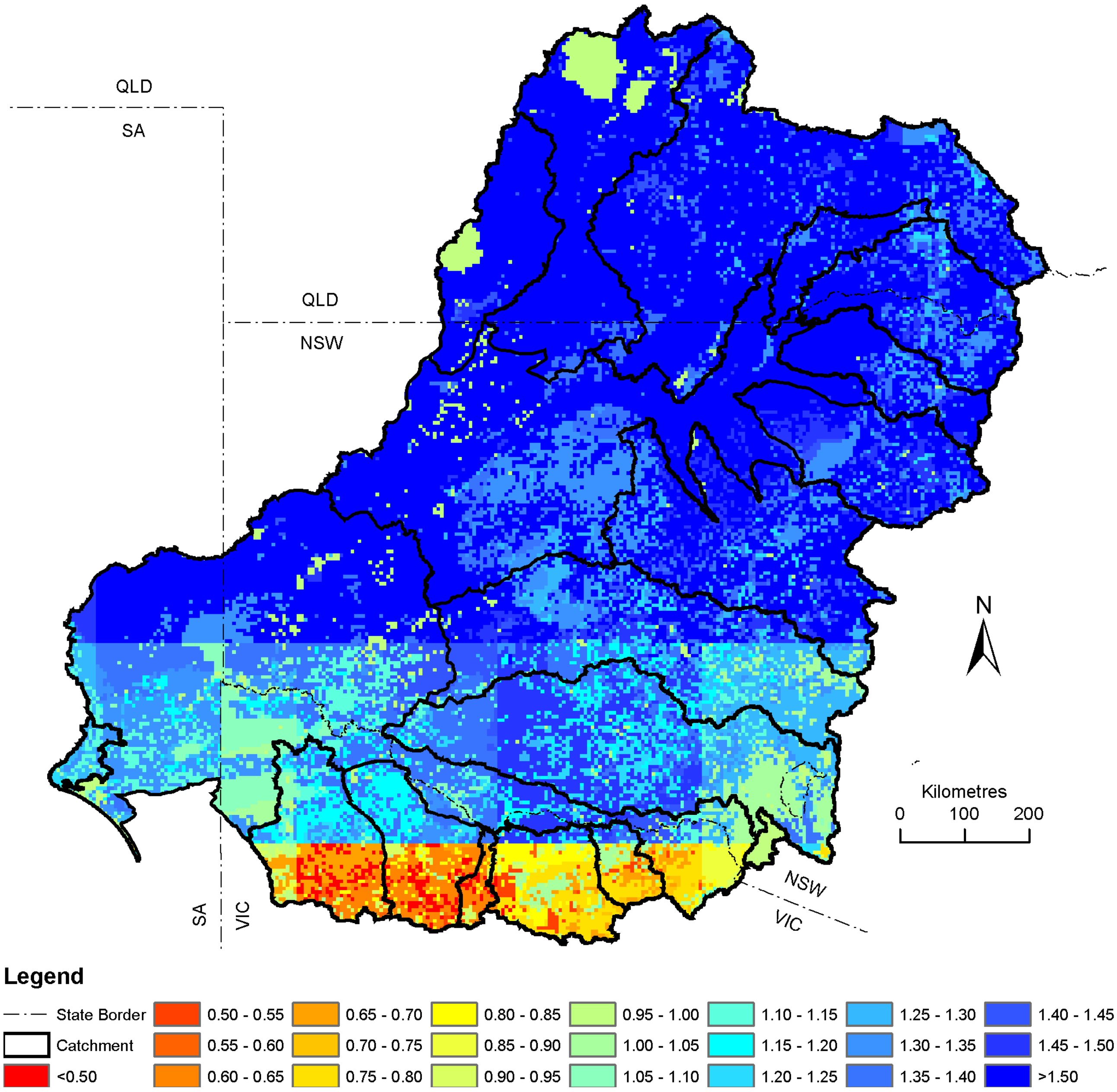

Figure 10-40. Recharge scaling factors for the miroc global climate model under the high global warming scenario

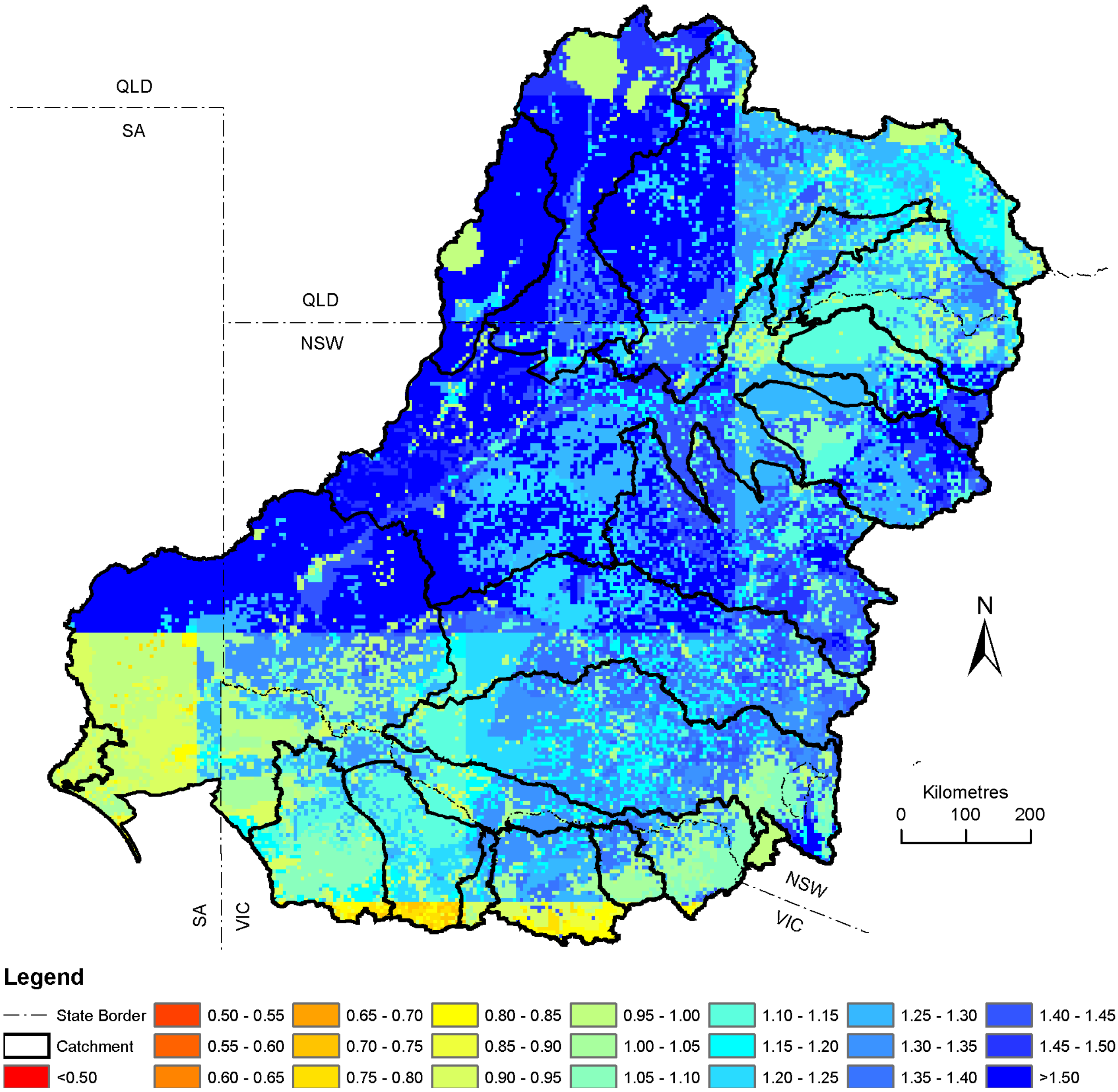

Figure 10-41. Recharge scaling factors for the miub global climate model under the high global warming scenario

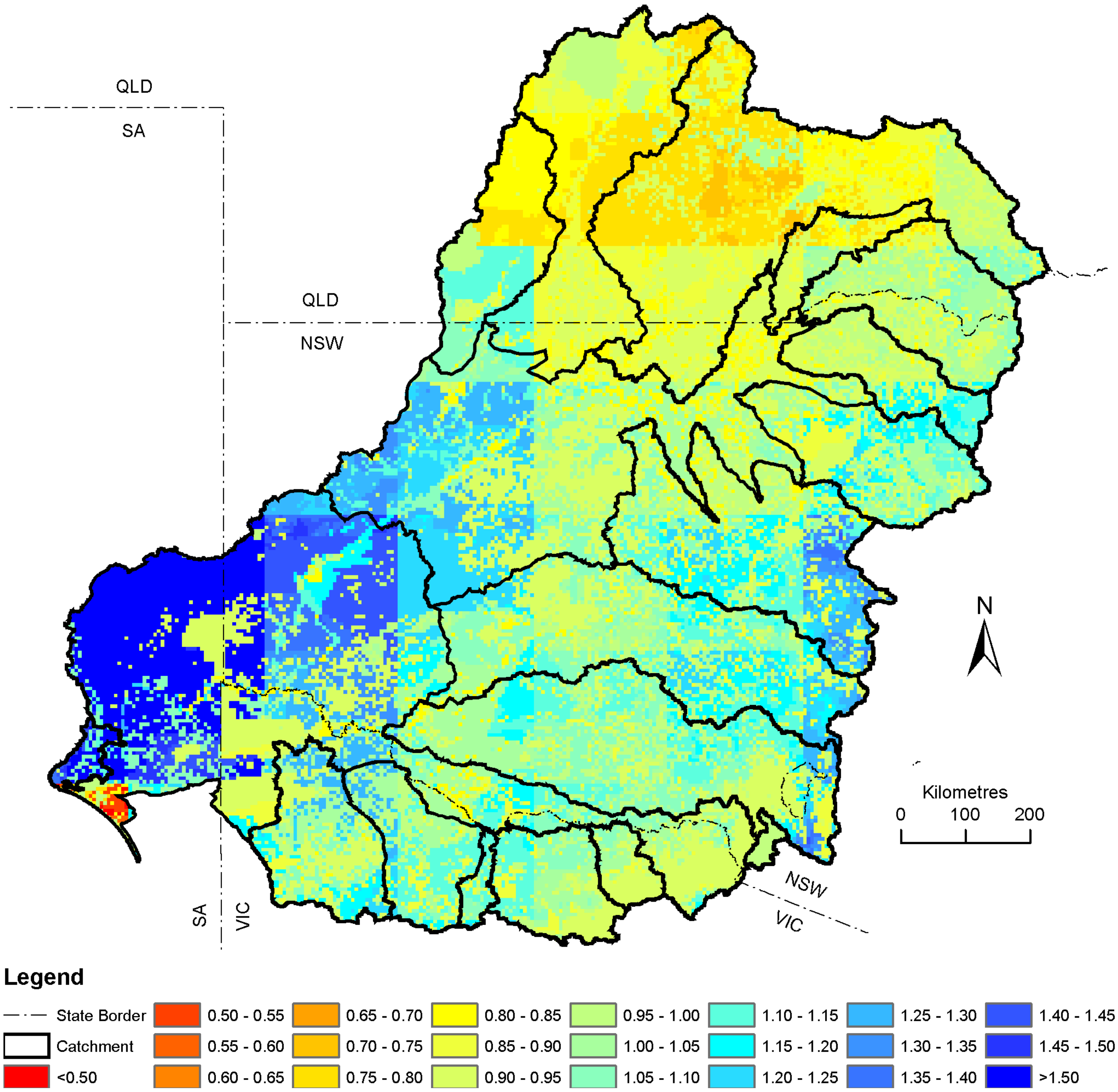

Figure 10-42. Recharge scaling factors for the mpi global climate model under the high global warming scenario

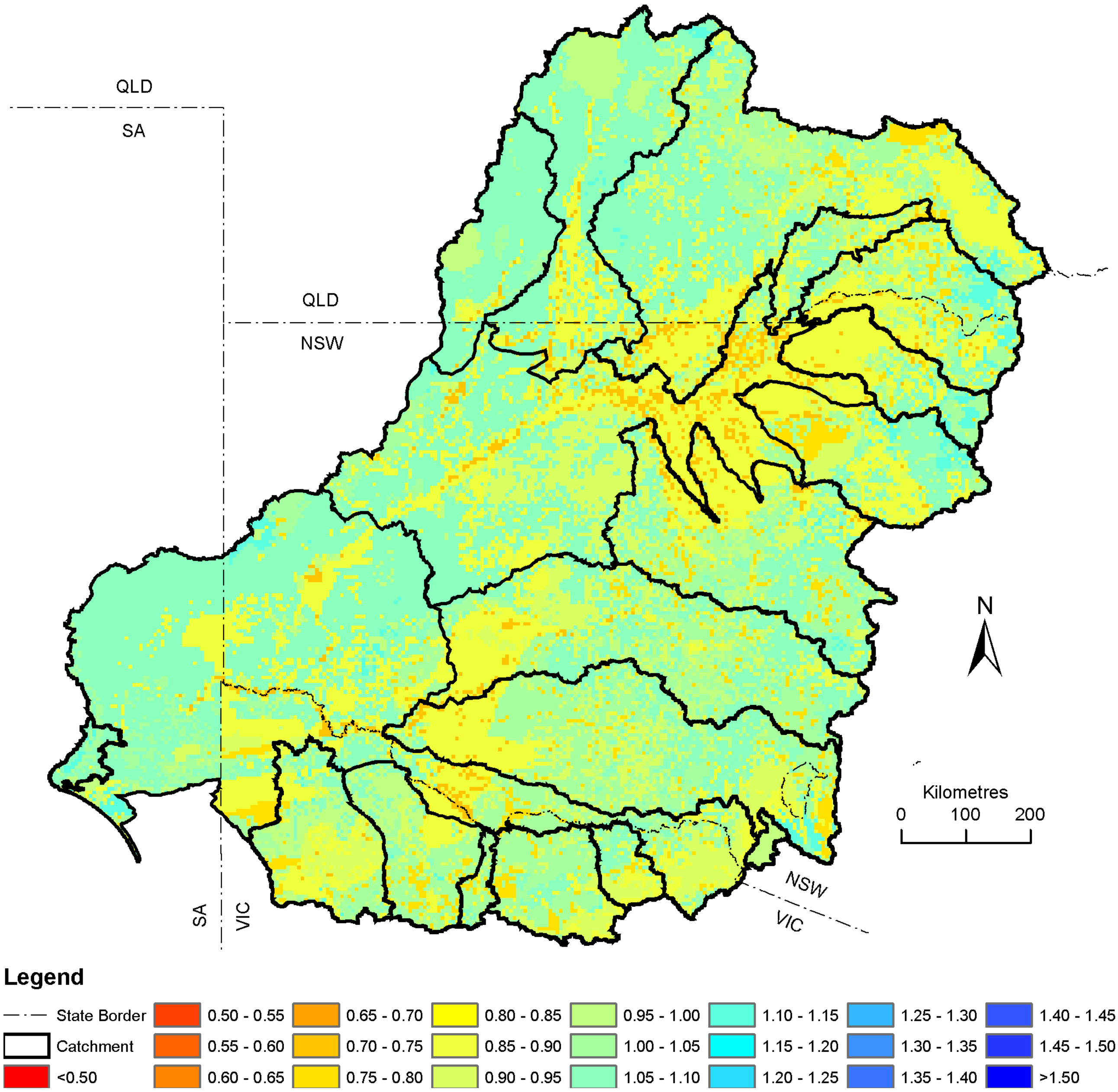

Figure 10-43. Recharge scaling factors for the mri global climate model under the high global warming scenario

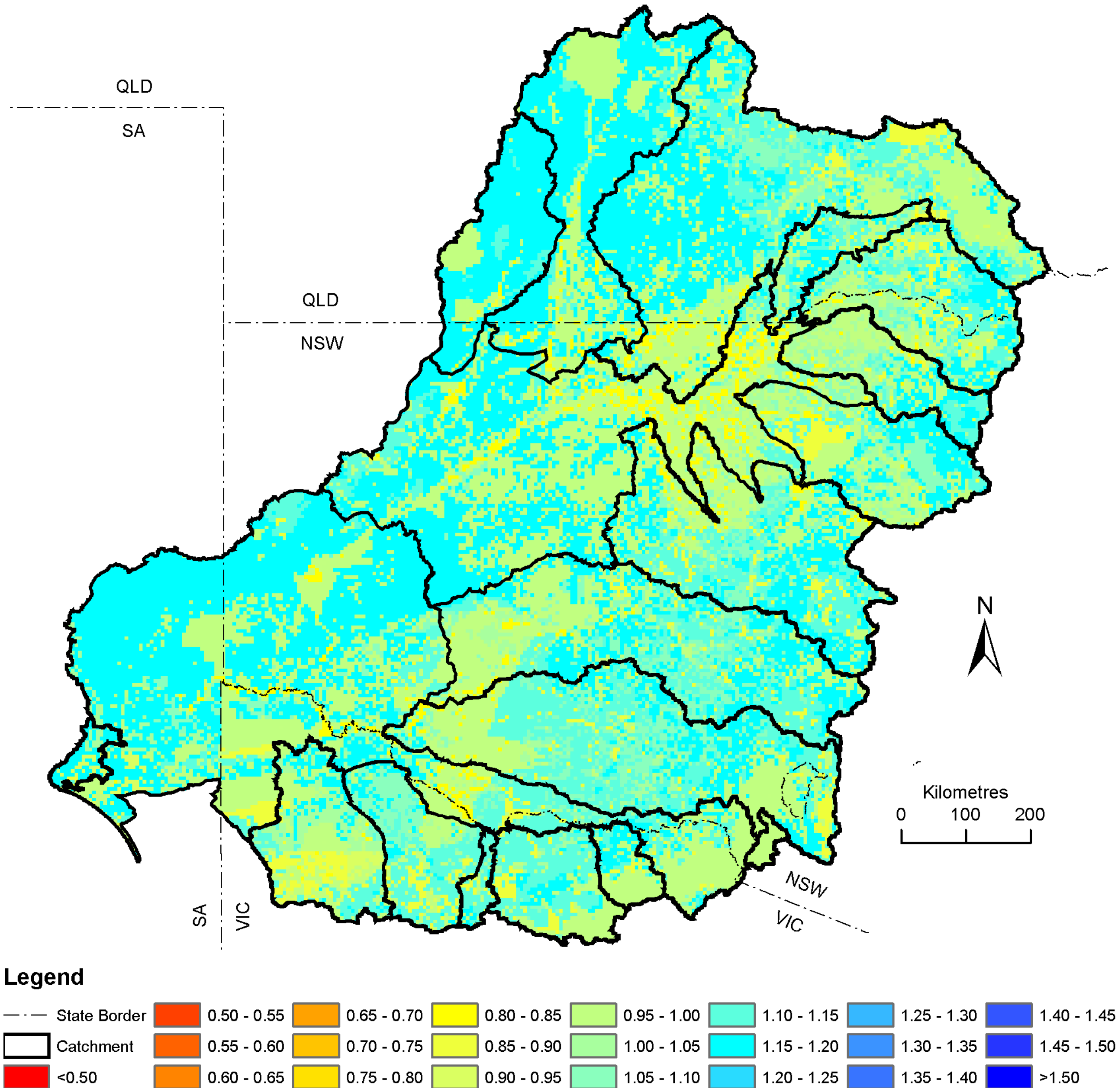

Figure 10-44. Recharge scaling factors for the ncar_ccsm global climate model under the high global warming scenario

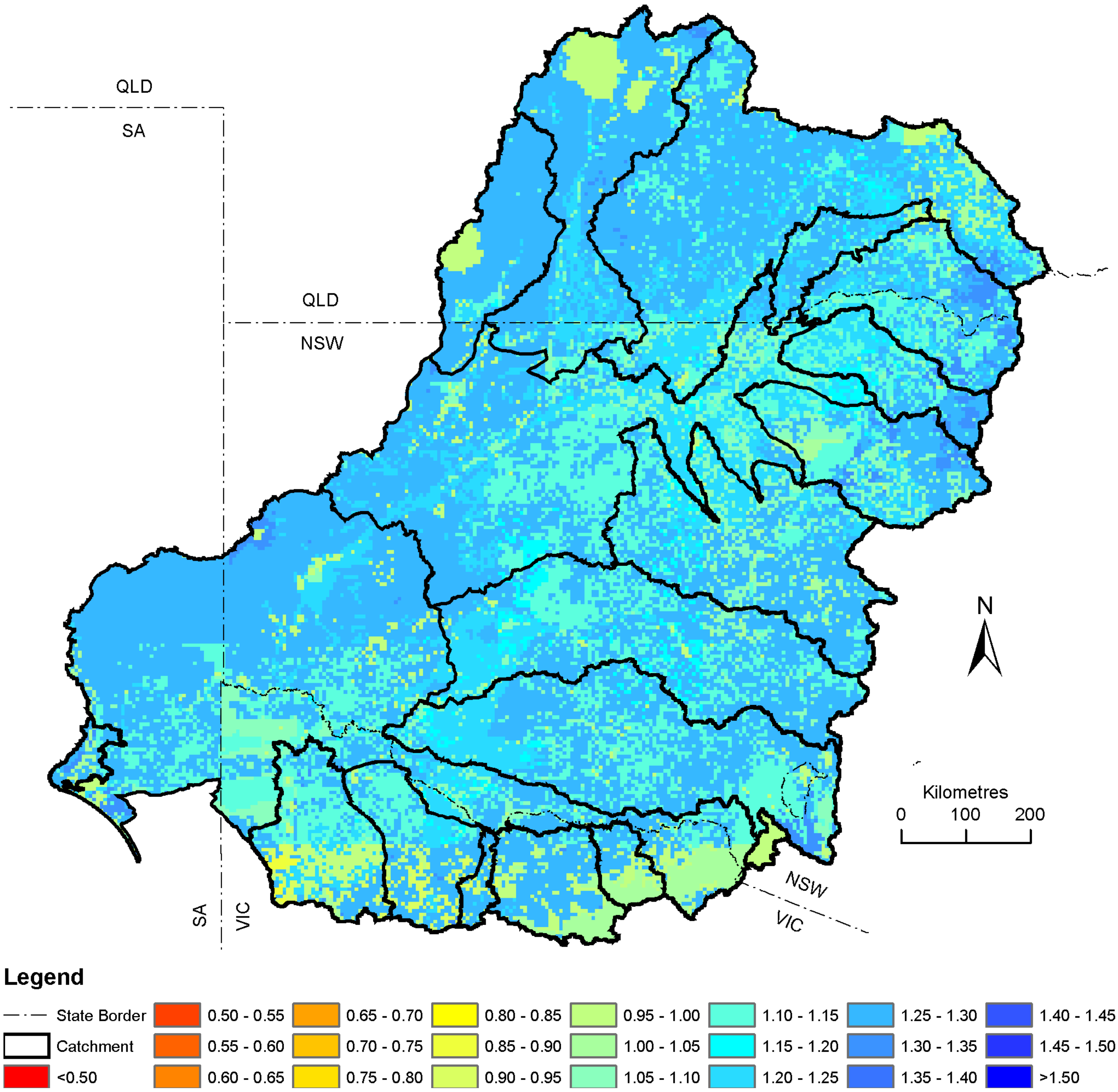

Figure 10-45. Recharge scaling factors for the ncar_pcm global climate model under the high global warming scenario

11 Appendix IV – Average change in recharge under Scenario C by region

The following tables give the change in rainfall and the change in recharge for the 45 C scenarios (three global warming scenarios and 15 global climate models). The results in bold type are those selected based upon the runoff modelling for further investigation as scenarios Cwet, Cmid and Cdry.

Table 11-1. Change in rainfall and recharge under 45 C scenarios in the Paroo region

High global warming			Medium global warming			Low global warming		
GCM	Rainfall	Recharge	GCM	Rainfall	Recharge	GCM	Rainfall	Recharge
ipsl	-12%	-34%	ipsl	-8%	-24%	ipsl	-3%	-12%
cnrm	-12%	-18%	cnrm	-7%	-13%	cnrm	-3%	-7%
iap	-5%	-9%	giss_aom	-7%	-7%	mpi	-2%	-5%
mpi	**-7%**	**-9%**	mpi	-5%	-6%	giss_aom	-3%	-4%
giss_aom	-12%	-8%	iap	-3%	-6%	iap	-2%	-3%
csiro	-8%	-3%	csiro	-5%	-3%	csiro	-2%	-2%
gfdl	-6%	1%	**gfdl**	**-4%**	**0%**	gfdl	-2%	-1%
mri	-7%	6%	mri	-5%	1%	mri	-2%	0%
inmcm	-1%	13%	inmcm	-1%	8%	inmcm	0%	3%
ncar_ccsm	3%	14%	ncar_ccsm	2%	8%	ncar_ccsm	1%	3%
ncar_pcm	9%	25%	ncar_pcm	6%	14%	ncar_pcm	2%	5%
cccma_t63	7%	27%	cccma_t63	5%	16%	cccma_t63	2%	6%
cccma_t47	13%	34%	cccma_t47	9%	20%	cccma_t47	4%	8%
miub	**13%**	**55%**	miub	8%	33%	miub	4%	13%
miroc	16%	57%	miroc	10%	34%	miroc	4%	13%

Table 11-2. Change in rainfall and recharge under 45 C scenarios in the Warrego region

High global warming			Medium global warming			Low global warming		
GCM	Rainfall	Recharge	GCM	Rainfall	Recharge	GCM	Rainfall	Recharge
ipsl	-11%	-30%	ipsl	-7%	-21%	mpi	-2%	-12%
cnrm	-10%	-19%	cnrm	-6%	-14%	ipsl	-3%	-10%
mpi	**-8%**	**-12%**	mpi	-5%	-8%	cnrm	-3%	-6%
iap	-4%	-9%	iap	-3%	-6%	iap	-1%	-3%
csiro	-8%	-6%	giss_aom	-7%	-5%	csiro	-2%	-3%
giss_aom	-11%	-5%	csiro	-5%	-5%	giss_aom	-3%	-3%
gfdl	-6%	1%	mri	-4%	-1%	mri	-2%	-1%
mri	-7%	1%	**gfdl**	**-4%**	**-1%**	gfdl	-2%	-1%
inmcm	-2%	6%	inmcm	-1%	3%	inmcm	0%	1%
ncar_ccsm	2%	10%	ncar_ccsm	1%	5%	ncar_ccsm	1%	2%
ncar_pcm	8%	21%	ncar_pcm	5%	13%	ncar_pcm	2%	5%
cccma_t63	6%	23%	cccma_t63	4%	14%	cccma_t63	2%	6%
cccma_t47	10%	31%	cccma_t47	7%	18%	cccma_t47	3%	7%
miub	**11%**	**41%**	miub	7%	24%	miub	3%	10%
miroc	15%	51%	miroc	10%	30%	miroc	4%	12%

Table 11-3. Change in rainfall and recharge under 45 C scenarios in the Condamine-Balonne region

High global warming			Medium global warming			Low global warming		
GCM	Rainfall	Recharge	GCM	Rainfall	Recharge	GCM	Rainfall	Recharge
ipsl	-8%	-17%	ipsl	-5%	-12%	mpi	-2%	-7%
cnrm	-10%	-15%	cnrm	-6%	-11%	ipsl	-2%	-6%
mpi	-8%	-10%	inmcm	-4%	-6%	cnrm	-3%	-5%
iap	-4%	-9%	mpi	-5%	-6%	mri	-2%	-3%
inmcm	-6%	-9%	csiro	-6%	-6%	inmcm	-2%	-3%
csiro	-9%	-8%	**iap**	**-3%**	**-6%**	csiro	-2%	-3%
mri	**-9%**	**-5%**	mri	-6%	-4%	iap	-1%	-2%
giss_aom	-8%	0%	gfdl	-4%	0%	gfdl	-2%	0%
gfdl	-6%	1%	giss_aom	-5%	0%	giss_aom	-2%	0%
ncar_ccsm	1%	4%	ncar_ccsm	1%	2%	ncar_ccsm	0%	1%
ncar_pcm	6%	15%	ncar_pcm	4%	9%	ncar_pcm	2%	4%
cccma_t63	6%	18%	cccma_t63	4%	12%	cccma_t63	2%	5%
miub	8%	24%	miub	5%	14%	miub	2%	6%
cccma_t47	**10%**	**28%**	cccma_t47	7%	17%	cccma_t47	3%	7%
miroc	13%	41%	miroc	8%	25%	miroc	4%	11%

Table 11-4. Change in rainfall and recharge under 45 C scenarios in the Moonie region

High global warming			Medium global warming			Low global warming		
GCM	Rainfall	Recharge	GCM	Rainfall	Recharge	GCM	Rainfall	Recharge
inmcm	-8%	-16%	cnrm	-6%	-12%	mpi	-2%	-6%
cnrm	**-9%**	**-15%**	inmcm	-5%	-12%	inmcm	-2%	-4%
ipsl	-3%	-11%	ipsl	-2%	-9%	cnrm	-3%	-4%
csiro	-9%	-10%	**csiro**	**-6%**	**-9%**	ipsl	-1%	-4%
mpi	-8%	-9%	iap	-2%	-7%	csiro	-2%	-3%
iap	-4%	-8%	mpi	-5%	-7%	mri	-2%	-3%
mri	-7%	-6%	mri	-5%	-5%	iap	-1%	-2%
giss_aom	-9%	-4%	giss_aom	-6%	-4%	giss_aom	-3%	-1%
gfdl	-7%	0%	gfdl	-4%	-2%	gfdl	-2%	0%
ncar_ccsm	2%	3%	ncar_ccsm	1%	1%	ncar_ccsm	1%	1%
miub	3%	12%	miub	2%	7%	miub	1%	4%
ncar_pcm	6%	13%	cccma_t63	4%	9%	ncar_pcm	2%	4%
cccma_t63	6%	17%	ncar_pcm	4%	9%	cccma_t63	2%	5%
cccma_t47	**9%**	**27%**	cccma_t47	6%	15%	cccma_t47	3%	7%
miroc	13%	37%	miroc	8%	22%	miroc	4%	10%

Table 11-5. Change in rainfall and recharge under 45 C scenarios in the Border Rivers region

High global warming			Medium global warming			Low global warming		
GCM	Rainfall	Recharge	GCM	Rainfall	Recharge	GCM	Rainfall	Recharge
inmcm	-9%	-15%	inmcm	-5%	-10%	inmcm	-2%	-4%
cnrm	-10%	-14%	cnrm	-6%	-9%	cnrm	-3%	-4%
iap	-3%	-9%	iap	-2%	-5%	mri	-2%	-3%
giss_aom	**-10%**	**-6%**	mri	-4%	-4%	iap	-1%	-2%
mri	-7%	-5%	giss_aom	-6%	-4%	mpi	-2%	-2%
mpi	-7%	-4%	mpi	-4%	-3%	giss_aom	-3%	-2%
csiro	-5%	-3%	csiro	-3%	-2%	ipsl	0%	-1%
ipsl	-1%	-1%	**ipsl**	**0%**	**-1%**	csiro	-1%	-1%
gfdl	-6%	2%	gfdl	-4%	1%	gfdl	-2%	0%
ncar_ccsm	2%	4%	ncar_ccsm	1%	3%	ncar_ccsm	0%	1%
miub	3%	15%	miub	2%	9%	miub	1%	4%
ncar_pcm	6%	15%	ncar_pcm	4%	9%	ncar_pcm	2%	4%
cccma_t63	4%	17%	cccma_t63	3%	11%	cccma_t63	1%	5%
cccma_t47	**9%**	**28%**	cccma_t47	6%	18%	cccma_t47	2%	7%
miroc	12%	37%	miroc	7%	23%	miroc	3%	10%

Table 11-6. Change in rainfall and recharge under 45 C scenarios in the Gwydir region

High global warming			Medium global warming			Low global warming		
GCM	Rainfall	Recharge	GCM	Rainfall	Recharge	GCM	Rainfall	Recharge
inmcm	-8%	-14%	inmcm	-5%	-9%	inmcm	-2%	-4%
cnrm	-10%	-13%	cnrm	-6%	-9%	cnrm	-3%	-4%
iap	-3%	-9%	iap	-2%	-5%	iap	-1%	-2%
giss_aom	**-10%**	**-6%**	mri	-4%	-4%	mri	-2%	-2%
mri	-6%	-5%	giss_aom	-6%	-3%	giss_aom	-3%	-2%
mpi	-7%	-2%	mpi	-4%	-2%	mpi	-2%	-1%
csiro	-4%	-1%	csiro	-3%	0%	ipsl	0%	0%
gfdl	-6%	1%	gfdl	-4%	1%	gfdl	-2%	0%
ipsl	0%	2%	**ipsl**	**0%**	**1%**	csiro	-1%	0%
ncar_ccsm	2%	5%	ncar_ccsm	1%	3%	ncar_ccsm	1%	1%
ncar_pcm	6%	16%	ncar_pcm	4%	10%	ncar_pcm	2%	4%
cccma_t63	5%	18%	cccma_t63	3%	13%	cccma_t63	1%	5%
miub	6%	24%	miub	4%	15%	miub	2%	6%
cccma_t47	**11%**	**32%**	cccma_t47	7%	21%	cccma_t47	3%	8%
miroc	12%	41%	miroc	8%	26%	miroc	3%	11%

Table 11-7. Change in rainfall and recharge under 45 C scenarios in the Namoi region

High global warming			Medium global warming			Low global warming		
GCM	Rainfall	Recharge	GCM	Rainfall	Recharge	GCM	Rainfall	Recharge
cnrm	-10%	-16%	cnrm	-6%	-12%	cnrm	-3%	-5%
inmcm	-7%	-12%	inmcm	-4%	-8%	inmcm	-2%	-3%
iap	-3%	-9%	iap	-2%	-6%	ipsl	-1%	-3%
ipsl	-3%	-7%	ipsl	-2%	-5%	iap	-1%	-2%
giss_aom	**-10%**	**-7%**	giss_aom	-6%	-5%	giss_aom	-3%	-2%
mri	-3%	-6%	mri	-2%	-5%	mri	-1%	-1%
mpi	-6%	-3%	mpi	-4%	-3%	mpi	-2%	0%
csiro	-3%	2%	**csiro**	**-2%**	**1%**	ncar_ccsm	1%	1%
ncar_ccsm	2%	3%	ncar_ccsm	2%	2%	gfdl	-1%	1%
gfdl	-4%	4%	gfdl	-3%	2%	csiro	-1%	1%
ncar_pcm	5%	13%	ncar_pcm	3%	8%	ncar_pcm	1%	4%
cccma_t63	5%	18%	cccma_t63	4%	11%	cccma_t63	2%	5%
miub	8%	23%	miub	5%	14%	miub	2%	6%
cccma_t47	**13%**	**33%**	cccma_t47	8%	19%	cccma_t47	4%	8%
miroc	12%	37%	miroc	8%	23%	miroc	3%	10%

Table 11-8. Change in rainfall and recharge under 45 C scenarios in the Macquarie-Castlereagh region

High global warming			Medium global warming			Low global warming		
GCM	Rainfall	Recharge	GCM	Rainfall	Recharge	GCM	Rainfall	Recharge
ipsl	-10%	-17%	ipsl	-7%	-12%	ipsl	-3%	-6%
cnrm	-11%	-15%	cnrm	-7%	-10%	cnrm	-3%	-5%
giss_aom	**-13%**	**-13%**	giss_aom	-8%	-9%	giss_aom	-4%	-4%
iap	-3%	-8%	inmcm	-4%	-5%	inmcm	-2%	-3%
inmcm	-6%	-8%	iap	-2%	-4%	iap	-1%	-2%
csiro	-7%	-6%	csiro	-4%	-4%	csiro	-2%	-2%
mri	-3%	-4%	**mri**	**-2%**	**-3%**	mri	-1%	0%
mpi	-6%	0%	mpi	-4%	0%	ncar_ccsm	1%	1%
ncar_ccsm	3%	6%	ncar_ccsm	2%	4%	gfdl	-1%	1%
gfdl	-3%	6%	gfdl	-2%	4%	mpi	-2%	3%
ncar_pcm	5%	14%	ncar_pcm	3%	8%	ncar_pcm	1%	4%
cccma_t63	6%	17%	cccma_t63	4%	12%	cccma_t63	2%	5%
miub	10%	27%	miub	7%	17%	miub	3%	7%
cccma_t47	13%	30%	cccma_t47	8%	18%	cccma_t47	4%	8%
miroc	**12%**	**35%**	miroc	8%	22%	miroc	3%	9%

Table 11-9. Change in rainfall and recharge under 45 C scenarios in the Barwon-Darling region

High global warming			Medium global warming			Low global warming		
GCM	Rainfall	Recharge	GCM	Rainfall	Recharge	GCM	Rainfall	Recharge
ipsl	-13%	-20%	cnrm	-7%	-15%	ipsl	-4%	-6%
cnrm	-10%	-19%	ipsl	-8%	-14%	cnrm	-3%	-6%
giss_aom	**-13%**	**-14%**	giss_aom	-9%	-11%	giss_aom	-4%	-4%
iap	-4%	-10%	csiro	-5%	-8%	csiro	-2%	-3%
csiro	-7%	-9%	**iap**	**-3%**	**-7%**	iap	-1%	-2%
mri	-5%	-9%	mri	-3%	-7%	mri	-1%	-2%
mpi	-6%	-5%	mpi	-4%	-4%	inmcm	-1%	-1%
inmcm	-2%	-1%	inmcm	-2%	-2%	gfdl	-2%	0%
gfdl	-6%	0%	gfdl	-4%	-1%	ncar_ccsm	1%	0%
ncar_ccsm	3%	0%	ncar_ccsm	2%	-1%	mpi	-2%	2%
ncar_pcm	8%	14%	ncar_pcm	5%	9%	ncar_pcm	2%	4%
cccma_t63	8%	17%	cccma_t63	5%	10%	cccma_t63	2%	5%
miub	**14%**	**29%**	cccma_t47	8%	16%	miub	4%	7%
cccma_t47	12%	32%	miub	9%	17%	cccma_t47	3%	7%
miroc	13%	37%	miroc	8%	22%	miroc	4%	10%

Table 11-10. Change in rainfall and recharge under 45 C scenarios in the Lachlan region

High global warming			Medium global warming			Low global warming		
GCM	Rainfall	Recharge	GCM	Rainfall	Recharge	GCM	Rainfall	Recharge
ipsl	**-18%**	**-34%**	ipsl	-12%	-21%	ipsl	-5%	-10%
giss_aom	-15%	-18%	giss_aom	-10%	-12%	cnrm	-4%	-6%
cnrm	-13%	-15%	cnrm	-8%	-12%	giss_aom	-4%	-5%
csiro	-10%	-12%	csiro	-7%	-9%	csiro	-3%	-4%
iap	-4%	-7%	iap	-2%	-5%	iap	-1%	-2%
inmcm	-4%	-4%	inmcm	-2%	-3%	inmcm	-1%	-1%
mri	-4%	1%	mri	-2%	-3%	mri	-1%	0%
gfdl	-5%	3%	**mpi**	**-4%**	**-2%**	gfdl	-1%	1%
mpi	-6%	5%	gfdl	-3%	2%	ncar_ccsm	1%	2%
ncar_ccsm	3%	9%	ncar_ccsm	2%	3%	mpi	-2%	2%
cccma_t63	6%	16%	ncar_pcm	4%	9%	ncar_pcm	2%	4%
ncar_pcm	**7%**	**21%**	cccma_t63	4%	10%	cccma_t63	2%	5%
cccma_t47	8%	23%	miub	5%	14%	miub	2%	6%
miub	8%	32%	cccma_t47	5%	14%	cccma_t47	2%	6%
miroc	8%	33%	miroc	5%	14%	miroc	2%	6%

Table 11-11. Change in rainfall and recharge under 45 C scenarios in the Murrumbidgee region

High global warming			Medium global warming			Low global warming		
GCM	Rainfall	Recharge	GCM	Rainfall	Recharge	GCM	Rainfall	Recharge
ipsl	**-19%**	**-30%**	ipsl	-12%	-20%	ipsl	-5%	-10%
cnrm	-14%	-18%	cnrm	-9%	-14%	cnrm	-4%	-8%
giss_aom	-15%	-16%	giss_aom	-10%	-10%	giss_aom	-4%	-5%
csiro	-11%	-13%	csiro	-7%	-8%	csiro	-3%	-4%
iap	-4%	-9%	iap	-3%	-5%	iap	-1%	-2%
mri	-4%	-5%	**mri**	**-2%**	**-4%**	inmcm	-1%	-2%
inmcm	-5%	-4%	inmcm	-3%	-3%	mri	-1%	-1%
mpi	-6%	-3%	mpi	-4%	-2%	mpi	-2%	-1%
gfdl	-6%	0%	gfdl	-4%	0%	gfdl	-2%	0%
ncar_ccsm	2%	3%	ncar_ccsm	1%	2%	ncar_ccsm	1%	1%
miroc	5%	13%	ncar_pcm	4%	9%	miub	1%	4%
miub	5%	14%	miroc	3%	9%	ncar_pcm	2%	4%
cccma_t63	4%	14%	miub	3%	9%	miroc	1%	4%
ncar_pcm	**6%**	**15%**	cccma_t63	3%	10%	cccma_t63	1%	4%
cccma_t47	4%	21%	cccma_t47	2%	14%	cccma_t47	1%	6%

Table 11-12. Change in rainfall and recharge under 45 C scenarios in the Murray region

High global warming			Medium global warming			Low global warming		
GCM	Rainfall	Recharge	GCM	Rainfall	Recharge	GCM	Rainfall	Recharge
giss_aom	-21%	-31%	giss_aom	-13%	-22%	giss_aom	-6%	-10%
ipsl	**-19%**	**-31%**	ipsl	-13%	-21%	ipsl	-5%	-9%
cnrm	-13%	-20%	cnrm	-8%	-15%	cnrm	-4%	-8%
csiro	-8%	-10%	csiro	-5%	-7%	csiro	-2%	-3%
inmcm	-6%	-10%	inmcm	-4%	-7%	inmcm	-2%	-3%
iap	-5%	-9%	iap	-3%	-6%	mri	-2%	-3%
mri	-7%	-7%	gfdl	-8%	-6%	gfdl	-3%	-2%
gfdl	-12%	-7%	mri	-4%	-5%	iap	-1%	-2%
mpi	-5%	-3%	**mpi**	**-3%**	**-3%**	ncar_ccsm	1%	0%
miroc	6%	-2%	ncar_ccsm	1%	0%	miroc	2%	1%
ncar_ccsm	2%	0%	miroc	4%	0%	mpi	-1%	2%
miub	4%	6%	miub	3%	4%	miub	1%	2%
ncar_pcm	**8%**	**8%**	ncar_pcm	5%	6%	ncar_pcm	2%	4%
cccma_t63	6%	12%	cccma_t63	4%	10%	cccma_t63	2%	4%
cccma_t47	3%	19%	cccma_t47	2%	12%	cccma_t47	1%	6%

Table 11-13. Change in rainfall and recharge under 45 C scenarios in the Ovens region

High global warming			Medium global warming			Low global warming		
GCM	Rainfall	Recharge	GCM	Rainfall	Recharge	GCM	Rainfall	Recharge
giss_aom	-22%	-37%	giss_aom	-14%	-26%	cnrm	-5%	-13%
ipsl	-18%	-29%	ipsl	-12%	-20%	giss_aom	-6%	-12%
miroc	-6%	-25%	cnrm	-12%	-19%	ipsl	-5%	-9%
cnrm	**-18%**	**-22%**	miroc	-4%	-13%	csiro	-3%	-5%
csiro	-10%	-17%	csiro	-6%	-12%	inmcm	-2%	-4%
inmcm	-6%	-14%	inmcm	-4%	-10%	miroc	-2%	-4%
iap	-2%	-10%	**mri**	**-4%**	**-7%**	mri	-2%	-4%
mri	-6%	-9%	iap	-2%	-7%	mpi	-2%	-4%
mpi	-7%	-7%	mpi	-4%	-6%	iap	-1%	-2%
gfdl	-9%	-5%	gfdl	-6%	-4%	gfdl	-2%	-2%
ncar_ccsm	0%	-1%	ncar_ccsm	0%	-1%	ncar_ccsm	0%	0%
ncar_pcm	3%	3%	miub	2%	3%	miub	1%	2%
miub	**3%**	**4%**	ncar_pcm	2%	4%	ncar_pcm	1%	4%
cccma_t63	1%	6%	cccma_t63	0%	9%	cccma_t63	0%	4%
cccma_t47	3%	20%	cccma_t47	2%	13%	cccma_t47	1%	7%

Table 11-14. Change in rainfall and recharge under 45 C scenarios in the Goulburn-Broken region

High global warming			Medium global warming			Low global warming		
GCM	Rainfall	Recharge	GCM	Rainfall	Recharge	GCM	Rainfall	Recharge
giss_aom	-22%	-36%	giss_aom	-14%	-25%	cnrm	-5%	-12%
ipsl	-19%	-30%	ipsl	-12%	-20%	giss_aom	-6%	-11%
miroc	-7%	-23%	cnrm	-12%	-19%	ipsl	-5%	-9%
cnrm	**-18%**	**-22%**	miroc	-5%	-12%	mpi	-2%	-5%
csiro	-10%	-13%	csiro	-6%	-9%	csiro	-3%	-4%
inmcm	-6%	-13%	inmcm	-4%	-9%	inmcm	-2%	-4%
iap	-2%	-9%	**mri**	**-4%**	**-6%**	miroc	-2%	-3%
miub	0%	-9%	iap	-2%	-6%	mri	-2%	-3%
mri	-6%	-9%	miub	0%	-5%	iap	-1%	-2%
mpi	-6%	-7%	mpi	-4%	-5%	gfdl	-3%	-2%
gfdl	-9%	-4%	gfdl	-6%	-4%	miub	0%	-1%
ncar_ccsm	0%	-1%	ncar_ccsm	0%	-1%	ncar_ccsm	0%	0%
ncar_pcm	2%	3%	ncar_pcm	1%	4%	ncar_pcm	1%	4%
cccma_t63	**0%**	**6%**	cccma_t47	0%	9%	cccma_t63	0%	5%
cccma_t47	0%	13%	cccma_t63	0%	9%	cccma_t47	0%	7%

Table 11-15. Change in rainfall and recharge under 45 C scenarios in the Campaspe region

High global warming			Medium global warming			Low global warming		
GCM	Rainfall	Recharge	GCM	Rainfall	Recharge	GCM	Rainfall	Recharge
giss_aom	-22%	-40%	giss_aom	-14%	-29%	giss_aom	-6%	-14%
ipsl	-19%	-34%	ipsl	-12%	-24%	ipsl	-5%	-11%
miroc	-10%	-28%	cnrm	-11%	-16%	cnrm	-5%	-9%
cnrm	**-18%**	**-20%**	miroc	-7%	-15%	miroc	-3%	-6%
csiro	-11%	-13%	csiro	-7%	-8%	csiro	-3%	-5%
iap	-2%	-11%	iap	-2%	-6%	inmcm	-2%	-3%
inmcm	-6%	-7%	**inmcm**	**-4%**	**-5%**	iap	-1%	-3%
gfdl	-13%	-7%	gfdl	-8%	-4%	mri	-2%	-3%
mri	-9%	-3%	mri	-6%	-3%	gfdl	-4%	-3%
miub	0%	-2%	miub	0%	-1%	miub	0%	0%
mpi	-6%	1%	mpi	-4%	0%	ncar_ccsm	0%	1%
ncar_ccsm	0%	5%	ncar_ccsm	0%	3%	ncar_pcm	0%	3%
ncar_pcm	1%	8%	ncar_pcm	1%	5%	mpi	-2%	3%
cccma_t63	**0%**	**14%**	cccma_t63	0%	12%	cccma_t63	0%	5%
cccma_t47	0%	20%	cccma_t47	0%	16%	cccma_t47	0%	7%

Table 11-16. Change in rainfall and recharge under 45 C scenarios in the Loddon-Avoca region

High global warming			Medium global warming			Low global warming		
GCM	Rainfall	Recharge	GCM	Rainfall	Recharge	GCM	Rainfall	Recharge
giss_aom	-23%	-44%	giss_aom	-15%	-29%	giss_aom	-7%	-14%
ipsl	**-20%**	**-36%**	ipsl	-13%	-24%	ipsl	-6%	-11%
cnrm	-15%	-13%	cnrm	-10%	-9%	cnrm	-4%	-5%
csiro	-10%	-12%	csiro	-7%	-7%	csiro	-3%	-3%
gfdl	-12%	-10%	gfdl	-8%	-6%	gfdl	-3%	-3%
iap	-3%	-7%	iap	-2%	-4%	mri	-2%	-2%
inmcm	-6%	-3%	**inmcm**	**-4%**	**-2%**	iap	-1%	-2%
mri	-8%	-2%	mri	-5%	-1%	inmcm	-2%	-1%
mpi	-6%	1%	mpi	-4%	0%	ncar_ccsm	0%	2%
miroc	-4%	5%	ncar_ccsm	0%	4%	miroc	-1%	2%
ncar_ccsm	0%	6%	miroc	-3%	4%	mpi	-2%	3%
miub	0%	8%	miub	0%	6%	miub	0%	3%
cccma_t47	-1%	9%	ncar_pcm	2%	6%	ncar_pcm	1%	3%
ncar_pcm	**3%**	**10%**	cccma_t47	-1%	7%	cccma_t47	0%	3%
cccma_t63	3%	14%	cccma_t63	2%	10%	cccma_t63	1%	4%

Table 11-17. Change in rainfall and recharge under 45 C scenarios in the Wimmera region

High global warming			Medium global warming			Low global warming		
GCM	Rainfall	Recharge	GCM	Rainfall	Recharge	GCM	Rainfall	Recharge
giss_aom	-23%	-46%	giss_aom	-15%	-32%	giss_aom	-7%	-14%
ipsl	**-20%**	**-37%**	ipsl	-13%	-25%	ipsl	-6%	-11%
gfdl	-15%	-18%	gfdl	-9%	-12%	cnrm	-4%	-6%
cnrm	-15%	-15%	cnrm	-10%	-12%	gfdl	-4%	-5%
csiro	-10%	-14%	csiro	-7%	-10%	csiro	-3%	-4%
inmcm	-8%	-11%	inmcm	-5%	-8%	inmcm	-2%	-3%
iap	-3%	-8%	iap	-2%	-5%	mri	-2%	-3%
mri	-9%	-5%	**mri**	**-6%**	**-3%**	iap	-1%	-2%
mpi	-5%	-1%	mpi	-3%	-1%	mpi	-2%	-1%
ncar_ccsm	-1%	0%	ncar_ccsm	-1%	0%	ncar_ccsm	0%	0%
miroc	-3%	1%	miroc	-2%	1%	miroc	-1%	1%
miub	0%	6%	miub	0%	4%	miub	0%	2%
ncar_pcm	3%	7%	ncar_pcm	2%	6%	ncar_pcm	1%	3%
cccma_t47	**0%**	**10%**	cccma_t47	0%	7%	cccma_t47	0%	4%
cccma_t63	2%	14%	cccma_t63	2%	9%	cccma_t63	1%	4%

Table 11-18. Change in rainfall and recharge under 45 C scenarios in the Eastern Mt Lofty Ranges region

High global warming			Medium global warming			Low global warming		
GCM	Rainfall	Recharge	GCM	Rainfall	Recharge	GCM	Rainfall	Recharge
ipsl	**-19%**	**-36%**	giss_aom	-13%	-25%	giss_aom	-6%	-11%
giss_aom	-20%	-34%	ipsl	-12%	-25%	ipsl	-5%	-11%
gfdl	-18%	-19%	gfdl	-12%	-14%	gfdl	-5%	-6%
inmcm	-10%	-17%	inmcm	-7%	-12%	csiro	-4%	-5%
csiro	-14%	-14%	csiro	-9%	-11%	inmcm	-3%	-5%
cnrm	-14%	-12%	cnrm	-9%	-11%	cnrm	-4%	-4%
miub	-8%	-7%	iap	-3%	-6%	iap	-1%	-2%
iap	-4%	-7%	**miub**	**-5%**	**-5%**	mri	-3%	-2%
ncar_ccsm	-4%	0%	ncar_ccsm	-2%	-1%	miub	-2%	-1%
mri	-10%	1%	mri	-6%	-1%	ncar_ccsm	-1%	0%
ncar_pcm	2%	7%	ncar_pcm	1%	5%	ncar_pcm	1%	2%
cccma_t47	-2%	11%	cccma_t47	-1%	6%	cccma_t63	0%	3%
cccma_t63	**1%**	**13%**	mpi	-2%	6%	cccma_t47	-1%	3%
miroc	1%	13%	cccma_t63	1%	7%	miroc	0%	4%
mpi	-4%	14%	miroc	1%	8%	mpi	-1%	13%

12 Appendix V – Recharge scaling factors for groundwater management units and model domains

Table 12-1. Recharge scaling factors calculated for each groundwater management unit under scenarios B and C

GMU	B	Cdry	Cmid	Cwet
ACT	83%	76%	93%	112%
Adelaide Fold Belt	58%	62%	120%	129%
Alexandra GMA	62%	74%	101%	128%
Barnawartha GMA	106%	72%	102%	134%
Bell Valley Aluvium	106%	96%	104%	158%
Belubula Valley Alluvium	82%	60%	110%	130%
Billabong Creek Alluvium (upstream of Mahonga)	73%	60%	97%	116%
Border Rivers Alluvium	101%	98%	101%	128%
Castlereagh Alluvium	116%	98%	96%	137%
Collaburragundry-Talbragar Valley	119%	98%	98%	153%
Condamine CGMA SA 1	70%	87%	93%	134%
Condamine CGMA SA 2	72%	91%	94%	132%
Condamine CGMA SA 3	79%	87%	94%	134%
Condamine CGMA SA 4	83%	94%	94%	130%
Condamine CGMA SA 5	83%	97%	94%	131%
Condamine River Alluvium (Cunningham to Ellangowan)	83%	94%	94%	133%
Condamine River Alluvium (Killarny to Murry Bridge)	75%	91%	93%	117%
Condamine River Alluvium (Murry Bridge to Cunningham)	93%	90%	93%	117%
Condamine River d/s of CGMA	71%	90%	94%	130%
Cudgegong Valley Alluvium	110%	95%	100%	173%
Dalrymple Creek Alluvium	74%	96%	93%	121%
Ellesmere GMA	55%	71%	96%	127%
EMLR	77%	65%	97%	114%
Emu Creek Alluvium	79%	104%	90%	153%
GAB Alluvial	116%	97%	102%	132%
Galarganbone Tertiary Basalt	125%	96%	90%	138%
Glengallen Creek Alluvium	75%	89%	93%	112%
Goorambat GMA	55%	86%	100%	130%
Goroke	66%	60%	97%	112%
Great Artesian Basin	115%	98%	99%	132%
Gunnedah Basin	113%	98%	99%	133%
Inverell Basalt	114%	98%	102%	130%
Kaniva	80%	65%	96%	111%
Kanmantoo Fold Belt	108%	93%	96%	140%
Kinglake GMA	83%	77%	94%	102%
King's Creek Alluvium	76%	88%	94%	114%
Lachlan Fold Belt	84%	78%	96%	118%
Liverpool Ranges Basalt	115%	98%	98%	137%
Lower Darling Alluvium	77%	65%	103%	119%
Lower Gwydir Alluvium	125%	99%	122%	132%
Lower Lachlan Alluvium (downstream of Lake Cargelligo)	92%	66%	96%	119%
Lower Macquarie Alluvium (downstream of Narromine)	101%	99%	97%	136%
Lower Murray Alluvium (downstream of Corowa)	79%	59%	98%	115%
Lower Murrumbidgee Alluvium (downstream of Narrandera)	82%	56%	97%	115%

GMU	B	Cdry	Cmid	Cwet
Lower Namoi Alluvium	123%	98%	96%	137%
Lower Oakey Creek Alluvium	70%	87%	93%	134%
Mallee-1	88%	66%	103%	112%
Marne	84%	66%	97%	114%
Mid Loddon WSPA	73%	59%	97%	103%
Mid Murrumbidgee Alluvium (upstream of Narrandera)	74%	62%	97%	115%
Miscellaneous Alluvium of Barwon Region	114%	96%	90%	143%
Mullindolingong GMA	84%	72%	95%	105%
Murmungee GMA	72%	81%	97%	116%
Myall / Moola Creek North Alluvium	69%	93%	95%	125%
Myall Creek Alluvium	70%	97%	95%	125%
New England Fold Belt	112%	97%	94%	132%
Nhill	76%	61%	98%	110%
Nobby Basalts	77%	92%	95%	114%
Noora	83%	62%	106%	113%
Oakey Creek Management Area	82%	99%	96%	124%
Orange Basalt	93%	81%	97%	121%
Oxley Basin	119%	98%	99%	134%
Peake, Roby and Sherlock	84%	66%	104%	112%
Peel Valley Alluvium	113%	97%	101%	132%
Peel Valley Fractured Rock	102%	97%	103%	133%
SA/VIC Border Water Supply Protection Area	83%	66%	97%	111%
Shepparton WSPA	66%	76%	98%	112%
Spring Hill WSPA	64%	65%	93%	99%
St. George Alluvium	111%	99%	95%	130%
Swan Creek Alluvium	92%	101%	90%	154%
Sydney Basin	83%	96%	103%	156%
Tintinara-Coonalpyn	82%	68%	100%	111%
Toowoomba City Basalt	40%	108%	94%	137%
Toowoomba North Basalt	73%	93%	95%	125%
Toowoomba South Basalt	75%	88%	93%	132%
Upper Darling Alluvium	119%	97%	93%	141%
Upper Hodgson Creek Basalt	66%	87%	93%	136%
Upper Lachlan Alluvium (upstream of Lake Cargelligo)	80%	62%	99%	114%
Upper Loddon WSPA	70%	59%	97%	103%
Upper Macquarie Alluvium (upstream of Narromine)	111%	96%	102%	154%
Upper Murray Alluvium (upstream of Corowa)	79%	60%	99%	120%
Upper Namoi Alluvium	116%	99%	102%	136%
Warwick Area Basalt	79%	93%	94%	118%
Western Murray Porous Rock	83%	71%	99%	121%
Young Granite	79%	75%	100%	115%

Table 12-2. Recharge scaling factors calculated for each model recharge zone under scenarios B and C

Model	B	Cdry	Cmid	Cwet
Border Rivers		91%	99%	124%
Campaspe	72%	67%	98%	113%
Lower Gwydir Zone 2		92%	112%	133%
Lower Gwydir Zone 3		92%	110%	134%
Lower Gwydir Zone 4		92%	112%	139%
Lower Gwydir Zone 5		92%	114%	131%
Lower Lachlan	92%	65%	96%	119%
Lower Murrumbidgee	82%	58%	97%	115%
Lower Namoi		92%	95%	143%
Lower Namoi Zone 1		84%	98%	143%
Lower Namoi Zone 2		92%	101%	137%
Lower Namoi Zone 3		92%	99%	138%
Lower Namoi Zone 4		92%	100%	136%
Lower Namoi Zone 5		91%	100%	144%
Lower Namoi Zone 6		84%	98%	143%
Lower Namoi Zone 7		93%	99%	127%
Lower Namoi Zone 8		91%	98%	143%
Lower Namoi Zone 9		92%	102%	132%
Lower Namoi Zone 10		90%	96%	135%
Lower Namoi Zone 11		90%	98%	135%
Lower Namoi Zone 12		88%	100%	147%
Macquarie	101%	99%	97%	137%
Mid Murrumbidgee	74%	59%	97%	115%
Super G	75%	66%	97%	114%
Upper Lachlan	84%	65%	100%	113%

Contact Us
Phone: 1300 363 400
+61 3 9545 2176
Email: enquiries@csiro.au
Web: www.csiro.au

Your CSIRO

Australia is founding its future on science and innovation. Its national science agency, CSIRO, is a powerhouse of ideas, technologies and skills for building prosperity, growth, health and sustainability. It serves governments, industries, business and communities across the nation.